RÉPUBLIQUE DÉMOCRATIQUE POPULAIRE D'ALGÉRIE
Ministère de l'Enseignement supérieur et
Recherche scientifique
ÉCOLE NATIONALE POLYTECHNIQUE

Département Hydraulique
Laboratoire de recherche en sciences de l'eau
End-of-studies project dissertation for obtaining
the state engineer diploma in hydraulics

USING MACHINE LEARNING TECHNIQUES AND RECONNAISSANCE DROUGHT INDEX FOR METEOROLOGICAL DROUGHT FORECASTING

Mohamed AMMOUR
Under the direction of Hamza BOUGUERRA and Salim BENZIADA
Presented and publicly supported on 03/07/2024

Composition of the Jury :

President	Mrs. Chahinez TCHEKIKEN	MCB	ENP
Promoter	Mr. Hamza BOUGUERRA	MCA	Annaba University
Promoter	Mr. Salim BENZIADA	MAA	ENP
Examiner	Mr. Salah Eddine TACHI	MCA	Annaba University
Examiner	Mr. Yacine HASNAOUI	PHD Student	ENP
Invited	Mr. Robert SZCZEPANEK	MCA	Jagiellonian University
Invited	Mrs. Maria HATZAKI	MCA	Athenes University

ENP 2024

RÉPUBLIQUE DÉMOCRATIQUE POPULAIRE D'ALGÉRIE
Ministère de l'Enseignement supérieur et
Recherche scientifique
ÉCOLE NATIONALE POLYTECHNIQUE

Département Hydraulique
Laboratoire de recherche en sciences de l'eau
End-of-studies project dissertation for obtaining
the state engineer diploma in hydraulics

USING MACHINE LEARNING TECHNIQUES AND RECONNAISSANCE DROUGHT INDEX FOR METEOROLOGICAL DROUGHT FORECASTING

Mohamed AMMOUR
Under the direction of Hamza BOUGUERRA and Salim BENZIADA
Presented and publicly supported on 03/07/2024

Composition of the Jury :

President	Mrs. Chahinez TCHEKIKEN	MCB	ENP
Promoter	Mr. Hamza BOUGUERRA	MCA	Annaba University
Promoter	Mr. Salim BENZIADA	MAA	ENP
Examiner	Mr. Salah Eddine TACHI	MCA	Annaba University
Examiner	Mr. Yacine HASNAOUI	PHD Student	ENP
Invited	Mr. Robert SZCZEPANEK	MCA	Jagiellonian University
Invited	Mrs. Maria HATZAKI	MCA	Athenes University

ENP 2024

RÉPUBLIQUE DÉMOCRATIQUE POPULAIRE D'ALGÉRIE
Ministère de l'Enseignement supérieur et
Recherche scientifique
ÉCOLE NATIONALE POLYTECHNIQUE

المدرسة الوطنية المتعددة التقنيات
Ecole Nationale Polytechnique

LRS EAU
ENP - ALGERIE

Département Hydraulique
Laboratoire de recherche en sciences de l'eau

Mémoire de projet de fin d'études pour l'obtention de diplôme d'état d'ingénieur en hydraulique

UTILISATION DES TECHNIQUES D'APPRENTISSAGE AUTOMATIQUE ET L'INDICE DE RECONNAISSANCE DE SÉCHERESSE POUR LA PRÉVISION DE SÉCHRESSE MÉTÉOROLOGIQUE

AMMOUR Mohamed

Sous la direction de BOUGUERRA Hamza et BENZIADA Salim

Présenté et soutenu publiquement le 03/07/2024

Composition du Jury :

Présidente	Mrs. TCHEKIKEN Chahinez	MCB	ENP
Promoteur	Mr. BOUGUERRA Hamza	MCA	Université d'Annaba
Promoteur	Mr. BENZIADA Salim	MAA	ENP
Examinateur	Mr. TACHI Salah Eddine	MCA	Université d'Annaba
Examinateur	Mr. HASNAOUI Yacine	Doctorant	ENP
Invité	Mr. SZCZEPANEK Robert	MCA	Université Jagellonne
Invitée	Mrs. HATZAKI Maria	MCA	Université d'Athènes

ENP 2024

الملخص : تؤثر تغيرات المناخ بشكل كبير على بيئتنا، مما يؤدي إلى زيادة الجفاف، وتزايد حرائق الغابات بشكل أكثر تواترًا، وأنماط غير متوقعة في التساقطات المطرية. تؤدي هذه التغييرات إلى اضطراب النظم البيئية وسبل العيش للإنسان، مما يبرز الحاجة الملحة لاتخاذ إجراءات مناخية فورية. فهم هذه التأثيرات أمر بالغ الأهمية لتطوير استراتيجيات فعالة للتكيف. في مشروعنا، نركز بشكل خاص على مشكلة الجفاف في الجزائر وتأثيراته العميقة على الزراعة. لذا، هدف هذا المشروع هو تطوير نموذج تنبؤي لتلبية الحاجة إلى نظام تحذير مبكر ضد الجفاف في الجزائر. وذلك باستخدام منهجية ربط بين انماط حركة الجو ومؤشرات الجفاف، مثل مؤشر التعرف على الجفاف في حالتنا، في منطقة شمال غرب الجزائر. هذا العمل لا يتناول فقط مخاوف السلامة الفورية، بل يضع أيضًا الأسس لمختلف النظريات المحتملة، مما قد يسهم في التقدم في تقليل الآثار السلبية للجفاف.

الكلمات الرئيسية : الجفاف، توقع الجفاف، مؤشر التعرف على الجفاف، انماط حركة الجو، الزراعة.

Résumé : Le changement climatique a un impact significatif sur notre environnement, entraînant une augmentation des sécheresses, des incendies de forêt plus fréquents et des schémas de précipitations imprévisibles. Ces changements perturbent les écosystèmes et les moyens de subsistance des populations, soulignant l'urgence d'une action climatique. Comprendre ces effets est crucial pour développer des stratégies efficaces d'atténuation et d'adaptation. Dans notre projet, nous nous concentrons spécifiquement sur le problème de la sécheresse en Algérie et ses effets profonds sur l'agriculture. Par conséquent, l'objectif de ce projet est le développement d'un modèle de prévision pour répondre au besoin d'un système d'alerte précoce contre la sécheresse en Algérie. Utilisant l'approche de liaison entre les indices de circulation atmosphérique et les indices de sécheresse, l'indice de reconnaissance de sécheresse dans notre cas, dans la région nord-ouest de l'Algérie. Ce travail ne répond pas seulement aux préoccupations immédiates de sécurité, mais jette également les bases de diverses perspectives, contribuant potentiellement aux avancées dans l'atténuation de la sécheresse.

Mots-clés : Sécheresse, Prévision de la sécheresse, l'indice de reconnaissance de sécheresse, Indices de circulation atmosphérique, Agriculture.

Abstract: Climate change significantly impacts our environment, leading to increase drought, more frequent wildfires, and unpredictable rainfall patterns. These changes disrupt ecosystems and human livelihoods, highlighting the urgent need for climate action. Understanding these effects is crucial for developing effective mitigation and adaptation strategies. In our project, we focus specifically on the issue of drought in Algeria and its profound effects on agriculture. Therefore, the objective of this project is the development of a forecasting model to address the need for an early warning system against drought in Algeria. Utilizing the approach of linking between atmospheric circulation indices and drought indices, the reconnaissance drought index in our case, in the northwest region of Algeria. This work not only addresses immediate safety concerns but also lays the groundwork for various perspectives, potentially contributing to advancements in drought mitigations.

Keywords: Drought, Drought forecasting, Reconnaissance drought index, Atmospheric circulation indices, Agriculture.

Acknowledgements

First and foremost, I thank ***GOD*** *for granting me health, energy, and determination to complete this work.*

I also wish to express my deep gratitude to the ***members of the jury*** *for their time, expertise, and meticulous evaluation of this project. Your constructive comments and suggestions have been invaluable to me and have contributed to improving the quality of my work. Your commitment to academic excellence is a source of inspiration and motivation for me. I am honored to have had the opportunity to present my work before a panel of high-level specialists, and I am grateful for your consideration and objective evaluation of my project.*

Finally, I would like to express my gratitude to all ***the teachers of the school*** *as well as* ***everyone*** *who contributed, directly or indirectly, to the development of this project.*

Dedications

In memory of my dear grandparents, may God rest their souls.

To my dear parents, who have always given us good advice and made many sacrifices to provide us with the best living conditions.
Please see in this work the proof of the love and respect I have for you.

I dedicate this work :

To my brother and sister To my dear uncles and aunts To my dear cousins To my friend ***Yacine*** *To my friend* ***Mahmoud*** *To my friend* ***Nadhir*** *To my friend* ***Yasser*** *To my friend* ***Zakaria*** *To my friend* ***Fawzi*** *To all* ***my friends*** *To all* ***my colleagues*** *To all* ***my teachers***

To all those who are close to my heart

Table of Contents

List of Figures

List of Tables

GENERAL INTRODUCTION

GENERAL INTRODUCTION

Climate change poses one of the most pressing global challenges, primarily driven by human activities, leading to profound and long-term shifts in Earth's climate patterns. These changes manifest in rising global temperatures, increased occurrences of extreme weather events, and alterations in precipitation patterns. Dry and semi-arid regions, covering over 25 percent of the Earth's land area, confront severe water scarcity issues, necessitating proactive measures to mitigate the impacts of drought [1].

Drought emerges when extended periods of insufficient precipitation disrupt the balance considered normal or expected, resulting in inadequate water supply for human activities and ecological sustenance. Notably, drought, while not inherently a disaster, escalates to a crisis when its effects on local communities and ecosystems become severe [2, 3]. With intensifying climate change and human interventions, natural disasters occur more frequently, with drought emerging as the foremost disaster type in terms of total human impact in 2022, surpassing floods in both casualties and economic losses [4, 5].

Drought, characterized by water deficits ranging from weeks to years, span vast areas and often evolve into destructive events due to their gradual onset compared to rapid-onset disasters like floods, wildfires, and earthquakes. They result in water shortages, crop yield reductions, economic downturns, ecological degradation, and social unrest [6, 7, 8, 5].

Our project focuses on utilizing Artificial Intelligence techniques and the Reconnaissance Drought Index for meteorological drought forecasting in northwestern Algeria, representing a vital step in drought management. By harnessing advanced technologies and innovative methodologies, we aim to enhance early warning systems and decision-making processes, thereby reducing vulnerability to drought impacts. This forecasting approach has proven its validity in several studies conducted worldwide, but unfortunately, it has never been used in Algeria. Therefore, this work represents the first attempt to apply it in the country.

Motivation and contribution

The use of artificial intelligence techniques and drought recognition indices for meteorological drought forecasting is an inspiring project, as it addresses a crucial need in our country, drought mitigation and water management through preventive measures for the northwestern region of Algeria. This region, renowned for its agriculture and livestock, is particularly known for the production of durum and soft wheat, barley, as well as various fruits and vegetables. It is a vital resource for Algeria in its pursuit of self-sufficiency and food security.

Our project makes a significant contribution by integrating a thorough analysis of current drought indices, focusing particularly on the Reconnaissance Drought Index (RDI), and examining the interactions between drought and atmospheric indices. This work is based on a comprehensive literature review that facilitated a comprehensive understanding of all aspects of this domain. Subsequently, a detailed characterization of the northwestern region of Algeria was conducted, encompassing geographical features, land use patterns, and climate conditions. Following this, a methodology was proposed that begins with data processing and extends to the modeling of this phenomenon. This approach was applied to assess drought conditions in northwestern Algeria across various temporal scales, using the Random Forest model to classify drought severity. Additionally, through a detailed analysis of variable importance, we identified critical atmospheric and environmental factors influencing drought variability, thereby providing actionable insights for effective drought management strategies in the region, such as the development of an early warning system tailored to this area.

Organization of the manuscript :

- Our exploration began with a comprehensive analysis of the current state of the art, encompassing various drought indices, with a specific focus on the Reconnaissance Drought Index, and the relationship between drought and atmospheric indices. This literature review provided the essential foundation for understanding the complexities and challenges within the field.
- The second phase focused on representing the study area, the northwestern region of Algeria. This involved exploring various aspects, including geographical location, boundaries, geological features, land use and land cover patterns, elevation, slope characteristics, stream network, and climate conditions.
- The third phase laid the groundwork for our research methodologies, including an in-depth analysis of foundational datasets, exploration of the reconnaissance drought index, examination of atmospheric circulation indices, and an exploration of Artificial Intelligence techniques for predictive modeling.
- In the final phase, we delved into the analysis and interpretation of the Reconnaissance Drought Index and its application to drought assessment in northwestern Algeria. This analysis included an evaluation of drought conditions across various temporal scales and an assessment of the Random Forest model's performance in classifying drought conditions. Additionally, a detailed variable importance analysis identified key atmospheric and environmental factors influencing drought variability.

Chapter I

STATE OF THE ART AND LITERATURE REVIEW

Introduction

In this chapter, we investigate the current understanding of drought through a comprehensive exploration of the state of the art. Initially, we provide an introductory overview of the phenomenon of drought, shedding light on its multifaceted nature and the implications it holds for regions worldwide. We emphasize its far-reaching impacts on ecosystems, agriculture, water resources, and socio-economic systems.

We then turn our attention to investigate a range of forecasting techniques that are required for prediction. We explore three main areas : physical-based models, machine learning approaches, and statistical methodologies. Every approach has unique benefits and predicting difficulties.

Following this, we turn our attention to the various indices employed to assess and quantify drought conditions in different geographical contexts. These indices serve as crucial tools in understanding the complex dynamics of drought, offering insights into its intensity, duration, and spatial extent.

Our focus then shifts to the Reconnaissance Drought Index (RDI), a pivotal tool we will utilize in our research. We delve into its conceptual framework and operational characteristics, highlighting its significance in drought monitoring and early warning systems. Additionally, we review existing studies that have utilized the RDI, offering insights into its applicability and effectiveness in assessing drought severity.

Furthermore, we investigate the emerging frontier of research that seeks to integrate atmospheric circulation indices with the Reconnaissance Drought Index. By exploring this novel approach, we aim to enhance our understanding of drought dynamics and develop more accurate forecasting models. This integration enables us to explore potential correlations between atmospheric circulation patterns and meteorological drought indices, providing valuable insights into the underlying mechanisms driving drought events.

Finally, we broaden our scope to identify agricultural drought utilizing meteorological drought indices. By linking meteorological drought to its agricultural impacts, we aim to provide valuable insights for agricultural planning, resource management, and drought mitigation strategies.

Through a synthesis of literature and current research trends, this chapter sets the stage for our subsequent methodology and contributes to the broader discourse on drought assessment and prediction.

I.1 Drought

I.1.1 Definition of drought

Drought occurs when there is a prolonged lack of precipitation compared to what is considered normal or expected. This leads to an insufficient supply of water to meet the needs of both human activities and the environment. Drought itself is not necessarily a disaster ; instead, it becomes a disaster when its impacts on local communities and the environment are severe [2, 3].

I.1.2 Categories of drought

Droughts are typically classified into four categories to aid in their understanding, description, monitoring, and mitigation : meteorological drought, agricultural drought, hydrological drought, and socioeconomic drought [9, 10, 11]. Rainfall deficits are the root cause of meteorological droughts. An extended meteorological drought causes a drop in soil water content, which causes an agricultural drought [12]. When levels in streams, lakes, groundwater, or reservoirs are much below average, it is referred to as a hydrological drought. This kind of drought typically lasts for a while after the end of a meteorological drought [10, 11, 13, 12]. A socioeconomic drought occurs when water resources systems are significantly unable to supply people with the water needs for their daily activities. This can have a negative influence on people's lifestyles and income, among other socioeconomic effects [14].

I.2 Forecasting methods

Given the profound impacts of droughts on both the environment and human societies, accurate forecasting has become an essential tool for mitigation and preparedness. Over the years, numerous methods have been developed to predict drought occurrences, each leveraging different approaches and technologies. These methods can be broadly categorized into statistical methods, machine learning techniques, and physical-based methods.

I.2.1 Statistical methods for forecasting

I.2.1.1 Definition and importance

Statistical methods for forecasting involve the use of historical data and mathematical models to predict future trends or outcomes. These methods rely on statistical techniques such as time series analysis, regression analysis, and probabilistic models to identify patterns and relationships within the data and extrapolate them into the future.

Statistical methods provide a systematic and rigorous framework for forecasting, allowing analysts to quantify uncertainty and assess the reliability of predictions. They are widely used in various industries, including finance, economics, and operations management, for short-term and long-term forecasting tasks [15].

I.2.1.2 Examples

- **Time series analysis :** Analyzing historical data to identify patterns, trends, and seasonality.
- **Regression analysis :** Modeling the relationship between a dependent variable and one or more independent variables to make predictions.
- **ARIMA (Autoregressive integrated moving average) :** A popular method for modeling time series data by incorporating autoregressive and moving average components.

I.2.2 Machine learning techniques for forecasting

I.2.2.1 Definition and importance

Machine learning techniques for forecasting leverage algorithms that learn patterns and relationships directly from data without being explicitly programmed[16]. These techniques aim to discover complex patterns in large datasets and make predictions based on these learned patterns.

Machine learning offers flexibility and scalability, allowing for the analysis of diverse types of data and the handling of non-linear relationships. It excels in scenarios where traditional statistical methods may struggle, such as handling high-dimensional data or capturing intricate patterns [17].

I.2.2.2 Examples

- **Supervised learning :** Training models on labeled historical data to predict future outcomes. This includes regression for continuous variables and classification for categorical variables.
- **Unsupervised learning :** Discovering hidden structures and patterns in data without labeled outcomes. Clustering, for instance, groups similar data points.
- **Deep learning :** Utilizing neural networks with multiple layers to learn hierarchical representations of data. Deep learning is particularly effective for tasks involving images, text, and time series data.

I.2.3 Physical-based methods for forecasting

I.2.3.1 Definition and importance

Physical-based methods for forecasting rely on mathematical models that describe the underlying physical processes governing the system being forecasted. These methods incorporate knowledge of the system's dynamics, principles, and laws to simulate future behavior.

Physical-based methods are valuable when there is a deep understanding of the underlying processes and when data availability is limited. They provide insights into causal relationships and can be used for scenario analysis and sensitivity testing [18].

I.2.3.2 Examples

- **Numerical weather prediction :** Simulating atmospheric dynamics using complex physical models to forecast weather conditions.
- **Hydrological modeling :** Predicting River flow, groundwater levels, and water quality based on knowledge of hydrological processes and inputs such as precipitation and temperature.
- **Economic models :** Forecasting economic indicators such as GDP, inflation, and unemployment rates using mathematical models based on economic theories and principles.

I.3 Drought indices

For drought forecasting, a widely accepted strategy for identifying and tracking it involves the specification of drought indicators [19, 20]. Comparing drought measurements

across regions and comparing previous drought occurrences require a numerical standard. Still, the Creating a global drought index is unfeasible due to the significant dispute on the definition of drought. Furthermore, it is challenging to assess the effects of drought due to its features and the broad range of economic sectors it affects. The complexity of drought has made it impossible for a single measure to fully represent its intensity, severity, and its effects on such a wide range of users [10]. According to [21], the two fundamental processes that are to be taken into account when defining drought objectively and creating a drought index are the time and spatial processes of supply and demand. According to [22], four fundamental requirements should be met by any drought index :

- A long accurate past record of the index should be available or computable.
- The timescale should be appropriate for the problem at hand.
- The index should be applicable to the problem being studied.
- The index should be a quantitative measure of large-scale, long-continuing drought conditions.

[23] gives a deep dive into indices :

I.3.1 Aridity anomaly index (AAI)

A real-time drought measure that considers water balance. Each week or two, the Aridity Index (AI) is determined. The actual and typical levels of aridity for each epoch are contrasted. Negative numbers indicate an excess of moisture, whereas positive values indicate moisture stress [23].

I.3.2 Deciles

The entire record of precipitation data for a given location is used to rank the frequency and distribution of precipitation. First decile rainfall levels that do not surpass the lowest 10% of the values are found here ; the fifth decile contains the median. A wet scale is also provided. If the current data is compared to the historical record for a specific period, the approach can be adjusted to account for values that are daily, weekly, monthly, seasonal, and annual [24].

I.3.3 Keetch–Byram drought index (KBDI)

Designed to use a consistent method appropriate for the local climate to identify dryness in its early stages. The amount of water needed to completely saturate the soil

and eliminate drought stress is indicated by the combination of evapotranspiration and precipitation, which results in a moisture deficit in the upper soil layers [25].

I.3.4 Percent of normal precipitation

Simple formula that may be used for comparison in any place and at any time. Computing on a daily, weekly, monthly, seasonal, and annual timeline can satisfy a number of user demands. calculated by dividing the actual precipitation by the average precipitation for the time under consideration and multiplying the result by 100 [26].

I.3.5 Standardized precipitation index (SPI)

Uses historical precipitation records for any location to develop a likelihood of precipitation that may be calculated at any number of timescales, from one month to 48 months or beyond. Unlike other meteorological indicators, the time series of data used to generate SPI does not have to be of a specific length. Wet and dry events are directly correlated with positive and negative scores on the SPI intensity scale [27, 28, 29, 30, 31, 32].

I.3.6 Weighted anomaly standardized precipitation (WASP)

Computed using gridded monthly precipitation data at $0.5^\circ \times 0.5^\circ$ resolution ; based on 12-month overlapping sums of weighted, standardized monthly precipitation anomalies [33].

I.3.7 Aridity index (AI)

Can be utilized to classify the climates of various locations since it provides a way to determine the climate regime of a certain area based on the precipitation to temperature ratio. It is feasible to use the monthly AI computation to forecast the start of a drought because the index takes temperature and precipitation effects into account [34, 35].

I.3.8 China Z Index (CZI)

CZI and SPI are equivalent because precipitation is used to determine wet and dry periods (assuming that the precipitation follows a Pearson type III distribution). Because it uses monthly time steps spanning from one to seventy-two months, it can discern between different drought lengths [36, 37].

I.3.9 Crop moisture index (CMI)

Palmer created CMI in reaction to some of the PDSI's shortcomings when they surfaced. Its capacity to respond fast to rapidly changing conditions makes it a drought index that is especially well-suited to the effects of drought on agriculture. The difference between potential evapotranspiration and moisture is deducted to calculate any deficiencies [38].

I.3.10 Drought area index (DAI)

Developed as a method to improve understanding of India's monsoon rainfall, monthly precipitation is used to pinpoint seasons of floods and drought. Monthly precipitation throughout the crucial monsoon period can be compared to estimate the intensity of the wet and dry periods. It is possible to assess the significance of the dryness by looking at how much precipitation each month contributed to the entire monsoon season [39].

I.3.11 Reconnaissance drought index (RDI)

Includes an equation for the simplified water balance that accounts for precipitation and potential evapotranspiration, as well as a drought indicator. Its three outputs are the original value, the normalized value, and the standardized value. Standardized DRI readings are similar in nature and directly comparable to SPI. DRI, however, is more representative than SPI since it considers the whole water balance instead of only precipitation [40].

I.3.12 Effective drought index (EDI)

Uses daily precipitation data to create and calculate several parameters, such as effective precipitation (EP), daily mean EP, deviation of EP (DEP), and the standardized value of DEP. These criteria can be used to determine when periods of water deficit begin and conclude. By conducting EDI calculations with input parameters for any area in the world and standardizing the results for comparison, it is possible to determine the exact start, end, and length of a drought. Since most drought indices were created using monthly data at the time the EDI was developed, the translation to daily data was special and essential to the index's usefulness [41].

I.3.13 Hydro-thermal coefficient of selyaninov (HTC)

Makes use of temperature and precipitation data, and it is sensitive to dry conditions specific to the climate regime being observed. It's flexible enough to be used with both monthly and decadal timetables [42].

I.3.14 NOAA drought index (NDI)

A precipitation-based measure that compares recorded actual precipitation with typical amounts for the growing season. The mean precipitation for each week is calculated by adding up and comparing the measured average precipitation over a period of eight weeks. If the actual precipitation for the current week surpasses 60% of the average precipitation for the eight-week period, then there is considered to be little to no water stress. Once stress has been diagnosed, it doesn't go away until precipitation is at least 60% of the typical level [43].

I.3.15 Palmer drought severity index (PDSI)

Calculated using monthly data on soil water-holding capacity, temperature, and precipitation. It takes into consideration the potential for moisture loss due to temperature effects in addition to accounting for moisture that is absorbed (precipitation) and maintained in the soil [44, 45].

I.3.16 Palmer Z Index

Referred to as the "Moisture Anomaly Index" occasionally, the computed values provide a comparable method for comparing the relative anomalies of wetness and dryness in a location to the overall record for that area [45]

I.3.17 Rainfall anomaly index (RAI)

Utilize normalized precipitation values obtained from the station history of a particular place. It provides a historical perspective by comparing the result with the present [46, 47].

I.3.18 Self-calibrated Palmer drought severity index (sc-PDSI)

Considers each and every PDSI constant, using an approach where the constants are dynamically determined based on the features of each station. Every station has a unique self-adjusting characteristic of sc-PDSI, which changes based on the local climate regime. It has both wet and dry scales [48].

I.3.19 Standardized anomaly index (SAI)

Based on the results of the RAI, it was developed to help identify droughts in susceptible regions, such as northeastern Brazil and the Sahel region of West Africa. RAI considers station-based precipitation in a region and normalizes annual amounts. The variances are then averaged over all local stations to obtain a single SAI result [47, 49].

I.3.20 Standardized precipitation evapotranspiration index (SPEI)

SPEI is a relatively new drought index that uses a simple water balance calculation to account for the influence of temperature on the development of droughts. It does this by incorporating a temperature component into its basis. SPEI has an intensity scale that computes both positive and negative values, allowing it to differentiate between wet and dry events. One month to at least 48 months of time intervals can be used to compute it. Monthly updates allow for operational use, and the longer the available time series of data, the more consistent the outcomes will be [50].

I.3.21 Agricultural reference index for drought (ARID)

Estimates the amount of moisture that is currently available in the soil. Using a combination of crop models and water stress approximations, it assesses the impact of water stress on plant growth, development, and productivity for specific crops [51].

I.3.22 Crop-specific drought index (CSDI)

By calculating a basic soil water balance, it accounts for the effects of drought and establishes when the crop was under drought stress as well as how much it will ultimately affect the final yield. Although PDSI and CMI are able to identify drought conditions in a crop, they are not able to forecast the potential effects of these circumstances on yields [52, 53].

I.3.23 Reclamation drought index (RDI)

Created to indicate the length and severity of droughts, as well as their beginning and ending dates. It contains both wet and dry scales and is calculated at the river basin level, much like the Surface Water Supply Index (SWSI). Evaporation can be included in the index because of the temperature and water demand components of the RDI [54].

For more information consult [23, 10].

I.4 Reconnaissance drought index

For our study we are going to be focusing on the Reconnaissance Drought Index (RDI). This index was given during the MEDROPLAN coordinating meeting [55]. The precipitation to potential evapotranspiration ratio is the basis for this indicator. This index's PET (potential evapotranspiration) factor was determined using the FAO Penman-Monteith equation [56]. [57] updated the RDI index to effective RDI (eRDI). The RDI index gains foundation because of its small dataset needs, high sensitivity, flexibility, and appropriateness for weather unsteadiness [58, 20, 59, 60].

I.5 Literature review

I.5.1 Rationale for choosing the reconnaissance drought index (RDI)

The vast majority of studies in the water resources discipline have recently taken the RDI into consideration when estimating the severity of droughts :

H. Vangelis et al [61] ; mentioned that in many different geographic locations, a number of drought indices of differing complexity have been employed. The Reconnaissance Drought Index (RDI), a potent drought index, has recently gained widespread adoption, mostly in the arid and semiarid climatic zones. And where the goal was to compare the RDI results over different reference periods utilizing a few widely used empirical potential evapotranspiration methods that require the least amount of data.

A. Zarch et al [58] ; examined the variations in the characteristics of drought in various aridity zones, both with and without taking potential evapotranspiration (PET) into account, in order to more accurately evaluate drought in a warming climate. The Standardized Precipitation Index (SPI), which is based just on precipitation, and the Reconnaissance Drought Index (RDI), which considers PET in addition to precipitation, are the two drought indices used. The findings showed that, despite both upward and downward drought trends occurring in every aridity zone, there is no discernible trend over a substantial portion of the zones. On the other hand, as one approaches the humid zone from the hyper-arid zone on the extreme left, the agreement between SPI and RDI decreases.

A Memon and N Shah [62] ; Used RDI and SPI to monitor and compare the drought. The findings demonstrated that the RDI is more weather-sensitive than the SPI, indicating that evapotranspiration plays a crucial role in drought assessments. The findings also demonstrated that while both indices exhibit similar behavior, RDI is more sensitive since it makes use of potential evapotranspiration under comparable climatic conditions.

The RDI index is recommended as the suitable drought index for water resource planning and management in drought surveillance programs based on the study's findings.

R Mohammed and M Scholz [20] ; stated that in several climate locations, a variety of intricate drought indexes have been employed. Currently, the semi-arid and dry climatologic regions are the main places where the reconnaissance drought index (RDI), which is thought to be a potent indicator of meteorological drought, is gaining favor. Since evapotranspiration (ET) and precipitation (P) are the foundations of the drought severity index (RDI), the ET estimation impacts the RDI-computed drought severity characterization. This study uses three of the most popular experimental ET estimations with minimal data requirements to illuminate how the ET methods, elevation, and climate affect the RDI annual results.

R Mohammed and M Scholz [63] ; where the goals were set to compute the likely relative change in the annual streamflow availability of the downstream country under the combined impacts of climate change ; estimate the expected consequences of climate change on runoff ; estimate the values of the streamflow drought index (SDI) and the standardised reconnaissance drought index (RDIst) in relation to the overall effects of climate change ; determine the expected correlations between the probable future fluctuations in precipitation (P) and potential evapotranspiration (PET) and the RDIst and SDI ; Assess the operational probability of failure (OPOF) of reservoirs in light of the overall effects of climate change and establish correlations that take capacity, yield, and reliability into account.

R Mohammed and M Scholz [64] ; expressed that it is crucial to assess the effects of climate variability and provide adequate adaptation strategies by looking into the spatiotemporal distribution of climate data and their influence on the distribution of regional aridity and meteorological dryness. The climate variability was assessed using the coefficient of variation, precipitation concentration index, and anomaly index. The trend analysis was conducted using Sen's slope, Mann-Kendall, and homogeneity tests. The reconnaissance drought index's alpha form was used to assess the degree of aridity. On the other hand, three widely used meteorological drought indices—the standardized reconnaissance drought index, the standardized precipitation index, and the standardized precipitation evapotranspiration index—were applied to forecast drought occurrences. The long-term study of climate data revealed that the number of dry years has increased over time, and the basin has seen consecutive years of drought.

Y Mohammed and A Yimam [60] ; Used monthly rainfall and maximum and minimum temperature records, to examine the meteorological drought's intensity, trend, and spa-

tiotemporal variability. The intensity of the drought at three and twelve-month intervals was calculated using the Reconnaissance Drought Index (RDI). The trend of the RDI time series' changes was ascertained using the Mann-Kendall trend test. Using ArcGIS's spatial analyst tool, the inverse distance weighted (IDW) method was used to interpolate the spatial extent of droughts. The research area's results showed that various intensity and trend signals occurred throughout the year and in different places. All stations recorded 33 extreme drought months in the summer and 168 extreme drought months in the year.

N Arain et al [59] ; assessed past droughts in Pakistan's Sindh region's Tharparkar district. To evaluate the drought, two methods were used : the Standardized Precipitation Index and the Reconnaissance Drought Index (RDI). SPI and RDI were computed using monthly precipitation (mm) and temperature data spanning 35 years. Based on the findings, it is suggested that RDI and SPI be used for planning water resources and mitigation as well as for monitoring the region's drought.

I.5.2 Investigating the relationship between atmospheric circulation indices and drought indices

However, while previous studies primarily focused on drought indices, our approach extends beyond this scope. In our research, we not only emphasize the significance of drought indices but also prioritize the identification and understanding of atmospheric circulation patterns that lead to drought events. Leveraging artificial intelligence techniques, we integrate atmospheric circulation data to enhance drought prediction accuracy. Our methodology incorporates the reconnaissance drought index to pinpoint specific atmospheric circulation patterns influencing drought occurrences. This comprehensive approach not only improves prediction accuracy but also enhances adaptability, flexibility, and the ability to recognize complex patterns in drought dynamics. While similar studies have been conducted worldwide and we enumerate the following :

I.5.2.1 Changes in meteorological drought in the Huai river basin, China

Y Yin et al [65] explore the relationship between circulation patterns and recent variations in meteorological drought in the Huai River basin (HRB), China. Despite extensive research, the link between these patterns and drought changes remains underexplored. The study examines summer drought changes in HRB and uses a self-organizing map neural network (SOM) to identify dry and wet circulation patterns (CPs), analyzing the thermodynamic and dynamic effects. Key findings include :

- Summer drought in HRB has significantly decreased.
- Changes in historical drought data align with the Standardized Precipitation Evapotranspiration Index (SPEI).
- Among twelve CPs identified by SOM, three are categorized as dry and nine as wet.
- The average and longest duration of dry CPs show a significant downward trend, while wet CPs show an upward trend.
- Wet CPs have recently had longer durations than dry CPs, which have shorter lifespans.
- Transitions between CPs require a transitional CP, with higher internal transfer rates within dry and wet CPs.
- Summer drought change is mainly driven by thermodynamic effects (over half of the total), with dynamic (circulation-related) effects accounting for about one-fourth.

This study highlights the crucial role of thermodynamic effects in summer drought changes and provides a detailed understanding of circulation patterns influencing drought in the HRB.

I.5.2.2 Linking SPEI and atmospheric circulation patterns

K Migala et al [66] analyzed the long-term trends and variability of the drought index SPEI (Standardized Precipitation Evapotranspiration Index) and related meteorological patterns during extreme wet and dry periods on West Spitsbergen Island (Svalbard) from 1979 to 2019. The study also examined correlations between SPEI values and various atmospheric circulation indices. Key findings include :

- **Positive SPEI values :** Linked with 500 hPa geopotential height and precipitable water anomalies across the North Atlantic, impacting extreme precipitation and wet conditions.
- **Negative SPEI values :** Associated with extreme dryness due to high-pressure systems over Greenland and the central Arctic or high-pressure ridges over Spitsbergen, preventing moisture from leaving the SW sector.
- **Dry summer weather :** Related to high-pressure ridges or elevated pressure between the Greenland Sea and the Barents Sea, anticyclonic conditions (Ka type), air advection from the NE–E–SE sector, and negative precipitable water anomalies.
- **Wet weather :** Caused by positive precipitable water anomalies and cyclonic conditions with atmospheric advection from the SW sector.

- **Climate model predictions :** Indicate increased precipitation across all seasons, with the largest increases in the northeast and the least in the southwest. Changes in atmospheric circulation and baric fields will alter the regional distribution of the drought index.

This study emphasizes the influence of atmospheric circulation patterns on drought and wet conditions in Svalbard, highlighting the complexity of climate dynamics in polar regions.

I.5.2.3 Investigating anthropogenic and natural influences

E Cherenkova [67] examined the influence of anthropogenic (results from the influence of human beings on nature) factors and natural climate variability on atmospheric circulation restructuring and the changes in summer drought features from the mid-20th to early 21st centuries, particularly their connection to large-scale atmospheric circulation. Key findings include :

- **Repeating drought patterns :** Summer droughts affecting more than 20% of land have occurred almost yearly since the mid-2000s, similar to patterns seen in the 1950s and 1960s. Since 2006, widespread droughts covering more than 50% of land have become more frequent, occurring almost annually from 2014 to 2021.
- **Circulation patterns and drought occurrence :** Large-scale droughts predominantly occurred during severely negative phases of the West Pacific (WP) and Eastern Atlantic/Western Russia (EAWR) circulation patterns. Statistically significant increases in drought frequency were noted during negative stages of the EAWR and WP patterns across consecutive summer months.
- **Increased stability and causes :** The increased stability of atmospheric conditions conducive to drought development is indicated by the simultaneous negative phases of both EAWR and WP during successive summer months. The positive phase of the Atlantic Multidecadal Oscillation (AMO), enhanced summertime heat, and decreased zonal atmospheric circulation in the Northern Hemisphere correlate with more frequent widespread droughts.
- **Link to AMO and anthropogenic warming :** There is a high correlation between EAWR, North Atlantic multidecadal variability, and the increased frequency of significant summer droughts in southern European Russia during the positive AMO phase. This linkage is due to known changes in atmospheric circulation and anthropogenic warming.

This study highlights the complex interplay between anthropogenic influences, natural climate variability, and large-scale atmospheric circulation patterns in shaping the frequency and severity of summer droughts.

I.5.2.4 Characterization and trends in drought patterns

H Bouguerra et al [68] utilized the Standardized Precipitation Index (SPI) to characterize meteorological droughts in northern Algeria from 1948 to 2005 at both seasonal and annual time scales. Principal Component Analysis (PCA) was employed to identify sub-regions affected by droughts, evaluate long-term temporal trends, and explore potential connections between large-scale atmospheric circulation patterns and drought variability. Key findings include :

- **Identification of sub-regions :** Four distinct drought sub-regions (RPCs) were identified in northern Algeria : central and eastern coastal, western, eastern, and west-central southern regions. These sub-regions exhibited different patterns of drought variability, determined through PCA and SPI analysis.
- **Temporal variability :** RPC1 and RPC3 sub-regions showed significant temporal variability, indicating seasonal variations in rainfall.
- **Association with atmospheric circulation patterns :** Drought variability was linked to atmospheric circulation patterns, particularly the North Sea Caspian Pattern (NCP) and Eastern Mediterranean Pattern (EMP), which influence drought prevalence in various sub-regions.
- **Correlation with atmospheric indices :** At both seasonal and annual time scales, several atmospheric indices (e.g., SOI, NAO, MOI1, MOI2, TPI, WI) demonstrated significant correlations with drought variability across different sub-regions.
- **Implications for drought forecasting and Water resource planning :** The study highlighted the importance of improved drought forecasting and water resource planning to enhance resilience against severe drought events, especially in regions with increasing drought trends like northwest Algeria. Understanding the spatial and temporal patterns of drought and their relationship with atmospheric circulation is crucial for effective management and planning.

This comprehensive analysis provides valuable insights into the spatiotemporal dynamics of drought in northern Algeria and underscores the critical role of atmospheric circulation patterns in influencing drought variability.

I.5.2.5 Long-term precipitation forecasting using artificial neural networks and multi-regression analysis for Maharloo lake, Iran

K Sigaroodi et al [1] investigated long-term precipitation forecasting for Maharloo Lake in Iran, focusing on improving drought risk management using multi-regression analysis and artificial neural network (ANN) approaches.Key findings include :

- **Methodology :**
  - **Climatic indices selection :** Out of forty indices, the most relevant were selected using cross-correlation and stepwise regression.
  - **Prediction models :** Two models were utilized : Multi-Regression Stepwise Method and ANN. The performance of these models was compared using observed rainfall data.
- **Important climatic indices :** El Niño, Pacific North America (PNA), and North Atlantic Oscillation (NAO) were identified as significant influencers of precipitation in the region.
- **Model Performance :**
  - **ANN superiority :** The ANN model outperformed the multi-regression model in precipitation forecasting, confirmed by metrics such as root mean square error (RMSE), Nash-Sutcliffe efficiency, and R^2 (coefficient of determination).
  - **Seasonal accuracy :** ANN showed higher accuracy in predicting rare rainfall occurrences during dry months (June to October), with the highest accuracy in September and the lowest in March.
- **Correlation findings :** A significant correlation was found between monthly precipitation anomalies and meteorological indices for the ten months prior.
- **Recommendations :**
  - The study highlighted the need for further research to understand better the relationship between climatic indices and precipitation, acknowledging some uncertainties due to coarse data and system complexity.
  - Incorporating additional climatic and physiographic factors, such as wind patterns and physiography, could enhance model accuracy.

These insights contribute to more accurate long-term precipitation forecasting and improved drought risk management for Maharloo Lake.

I.5.2.6 Investigating large-scale heavy precipitation events and circulation types

In their 2024 study, R Bernova and J Kysely [69] propose a criterion for identifying large-scale heavy precipitation events (LHPEs) that considers both precipitation amounts and the affected area's extent, aiming for easy application to model simulations. They examined the characteristics of LHPEs across the Czech Republic and their connection to circulation indices, highlighting differences between the western and eastern regions influenced by Atlantic and Mediterranean factors, respectively. The research aims to shed light on the primary factors driving LHPE occurrences in the area. Furthermore, the study assesses the capability of CORDEX RCMs in capturing the fundamental links between circulation patterns and precipitation, identifying potential discrepancies in simulated relationships and paving the way for model enhancements. This work serves as a foundational step towards developing future climate scenarios for LHPEs, with a focus on addressing limitations and uncertainties inherent in climate model simulations.

I.5.2.7 Understanding extreme weather events in the Yangtze river valley

In their study, Z Qian et al [70] investigated the profound impacts of heat waves, droughts, and compound drought and heat waves (CDHWs) on various sectors, emphasizing agriculture, ecosystems, human health, and societal well-being. key findings :

- **Indexes computation :** The authors computed the heat wave magnitude index (HWMI), drought magnitude index (DMI), and compound drought and heat wave magnitude index (CDHMI) for the Yangtze River Valley (YRV) from July to August between 1961 and 2022.
- **Atmospheric circulation characteristics :** They compared the large-scale atmospheric circulation characteristics during different extreme events using the computed indexes.
- **Heat wave events :** Heat wave events were found to be favored by a positive center with sinking motion in East Asia.
- **Drought events :** Droughts were mainly influenced by a zonal wave train characterized by a significant negative anomaly in Siberia, along with a high-pressure anomaly upstream and anticyclonic water vapor with strong divergence over the Yangtze River basin.
- **Compound drought and heat wave events :** During CDHW events, both anomalous systems affecting heat waves and droughts were observed to occur and streng-

then simultaneously.

- **Interaction of circulation patterns :** The positive anomaly and water vapor anomaly brought by two circulation patterns at different latitudes were superimposed over the YRV, leading to severe CDHWs.
- **Stable pressure features :** Warm positive eddy (a swirling motion of fluid) centers and cold negative eddy centers in high latitudes exhibited more stable positive pressure features, contributing to the persistent development and strengthening of CDHWs.
- **Sea surface temperature influence :** Anomalous warm sea surface temperatures in the western Pacific, moderating favorable circulation patterns, were found to potentially promote the occurrence of CDHWs in the YRV during the same period.

These findings provide insights into the complex dynamics of extreme events in the YRV, shedding light on the interconnectedness of atmospheric circulation patterns and the occurrence of heat waves, droughts, and CDHWs.

I.5.2.8 Investigating Interdecadal Variability of Summer Precipitation in Northwest China

T Xue et al [71] delved into the interdecadal variability of summer precipitation in Northwest China, utilizing daily precipitation data from 149 rain gauge sites in China and NCEP–NCAR reanalysis data spanning from 1961 to 2018. key findings include :

- **Shift to rainy period :** Northwest China experienced a shift to a rainy period on the interdecadal timescale starting in 1987, characterized by an increase in precipitation intensity and quantity.
- **Rainfall patterns :** There was a notable increase in the likelihood of moderate, heavy, torrential, and extremely heavy rain, coupled with a decrease in the likelihood of light rain. Heavy rainfall events contributed significantly to the overall increase in precipitation.
- **Atmospheric circulation features :** Interdecadal variability in atmospheric circulations over midlatitude Eurasia during summer revealed the prominence of the Silk Road pattern (SRP), featuring enhanced ascending motion and atmospheric instability in Northwest China. Strengthened easterly winds due to the Mongolian anticyclonic anomaly and circulation anomalies over central Asia and Mongolia were also noted.

- **Water vapor transport :** The rise in summer precipitation was attributed to increased water vapor transported by easterly winds from the Pacific, Indian, and South China Sea to Northwest China, particularly on the south side of the Mongolian anticyclone.
- **Role of atlantic multidecadal oscillation (AMO) :** The study highlighted the transition of the AMO to a positive phase as a major factor influencing the rise in precipitation. This transition impacted the SRP, contributing to the observed interdecadal variability.

Through their comprehensive analysis, [71] shed light on the complex interplay of atmospheric circulation patterns and oceanic oscillations in driving interdecadal variations in summer precipitation over Northwest China.

I.5.2.9 Impact of atmospheric circulation on dry and wet periods in Kujawy region, Poland

The impact of atmospheric circulation on the occurrence of dry and wet periods in the Kujawy region of central Poland was presented by [72]. Monthly totals of precipitation from 10 meteorological stations between 1954 and 2018 were used. The Standardized Precipitation Index (SPI) monthly measurements were used to identify both dry and wet seasons. In addition, the atmospheric circulation indices—western (W), southern (S), and cyclonicity (C)—were calculated using the calendar of circulation types over Central Poland. According to the data that was provided, the area receives less precipitation overall than the rest of Poland. The circulation indices W, S, and C show that air mass advection from the West outweighs that from the East in Central Poland. Furthermore, there was a noticeable increase in the frequency of air entry from the South compared to the North. In this region of Europe, anticyclonic conditions were shown to occur more frequently than cyclonic ones. In the research region, anticyclonic circulation—which mostly involved air influx from the North and enhanced westerly circulation—was clearly dominant during dry spells. On the other hand, cyclonic circulation during the advection of air masses from the South and West was the primary factor influencing the occurrence of wet spells. 28 percent and 27 percent of the study period, respectively, were made up of dry and wet periods.

I.5.2.10 Understanding hydroclimate variability in the Nile river basin

H Mahmoud et al [73] investigated the causes of periodic droughts and hydroclimate fluctuations in the Nile River Basin (NRB), which remain poorly understood. Notable

hydroclimatic changes since the 1970s have led to increased aridity in the basin, influenced by global warming and changes in the strength of ENSO and the Indian Ocean Dipole (IOD). Key Findings :

- Hydroclimate variability in the NRB has been significantly influenced by warming, El Niño, and IOD, with IOD having a greater effect over longer timeframes.
- Positive phases of ENSO and IOD lead to stronger impacts on the NRB hydroclimate than negative phases.
- Changes in regional atmospheric circulations during persistent and stronger El Niño events contribute to a drier NRB, evidenced by anomalies in stream function, geopotential height, and U-wind.
- Increased frequency and severity of El Niño and IOD events since the 1970s have resulted in more severe droughts in the NRB.
- Nile flow is better predicted by IOD and the western pole of the Indian Ocean Dipole (WIO) than by El Niño, with a significant decline in flow after 1964.
- Future droughts in the NRB are predicted to worsen due to the combined effects of warming, higher IOD, and El Niño.

The study provides insights into the complex interactions driving hydroclimate variability in the NRB, highlighting the importance of understanding and mitigating the impacts of climate change on water resources in the region.

I.6 Linking meteorological drought to agricultural drought

Furthermore, we expand on the domain of agricultural drought using one- and three-month time frames. This emphasis stems from the knowledge that agricultural drought repeatedly precedes meteorological drought, which affects crop output and food security. Our goal is to give the agricultural community more quick and useful insights by utilizing shorter time spans. [74] assert that understanding the relationship between agricultural dryness and climatic conditions is essential for managing resources and intervening in time. Our research thus provides a comprehensive strategy to drought management and mitigation by addressing not only the climatic causes to drought but also extending its applicability to agricultural environments.

Y Zhang et al [74] examined the ideal time-scale for the Standardized Precipitation Index (SPI) to be used in the Huang-Huai-Hai (HHH) region for early drought identification, focusing on summer maize. Previous studies typically computed SPI across various

time intervals, but longer time-scales were deemed inappropriate for maize due to its shorter growth phase. Early detection of meteorological drought is crucial as it often precedes agricultural drought, impacting crop production.

Key Findings :

- The 10-day SPI (SPI10) was identified as the best index for drought identification, exhibiting the highest sensitivity (77.72%) and accuracy (95.8%).
- SPI10 detected dryness 0–16 days before the observed onset date, enabling almost real-time monitoring and early warning for summer maize drought disasters in the HHH region.
- Sensitivity and accuracy of drought identification were evaluated across SPI time-scales ranging from 5 to 180 days, with SPI10 outperforming other intervals.
- The study underscores the need to tailor SPI time-scales to the growth phases of crops like maize and emphasizes the importance of meteorological drought signals in mitigating agricultural drought effects.

By focusing on shorter SPI time-scales and early drought detection, this research provides valuable insights for strengthening agricultural resilience and implementing early warning systems in the HHH region, ultimately contributing to better crop production management and disaster prevention.

Conclusion

In conclusion, this chapter has provided a comprehensive overview of the current understanding of drought, emphasizing its multifaceted nature and far-reaching impacts on ecosystems, agriculture, water resources, and socio-economic systems worldwide. We have explored various forecasting techniques, including physical-based models, machine learning approaches, and statistical methodologies, each with its unique benefits and challenges.

Furthermore, we have searched for the importance of drought indices in assessing and quantifying drought conditions, with a particular focus on the Reconnaissance Drought Index (RDI). Through reviewing existing studies and emerging research, we have highlighted the significance of integrating atmospheric circulation indices with the RDI to enhance our understanding of drought dynamics and improve forecasting accuracy.

Our research aims to fill the gap in meteorological drought forecasting in Algeria by utilizing artificial intelligence techniques and the RDI. By identifying the atmospheric circulation indices responsible for drought in the region, we seek to tailor our approach

to the unique environmental and climatic conditions of Algeria. Additionally, our study extends its scope to agricultural drought, recognizing the importance of early warning systems and resilience-building measures for agricultural sustainability.

By synthesizing literature and current research trends, our chapter contributes to the broader discourse on drought assessment and prediction, while also laying the groundwork for our subsequent methodology. Through collaboration and innovation, we aim to develop more accurate forecasting models and enhance drought mitigation strategies, ultimately fostering resilience in the face of this critical global challenge.

Chapter II

STUDY AREA

Introduction

Algeria's northwest region is a vibrant and diverse region distinguished by its distinct climate, geology, and geography. This chapter offers an overview of the research region, exploring its location, boundaries, geological features, land use and cover, elevation, slope, stream network, and climate. Gaining a comprehensive grasp of the environmental dynamics of the area requires a comprehension of these essential concepts. We highlight the complexity of the region using detailed maps and analyses created using Geographic Information Systems (GIS) and several data sources.

II.1 Geographical location and delimitation

In this study, we focus on the northwest region of Algeria, The study area covers approximately 132,100 km^2. It is located between 2°10'10" West and 3°10'11" East longitude, and between 33°18'54" and 36°4812" North latitude Figure II.1. It stretches over 250 km from south to north and about 500 km from west to east [75, 76]. The region is delimited by the Mediterranean Sea to the north, the Algerian Sahara to the south, Morocco to the west, and Algiers, Bouira, Bou Saâda, and Biskra to the east. As shown in Figure II.1, this map was created using GIS software. The northwest of Algeria includes the following watersheds : Coastal West Oran, Tafna, Coastal Center Oran, Coastal East Oran, Macta, Oran Highlands, and Chélif. Additionally, this region partially contains the watersheds of Isser, Chott el Hodna, Coastal West Algiers, Zahrez, and Chott Melrhir.

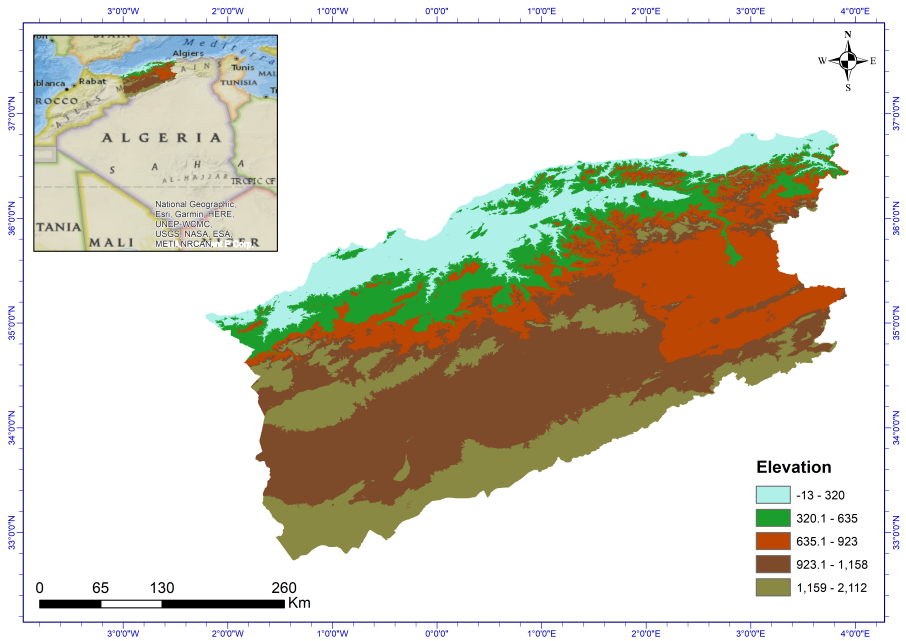

Figure II.1 — Northwest of Algeria (m)

II.2 General Characteristics of the northwest of Algeria

II.2.1 Geology

Geology, the study of Earth's physical structure and substance, serves as a fundamental pillar in understanding the landscape and natural resources of a region. It provides insights into the formation of rocks, minerals, and landforms, offering critical information for resource management, environmental conservation, and hazard assessment.

The geologie of the northwest region of Algeria is summarized in the Table II.1, which presents the area percentage for each class :

Table II.1 — Area percentage of different geological classes

Class	**Area percentage**
Sea	0.46
Tertiary Igneous	0.03
Tertiary	46.99
Cretaceous	11.85
Holocene	1.80
Lower Cretaceous	10.60
Precambrian	0.13
Lower Jurassic	0.52
Carboniferous-Devonian	0.04
Jurassic	11.91
Triassic	0.70
Quaternary (undivided)	11.45
Paleozoic Igneous	0.06
Cretaceous-Jurassic	0.17
Quaternary Igneous	0.41
Carboniferous	0.04
Pleistocene	2.58
Jurassic-Triassic	0.01
Devonian	0.13
Mesozoic Igneous	0.02
Silurian	0.009

The geological composition of the northwest region of Algeria, derived from GIS-based mapping, reveals a diverse and complex geological history. The region is predominantly

covered by Tertiary formations, accounting for approximately 47% of the area, highlighting the significance of this period. Significant contributions from the Cretaceous (11.85%) and Jurassic (11.91%) periods also play a crucial role. Additionally, the region features various other geological classes, such as Holocene, Precambrian, Carboniferous-Devonian, and Quaternary formations, indicating a dynamic geological past with multiple eras of sedimentation, erosion, and tectonic activity.

Minor contributions from igneous formations and sparse representations of certain classes like Silurian and Devonian add to the region's geological diversity. This varied geological composition has significant implications for the region's hydrology, soil types, and potential natural resources. Understanding these formations is essential for effective resource management and environmental conservation.

The Figure II.2 presents a geological map of the region, offering a visual representation of its diverse geological characteristics, was created utilizing GIS software.

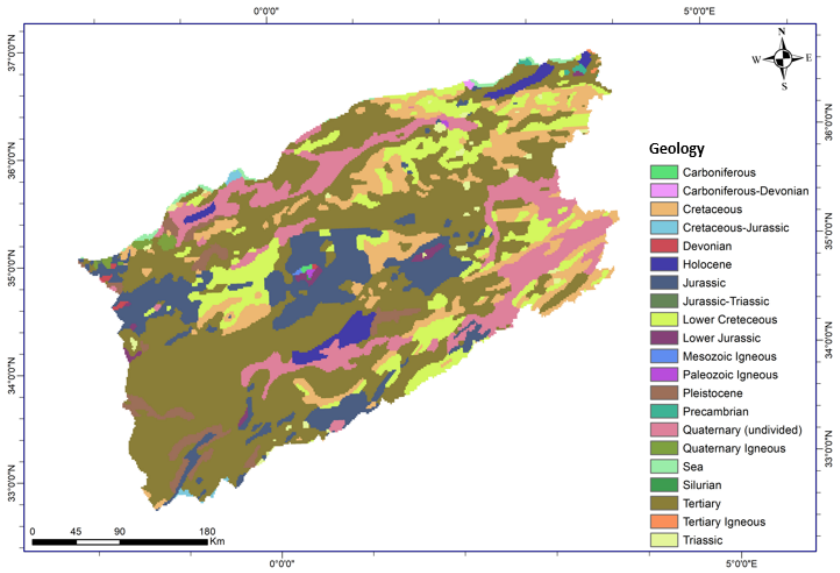

Figure II.2 — Geology map of the northwest of Algeria

II.2.2 Land use and land cover

Understanding the land use and land cover of a region is crucial for comprehending its environmental dynamics and human interactions. Land use refers to the human activities that take place on the land, such as agriculture, urbanization, and industrial development, while land cover describes the physical material covering the Earth's surface, including vegetation, water bodies, and built-up areas.

The land use and land cover of the northwest of Algeria are summarized in the Table II.2, which presents the area percentage for each class :

Table II.2 — Land use and land cover area percentages

Class	Area percentage
Water	0.13
Trees	4.08
Flooded vegetation	0.005
Crops	13.18
Built Area	3.02
Bare ground	4.45
Rangeland	75.10

From the table, it is evident that the largest land cover is rangeland, accounting for approximately 75% of the area. This is followed by crops at around 13%, and built-up areas at 3%. Bare ground and trees each cover about 4% of the region, while water and flooded vegetation cover very small portions.

The Figure II.3 is a land use and land cover map that provides a visual representation of the data presented in the table, was created utilizing GIS software from Sentinel 2 Land-use/Land-cover (10m). [77].

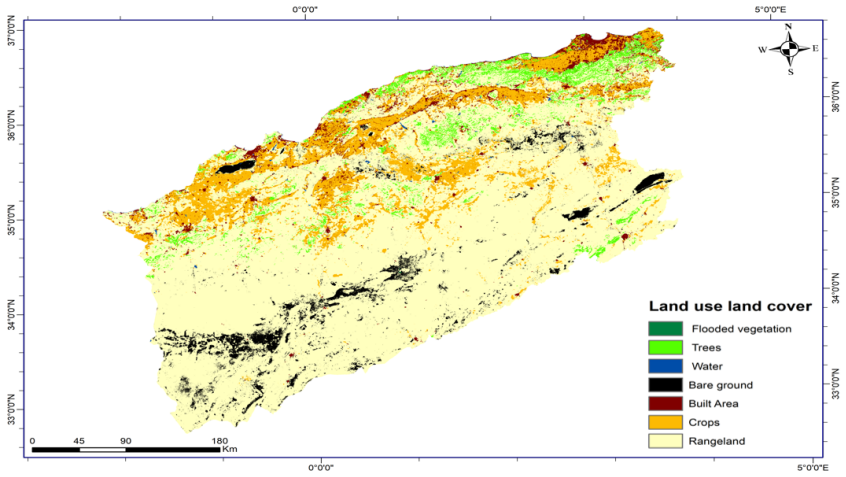

Figure II.3 — Land use, land cover map of the northwest of Algeria

II.2.3 Elevation

Elevation data is fundamental in understanding the topography and landscape of a region. It affects climate, vegetation, and human activities, influencing everything from agricultural suitability to urban planning and infrastructure development. Higher elevations typically experience cooler temperatures and different precipitation patterns compared to lower areas. Understanding the elevation variations within a region can provide

valuable insights into its environmental and developmental characteristics.

The elevation of the northwest region of Algeria ranges from 2112 meters above sea level to -13 meters below sea level. The Figure II.4 is an elevation map, providing a visual representation of the region's topography. This map was created using data from the United States Geological Survey (USGS), utilizing GIS software.

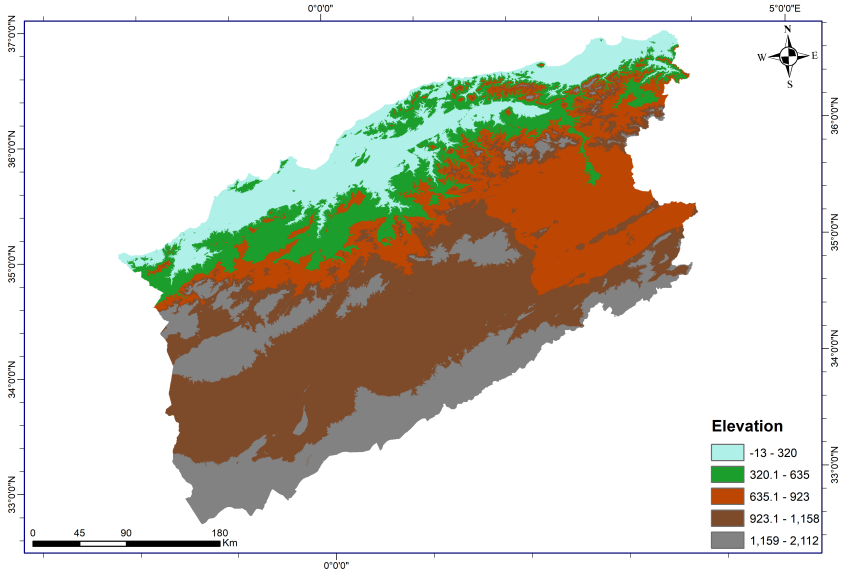

Figure II.4 — Elevation map (m) of the northwest of Algeria

II.2.4 Slope

The slope of a region is a crucial factor in understanding its topography and landscape. It influences various environmental and geological processes, including water runoff, soil erosion, and vegetation distribution. Analyzing the slope can provide insights into the region's potential for agriculture, construction, and land management. The following figure presents a slope map of the northwest region of Algeria, illustrating the gradient and steepness of the terrain.

In the northwest region of Algeria, significant variations in slope are observed, generally in the north and particularly in the northeastern and northwestern parts of the region where steep inclines prevail. The Figure II.5 visually illustrates the gradient and steepness of terrain across the northwest region, providing valuable insights into the topographical characteristics that influence the region's environmental and socio-economic dynamics, was created utilizing GIS software.

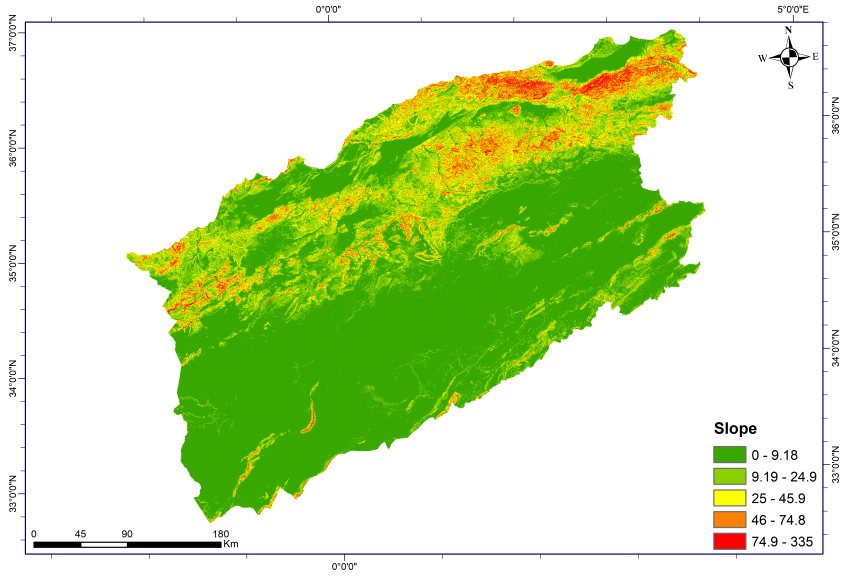

Figure II.5 — Slope map (°) of the northwest of Algeria

II.2.5 Stream network

The Figure II.6 provides a visual representation of the stream network within the northwest region of Algeria, was created utilizing GIS software.

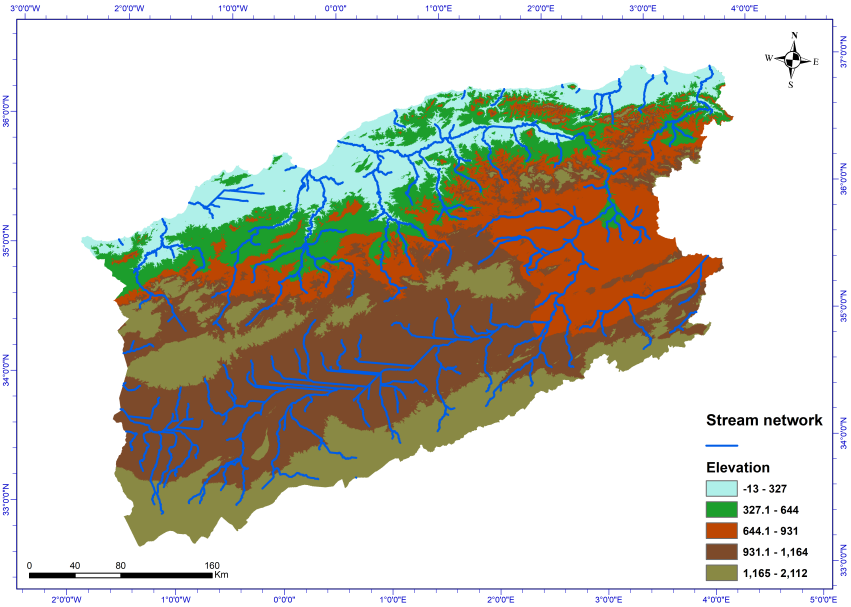

Figure II.6 — Stream network map of the northwest of Algeria (m)

The stream network of a region serves as a vital component of its hydrological cycle, shaping the landscape and influencing ecological processes, water availability, and human activities. Streams, rivers, and watercourses form interconnected networks that channel surface water runoff, transporting sediments, nutrients, and pollutants across the landscape. Understanding the stream network of a region provides valuable insights into its

hydrological dynamics, watershed boundaries, and freshwater ecosystems.

II.2.6 Climatology

A temperate climate, comparatively high humidity, and an annual precipitation range of 400 mm in the west to 900 mm in the east define the coastal region [76]. Algeria's northwest is latitude-wise, protected by Morocco's Middle Atlas-Rif mountain range. Numerous shelters from marine effects are provided by the study area's difficult topography [76, 78]. These two elements have a direct impact on the geographical variability of rainfall and help to lower the local precipitation levels. The east winds, which bring heavy rains, are uncommon in the winter and mostly originate from the west-northwest. Summertime brings regular northeastern winds that provide mild rain. The Azores High and the Saharan High have an impact on atmospheric circulation [76, 78]. Algeria's northern region experiences hot, dry summers and comparatively cold, rainy winters due to its Mediterranean climate. Along the shore, annual rainfall amounts to 400 mm in the west, 700 mm in the center, and 1,000 mm in the east. The Tell Atlas mountain ranges are similarly impacted by this climate ; in the eastern summits, total rainfall ranges from 800 to 1,600 mm, while values decrease towards the middle (700 to 1,000 mm) and the west (600 mm). The Tell Atlas plains experience 500 mm of rainfall in the west, 450 mm in the center, and 700 mm in the east. Because to its distance from the sea, the Saharan Atlas has milder winters with less rainfall than the north and extremely hot and dry summers [79, 80, 76].

Conclusion

In conclusion, the northwest region of Algeria is a multifaceted area with a rich geological composition, varied land use patterns, diverse topography, and complex hydrological networks. The region's Mediterranean climate, influenced by its proximity to the Mediterranean Sea and the Middle Atlas-Rif mountain range, results in significant spatial variability in precipitation and weather patterns. These factors collectively shape the region's environmental and socio-economic landscape, impacting everything from agriculture and urban development to natural resource management and environmental conservation. By understanding these characteristics, we can better appreciate the challenges and opportunities faced by the northwest region of Algeria, laying the groundwork for informed decision-making and sustainable development initiatives.

Chapter III

METHODOLOGY

Introduction

We undertake an in-depth look of the research procedures that serve as the foundation for our work in this chapter. We begin with an in-depth analysis of our foundational datasets, which include atmospheric circulation indicators, average minimum and maximum temperatures, and rainfall records. We identify the complex patterns and trends contained in these datasets through rigorous statistical analysis and graphical representations, offering a strong basis for additional study.

The reconnaissance drought index (RDI) is then discussed, along with its definition, the reasons it was created, and the methods used to calculate it. By clarifying the role of the RDI in drought assessment, we also set the foundation for our efforts in predictive modeling.

Next, we shift our focus to a summary of atmospheric circulation indices, delving into the computation techniques and definitions of the used indices. This chapter contributes to our understanding of meteorological processes by providing insightful information about the complex relationships between atmospheric events and drought occurrences.

We follow-up on to the topic of artificial intelligence (AI), covering both basic ideas and cutting-edge techniques with an emphasis on machine learning. Highlight its advantages, disadvantages, and special applications.

In the context of machine learning, we focus on the Random Forest method, which is well-known for its adaptability and ability to make accurate predictions. By clarifying its theoretical foundations and useful benefits, we give ourselves an effective tool for modeling drought prediction.

Finally, we combine all of the approaches mentioned into a unified modeling framework. By using a methodical procedure that includes preprocessing data, training models, and evaluating them, we want to create prediction models that can identify meteorological drought and how it affects agricultural sustainability.

III.1 Data processing

In this section, we cover the intricacies of data processing, a pivotal step in our methodology aimed at extracting meaningful insights. Firstly, the meteorological observations collected at four key stations : Chlef, Maghnia, Oran, and Saida. These stations have been strategically selected to represent the climatic diversity of the northwest region of Algeria, each contributing valuable data to our study, the data was collected from the National Meteorological Office Algeria (Office National de Météorologie Algérie). And where the gaps

were filled using the methods and datasets [81, 82, 83]. Secondly, regarding atmospheric circulation indices : Southern Oscillation Index (SOI), North Atlantic Oscillation (NAO), Paris-London Westerly Index (WI), Mediterranean Oscillation Indices (MOI),North Sea Caspian Pattern (NCP) and Trans Polar Index (TPI), the data was collected from [84]. These indices going to be defined later on.

III.1.1 Meteorological data

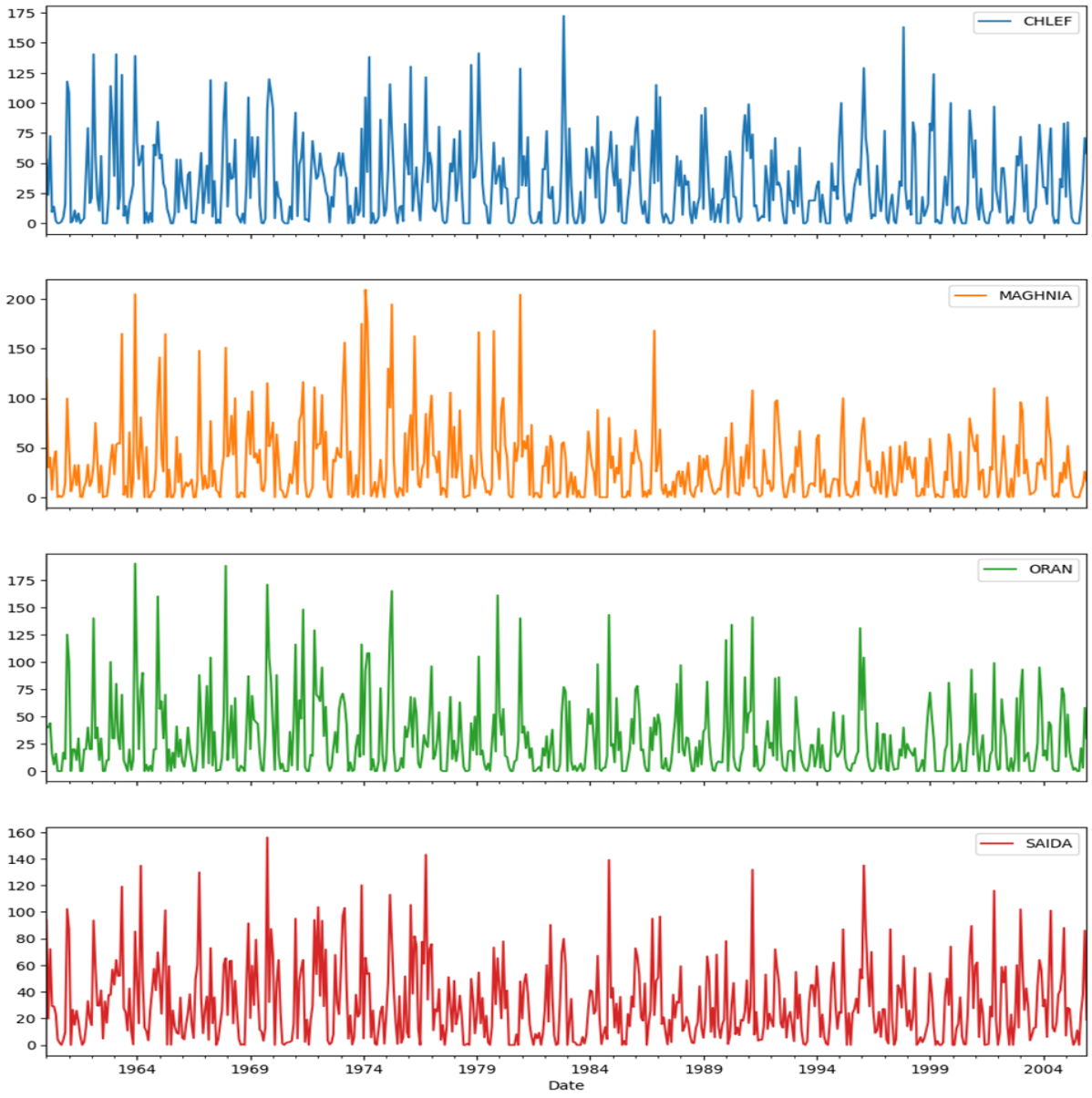

Figure III.1 — Rainfall in mm for stations : Chlef, Maghnia, Oran and Saida

Our analysis begins with a comprehensive statistical analysis of the rainfall and temperature data recorded at each station. And a representation of the data for 45years from 1960 to 2005. These statistics and representation offer critical insights into the climatic

characteristics of the region, including average precipitation levels, temperature fluctuations, and seasonal variations.

Furthermore, providing a precise locational information within the study area. By understanding the spatial distribution of our data collection points, we ensure comprehensive coverage of the region's climatic variability.

The Graphs in Figure III.1, Figure III.2 and Figure III.3 gives an overview of the data for the period from 1960 to 2005. Firstly, the rainfall graphs. Secondly, average, minimum and maximum temperature graphs. Finally, a map that gives a visual representation on the region for rainfall.

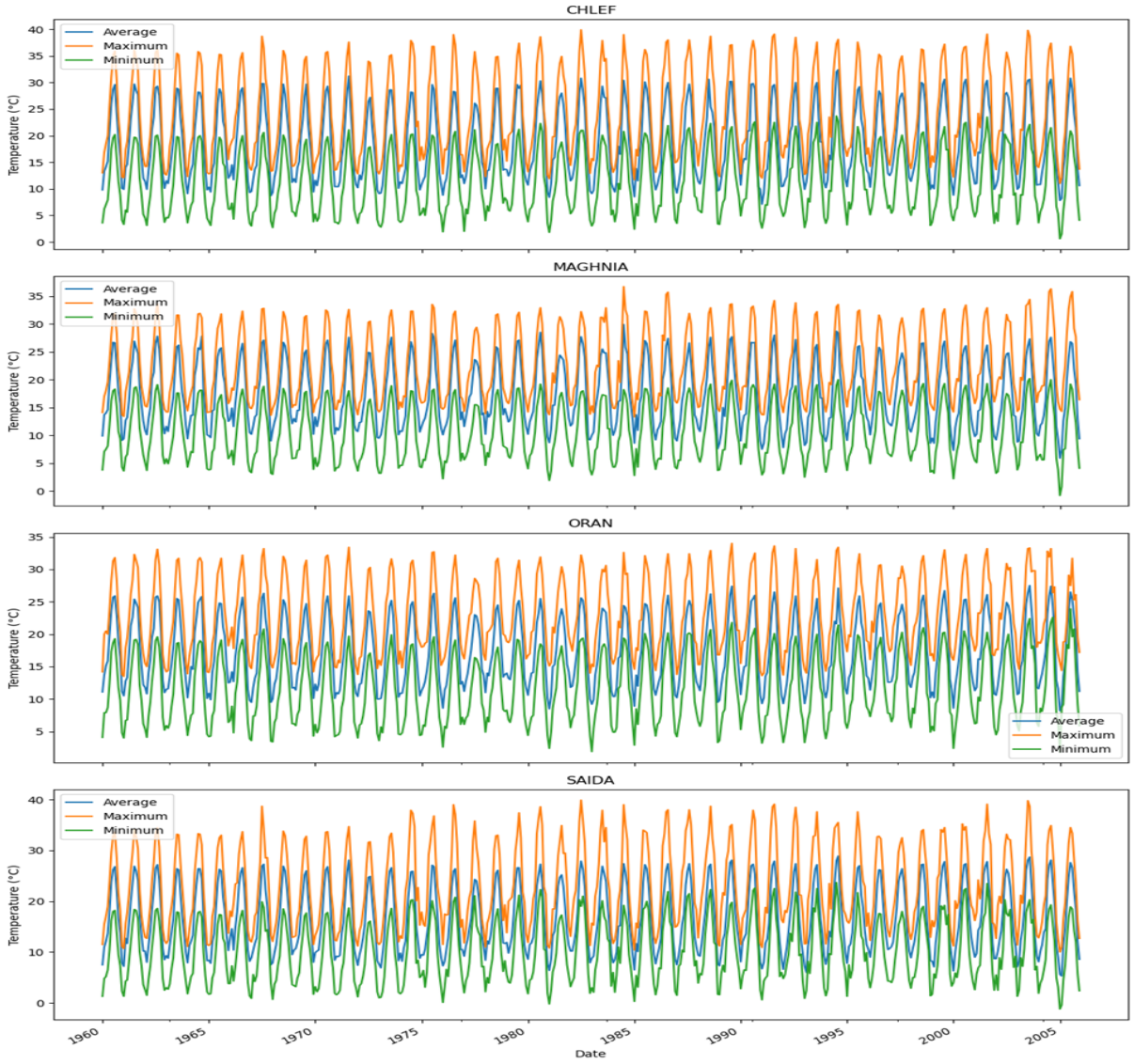

Figure III.2 — Average, minimum and maximum temperature for stations : Chlef, Maghnia, Oran and Saida

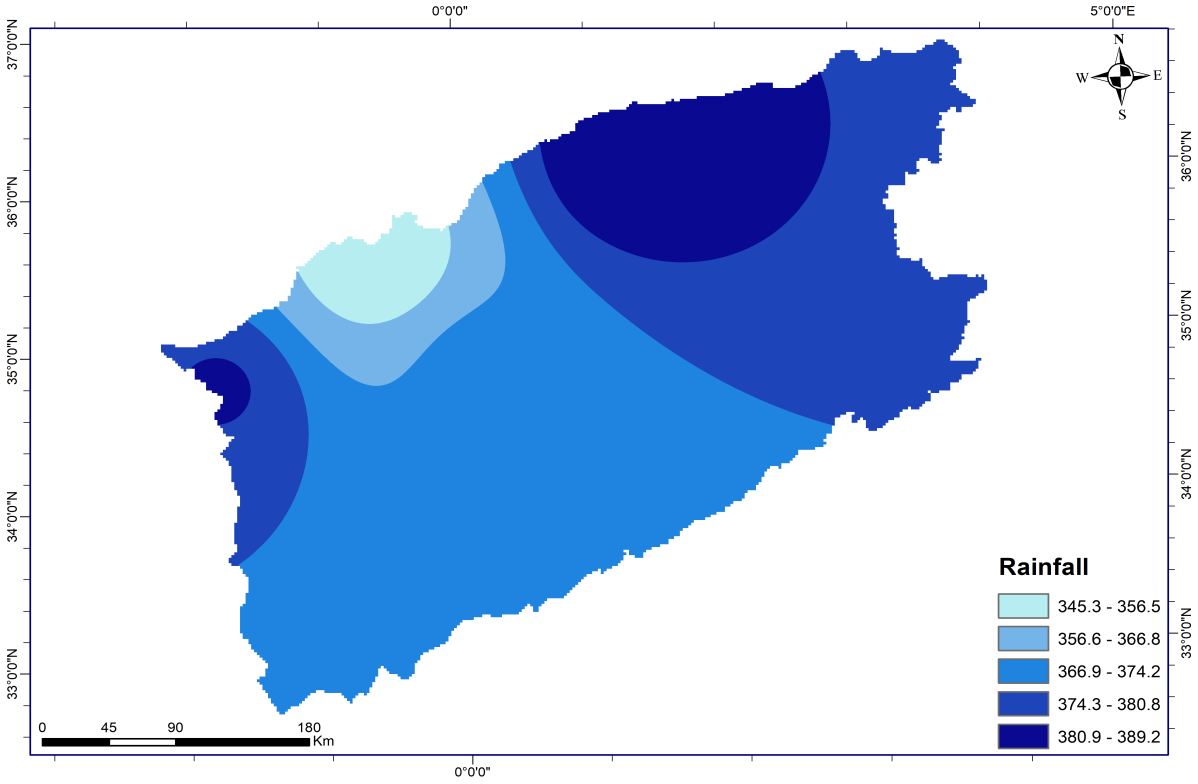

Figure III.3 — Rainfall map in (mm) of the northwest of Algeria

The histograms shown in Figure III.4, Figure III.5, Figure III.6 and Figure III.7 gives a representation of average annual rainfall (1960-2005) for each station. The histograms shown in Figure III.8, Figure III.9, Figure III.10 and Figure III.11 gives a representation of average monthly temperatures (1960-2005) for each station.

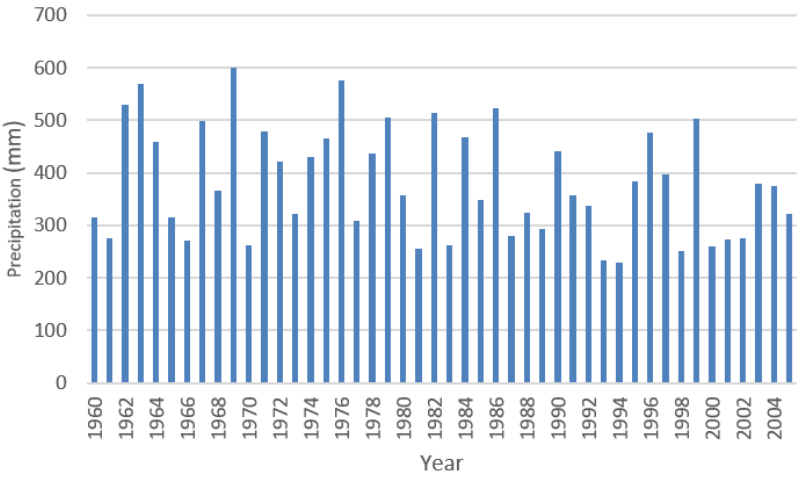

Figure III.4 — Average annual rainfall in (mm) of Chlef

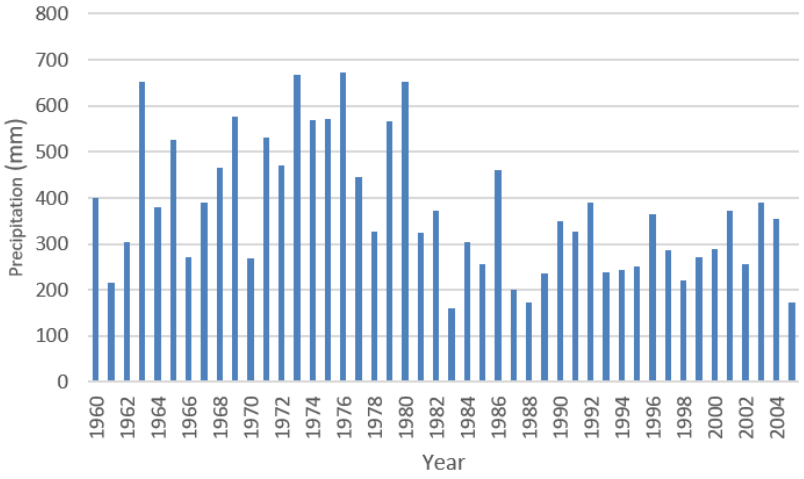

Figure III.5 — Average annual rainfall in (mm) of Maghnia

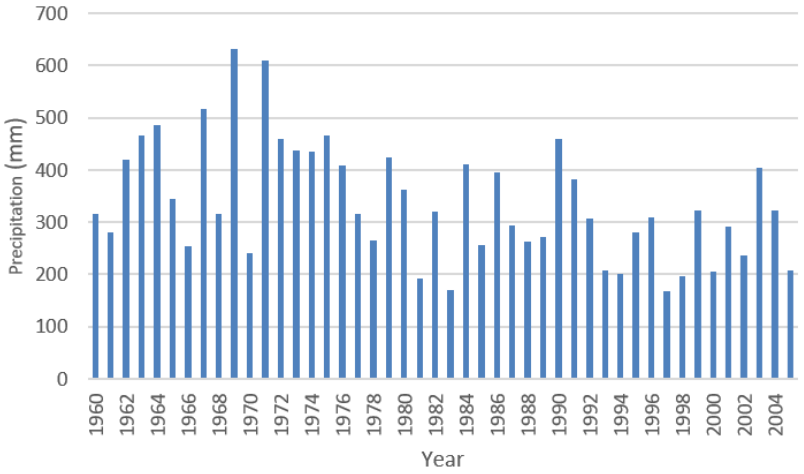

Figure III.6 — Average annual rainfall in (mm) of Oran

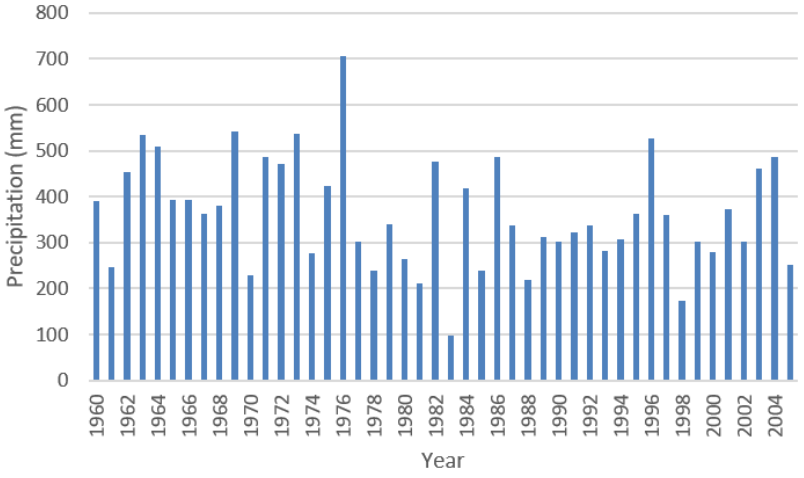

Figure III.7 — Average annual rainfall in (mm) of Saida

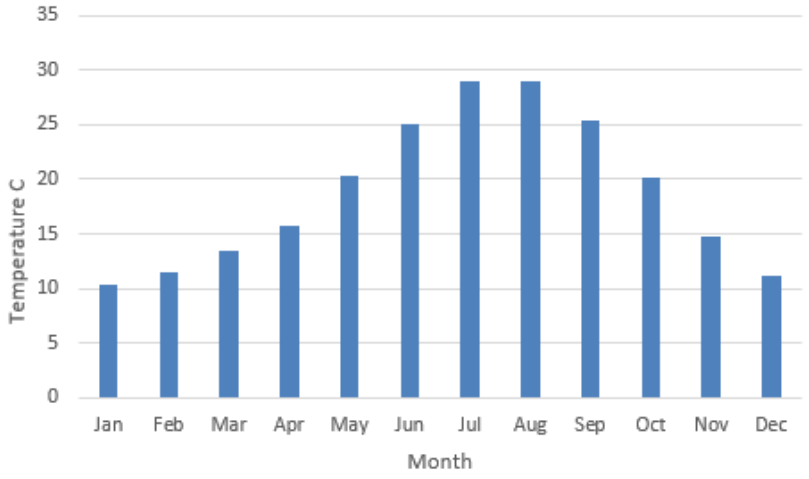

Figure III.8 — Average monthly temperature in °C of Chlef

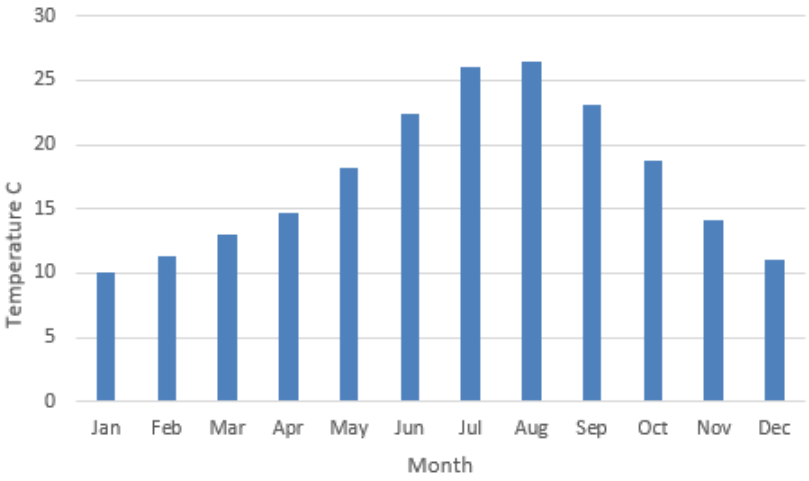

Figure III.9 — Average monthly temperature in °C of Maghnia

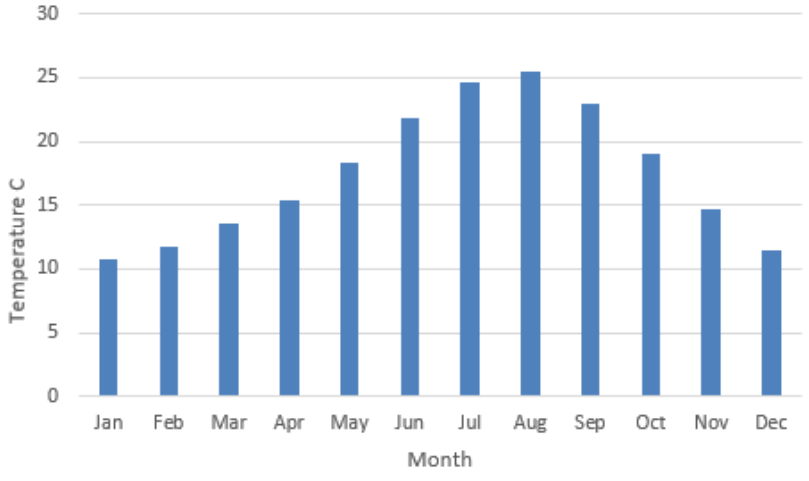

Figure III.10 — Average monthly temperature in °C of Oran

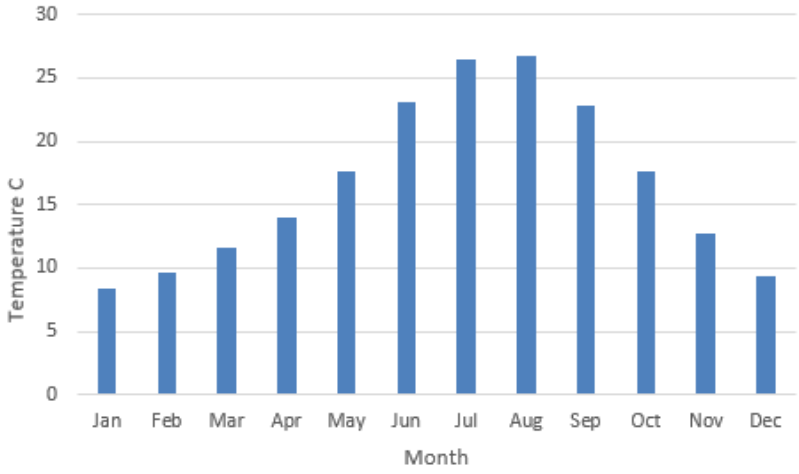

Figure III.11 — Average monthly temperature in °C of Saida

The average monthly temperature histograms shown in Figure III.8, Figure III.9, Figure III.10 and Figure III.11, display distinct seasonal patterns. Winter temperatures (December to February) are mild for Chlef, Maghnia, and Oran, ranging from about 10°C to 12°C, while Saida is cooler, ranging from 8°C to 10°C. Spring (March to May) sees a steady increase in temperatures, peaking in May at around 18°C to 20°C for Chlef and Maghnia, and slightly lower for Oran and Saida. The summer months (June to August) are the hottest, with Chlef and Saida experiencing the highest temperatures, around 29°C and 27°C, respectively. Autumn (September to November) shows a gradual decline in temperatures, from around 23°C in September to 13°C to 15°C in November. Overall, Chlef and Maghnia have higher summer temperatures, while Saida remains the coolest station year-round. The histograms illustrate these seasonal trends, with noticeable peaks in summer and troughs in winter.

For the average annual rainfall histograms shown in Figure III.4, Figure III.5, Figure III.6 and Figure III.7, reveal distinct patterns and variations over the 45-year period from 1960 to 2005. Chlef experiences considerable fluctuations, with notable peaks in years like 1963 (569 mm) and 1969 (600.1 mm), while also having lower precipitation years like 1970 (261 mm) and 1994 (229 mm). Maghnia shows similar variability, with the highest precipitation in 1973 (668.2 mm) and the lowest in 1983 (160.1 mm). Oran generally receives less precipitation, with significant highs in 1969 (632.8 mm) and lows in 1983 (171 mm). Saida tends to have a moderate to high range of precipitation, peaking in 1976 (705.7 mm) and dropping to its lowest in 1983 (96.7 mm). Across all stations, there are evident periods of increased precipitation in the late 1960s and early 1970s, contrasted by drier periods in the early 1980s and mid-1990s. These histograms highlight the inter-annual variability and distinct precipitation patterns experienced by

each station.

Next, geographical coordinates of each station are presented in the Table III.1

Table III.1 — Geographical coordinates and altitudes for each station

/	Chlef	Maghnia	Oran	Saida
Latitude	36.22	34.81	35.63	34.88
Longitude	1.32	-1.78	-0.61	0.16
Altitude	150	428	90	751

III.1.2 Statistics of atmospheric indices

Understanding atmospheric indices is crucial for comprehending climate dynamics and predicting future climatic conditions. These indices serve as key indicators of various atmospheric phenomena, such as temperature anomalies, precipitation patterns, and atmospheric circulation. By analyzing these indices over time, we can discern long-term trends and fluctuations in the Earth's climate system.

In this subsection, we explore nine significant atmospheric indices and their historical trends from 1960 to 2005. Through graphical representations and statistical analysis, we aim to provide insights into the changing dynamics of these indices and their implications for global climate patterns. The Figure III.12 offers a visual narrative of how these indices have evolved over the decades.

The Table III.2 gives a statistical representation of each atmospheric circulation index.

Table III.2 — Statistics of atmospheric circulation indices

/	NAO	SOI	TPI	WeMOi	NCP	WeI	EMP	MOI1
Count	552	552	552	552	552	552	552	552
Mean	0.024	-0.206	0.119	0.245	0.020	-0.009	-182.921	-0.008
Std	1.730	1.107	1.480	1.080	0.932	0.383	74.321	0.467
Min	-4.704	-3.463	-4.380	-3.210	-2.520	-1.256	-395.300	-1.389
25%	-1.126	-0.883	-0.845	-0.480	-0.573	-0.251	-230.875	-0.325
50%	0.043	-0.165	0.295	0.265	0.030	0.013	-183.470	0.002
75%	1.202	0.555	1.093	0.952	0.650	0.251	-130.975	0.342
Max	5.258	2.847	4.200	3.960	2.420	1.077	76.419	1.243

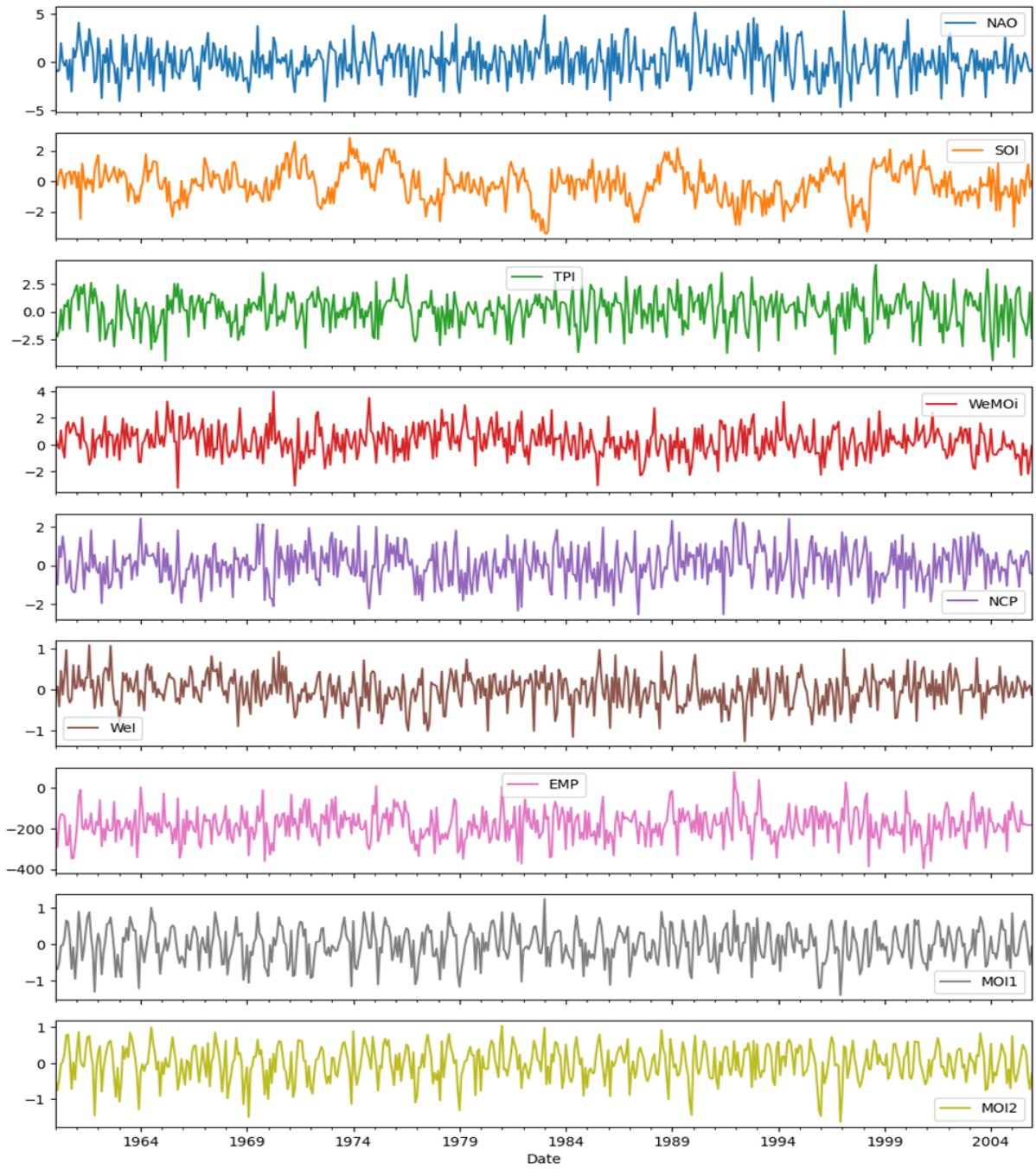

Figure III.12 — Atmospheric circulation indices

III.2 Reconnaissance drought index

III.2.1 Development and motivation behind the reconnaissance drought index (RDI)

The development of the reconnaissance drought index (RDI) stems from the necessity to address the complexities of characterizing meteorological droughts accurately. While the standardized precipitation index (SPI) has gained popularity due to its minimal data

requirements and established drought thresholds, it primarily focuses on precipitation data alone, overlooking the intricate balance between input and output factors in drought assessment [55, 40, 85].

Recognizing the fundamental importance of considering both precipitation (input) and potential evapotranspiration (PET) (output), the RDI seeks to provide a more comprehensive approach to drought evaluation. By assessing the equilibrium between these key meteorological parameters, the RDI acknowledges the essential role of PET in representing the atmosphere's intensity in extracting water from the environment [55, 40, 85].

Moreover, the RDI acknowledges that the effectiveness of precipitation varies across different systems and environments. Instead of relying solely on recorded precipitation data, the RDI accounts for the portion of precipitation that is truly beneficial and utilized by the system under study, such as infiltrated precipitation in rainfed agricultural areas [55, 40, 85].

For practicality and simplicity, the RDI primarily considers recorded precipitation and potential evapotranspiration, calculated preferably through established methods such as the Thornthwaite formula or evaporation from a class A pan. This streamlined approach ensures that only readily available precipitation and temperature data are essential for the analysis, facilitating widespread applicability and accessibility of the index [55, 40, 85].

In summary, the motivation behind the creation of the RDI lies in the recognition of the inherent complexities of meteorological drought assessment and the necessity for a comprehensive index that accounts for both input and output factors in drought characterization. This motivation, as articulated by [55, 40, 85] underscores the importance of developing innovative approaches to address the challenges of drought monitoring and management.

III.2.2 Reconnaissance drought index advantages

- **Physically sound calculation** : The RDI calculates the aggregated deficit between precipitation and the evaporative demand of the atmosphere, ensuring a physically sound assessment of drought conditions.
- **Flexible time periods** : It can be calculated for any period of time, such as monthly, bi-monthly, or seasonal intervals, allowing for customized analyses based on specific needs and data availability.
- **Meaningful results** : The calculation always leads to a meaningful figure, providing clear and interpretable indicators of drought severity.
- **Effectiveness in agricultural context** : The RDI can be effectively associated

with agricultural drought, making it a valuable tool for assessing the impact of drought on agricultural systems and informing related management decisions.

- **Link to climatic conditions** : It is directly linked to the climatic conditions of the region, allowing for comparisons with established indices such as the FAO Aridity Index. This linkage enhances its relevance and applicability to specific climatic contexts.
- **Utility in examining climate instability** : The RDI can be used under "climate instability" conditions to examine the significance of various changes in climatic factors related to water scarcity, providing insights into evolving drought patterns and trends.

Based on these advantages, the RDI emerges as an ideal index for the reconnaissance assessment of drought severity, particularly in large geographical areas like the Mediterranean region. Its comprehensive approach, flexibility in calculation, and direct relevance to agricultural and climatic conditions make it a valuable tool for drought monitoring and management.

Moreover, in regions like the Mediterranean where droughts are often accompanied by high temperatures and increased evapotranspiration rates, the RDI's sensitivity to both precipitation and evaporative demand makes it more effective than indices solely based on precipitation, such as the SPI. This heightened sensitivity enhances its ability to accurately capture and assess drought conditions, providing valuable insights for decision-makers and stakeholders [86].

III.2.3 Reconnaissance drought index calculations

The Reconnaissance Drought Index (RDI) is calculated in three stages : Initial value of RDI (a_0), normalized RDI (RDI_n), and standardized RDI (RDI_{st}). Initial value may be calculated for each month, seasons (3-month, 4-month, etc.), or hydrological year. The a_0 is calculated by using the Equation (III.1) [85, 87] :

$$a_0^{(i)} = \frac{\sum_{j=1}^{12} P_{ij}}{\sum_{j=1}^{12} \mathrm{PET}_{ij}}, \quad i = 1, \ldots, N \text{ and } j = 1, \ldots, 12 \tag{III.1}$$

Where P_{ij} and PET_{ij} are the precipitation and potential evapotranspiration of the jth month of the ith hydrological year. The hydrological year starts from October. N is the total number of years of the available data.

A second step, the Normalized RDI (RDI_n), is computed using the Equation (III.2) for

each year, in which it is evident that the parameter a_0 is the arithmetic mean of a_0 values [85, 87] :

$$\mathrm{RDI}_n^{(i)} = \frac{a_0^{(i)}}{\bar{a}_0} - 1 \tag{III.2}$$

The third step, the Standardized RDI (RDI_{st}), is given by the Equation (III.3) :

$$\mathrm{RDI}_{st(k)}^{(i)} = \frac{y_k^{(i)} - \bar{y}_k}{\hat{\sigma}_{yk}} \tag{III.3}$$

Where y_k is $\ln(a_0)$, $\bar{y}_k$ is its arithmetic mean, and $\hat{\sigma}_{yk}$ is its standard deviation.
The RDI is based on the ratio of two aggregated quantities, which are precipitation and potential evapotranspiration. It can be estimated for all time scales. However, 3, 6, 9, and 12 months are suggested since they are more useful for comparing different locations [40, 88].

III.3 Atmospheric indices

An atmospheric circulation index is a quantitative measure used to describe the patterns and behaviors of large-scale air movement within the Earth's atmosphere. These indices help in understanding and predicting climatic phenomena by summarizing complex atmospheric data into more manageable and interpretable forms. Key aspects include :
Definition : Atmospheric circulation indices are numerical representations of atmospheric patterns, such as pressure systems, jet streams, and wind patterns. They often relate to specific modes of variability in the atmosphere, like the El Niño-Southern Oscillation (ENSO), the North Atlantic Oscillation (NAO), and the Arctic Oscillation (AO) [89].
Purpose : These indices are used for predicting weather and climate conditions. By analyzing past and present values, scientists can forecast atmospheric behavior and its impact on global weather patterns, such as droughts, storms, and temperature anomalies [90].
Calculation : They are typically derived from various atmospheric parameters, including air pressure, temperature, wind speed, and precipitation, averaged over specific periods and geographical areas [91].

Understanding atmospheric circulation indices is crucial for climate science as they encapsulate the dynamic interactions within the atmosphere that drive weather systems globally.

III.3.1 Southern oscillation index (SOI)

The normalized pressure differential between Tahiti and Darwin is known as the SOI. The SOI values determined at different centers differ slightly in multiple instances. In this case, we compute the SOI using the technique described by [92]. It was the standard procedure used by the Climate Analysis Centre in 1987 and involved a second normalizing phase. Consult [93, 94] for information on the early pressure sources and the procedures used in the compilation of the series starting in 1866. [92] also conclude that the early Tahiti data quality is enough for use as a SO index. The pre-1935 data are perhaps a little less trustworthy than the post-1935 data.

III.3.2 North atlantic oscillation (NAO)

NAO is measured by the difference between the normalized sea level pressure over Gibraltar and the normalized sea level pressure over Southwest Iceland. NAO is one of the main forms of atmospheric variability in the Northern Hemisphere [95]. It is especially significant during the winter months since it has a significant influence on the Northern Hemisphere's climate [96]. According to [97], there is also a significant interdecadal variability throughout this season. [98] extended this index back to 1823 using early instrumental data. The normalized pressure difference between an Icelandic and Azorean station is the standard definition of the NAO. Using a station in the southwest of the Iberian Peninsula, an expanded version of the index can be calculated for the winter half of the year [95].

NAO modifications

The NAO modifications by [99] are pivotal in refining historical NAO data. By comparing the Gibraltar pressure record with digitized measurements from Cadiz and San Fernando, they identified discrepancies, particularly between 1821 and 1856. This analysis led to the development of a revised NAO index, incorporating data from Cadiz and San Fernando for the aforementioned period. Consequently, future NAO reconstructions benefit from a more robust dataset, offering a stronger foundation for understanding the NAO's impact on Northern Hemisphere climate in the 19th century. This enhanced dataset, which combines measurements from Cadiz, San Fernando, Gibraltar, and Southwest Iceland, forms the basis of the Iberia/Iceland Monthly NAO Index for the years 1821-1999. Specifically, data from Cadiz and San Fernando are utilized for the period 1821-1856, while later observations are based on measurements from Gibraltar and Southwest Iceland. Additionally, [100] contribute to the understanding of historical NAO

variability by reconstructing monthly NAO indices dating back to December 1658. Their reconstructions, which extend to seasonal estimates from 1500–1658, utilize a standardized methodology based on pressure differences between grid points over the Azores and Iceland. This approach, grounded in Principal Component Regression Analysis, provides valuable insights into the long-term behavior of the NAO and its implications for historical climate patterns.

III.3.3 Paris-London westerly index (WI)

For the city of London (1692-2007), [101] recovered, quality checked, and homogenized a >300-year daily series of sea-level pressure (SLP). For Paris (1670-2007), [102] created another extremely lengthy daily series of SLP by digitizing and correcting several records. There are some data gaps in both sets, especially for Paris (1726–1747). Additionally, [102, 101] evaluated the final series homogeneity. [103] created a monthly Paris-London Westerly index from 1692 onwards using the monthly means of the Paris and London SLP series.

III.3.4 Mediterranean oscillation indices (MOI)

The normalized pressure differential between Cairo (30.1°N, 31.4°E) and Algiers (36.4°N, 3.1°E) is the definition of the MOI, according to [104, 105]. From the Northern Frontier of Gibraltar (36.1°N, 5.3°W) and Palestine (32.0°N, 34.5°E), a second version of the index can be computed [106]. MOI1 covers Algiers/Cairo, MOI2 covers Gibraltar/Palestine, and WeMOi covers Padua/Cadiz (starts 1821).

III.3.5 North sea caspian pattern (NCP)

The normalized 500 hPa pressure difference between the averages of the North Sea (0°E, 55°N and 10°E, 55°N) and North Caspian (50°E, 45°N and 60°E, 45°N) centers of action is used to compute the NCP dataset. This formulation is identical to that used by [107], who employed a GIS technique and linear correlation between pressure grid points to identify these places.

III.3.6 Trans polar index (TPI)

The normalized pressure differential between Stanley and Hobart is known as the TPI. The index was first proposed by [108, 109, 110] updated and further analyzed it. The Trans Polar Indicator (TPI), which is based on the normalized pressure difference between Stanley, Falklands (51°41'27" S, 57°51'55" W) and Hobart, Tasmania (42°53'09" S,

147°19'53" E), is the only large-scale station pressure-based extratropical SH indicator that has been presented.

III.3.7 Eastern mediterranean pattern (EMP)

The Eastern Mediterranean Pattern index is defined as the normalized geopotential height difference at 500 hPa level between the north-eastern Atlantic (25°W, 52.5°N) and the eastern Mediterranean (22.5°E, 32.5°N) poles [111].

III.4 Artificial intelligence

This section delves into the foundational aspects and advanced methodologies within AI, specifically focusing on machine learning and deep learning.

In this section, we explore the differences between machine learning and deep learning, highlighting their unique applications, strengths, and challenges. We also discuss critical concepts such as over-fitting and under-fitting, which are pivotal in ensuring model accuracy and generalization.

Furthermore, we examine a specific machine learning techniques, Random Forest its definition, theory and advantages.

Through this exploration, we aim to provide a comprehensive understanding of how artificial intelligence, through its various methodologies and techniques, is shaping the future of technology and its applications across diverse industries.

III.4.1 Definition

The ability of technology, especially computer systems, to mimic human intelligence processes is known as artificial intelligence (AI). It includes a range of technologies, including machine learning, deep learning, natural language processing, and others that allow computers and other digital devices to learn, analyze, create, and interact. Artificial intelligence (AI) gives computers the ability to do tasks that are normally performed by intelligent beings, like sensing, reasoning, learning, and problem-solving. Decision-making, speech recognition, and picture analysis are among the activities that this technology makes easier [112]. According to [113], artificial intelligence (AI) had its start in the middle of the 1950s around the US.

III.4.2 Machine Learning

A branch of artificial intelligence called machine learning (ML) focuses on creating methods and algorithms that let computers learn from data and make judgment calls or predictions without needing to be explicitly programmed for every task [114].

Definition : Machine learning is the process of building models from data that can identify patterns and relationships, enabling them to generalize and forecast on previously unknown data [114].

Learning process : As ML algorithms process data, they iteratively learn from it. Over time, they modify their internal representations and parameters to increase performance [114].

Learning types : Machine Learning (ML) includes several learning types, such as reinforcement learning, unsupervised learning, semi-supervised learning, and supervised learning. These types of learning are appropriate for diverse tasks and data sets [114].

Applications : There are many different fields in which machine learning is used, such as computer vision, e-commerce, healthcare, finance, and autonomous vehicles [114].

Impact : By enabling automation, tailored suggestions, fraud detection, predictive maintenance, and other data-driven solutions, machine learning has revolutionized several sectors. Because of improvements in data availability, processing power, and algorithmic creativity, machine learning algorithms are always changing. This results in more complex models with more applications and a bigger social impact [114]

III.4.3 Learning types

Supervised learning : The algorithm gains knowledge from labeled data in which every input is matched with the appropriate output. To enable the model to forecast on data that hasn't been seen yet, the objective is to develop a mapping function from input to output [115]. Regression and classification tasks are two examples.

Unsupervised learning : In unsupervised learning, models are trained on unlabeled data with the goal of uncovering hidden patterns or structures in the data. The technique uses dimensionality reduction or clustering related data points to simplify data representation while exploring the data on its own [116]. Clustering, dimensionality reduction, and generative modeling are a few examples.

Semi-supervised learning : Training with a combination of labeled and unlabeled data is the basis of semi-supervised learning. It makes use of a smaller pool of labeled data in conjunction with a larger one of unlabeled data, enhancing model performance by adding details from unlabeled instances [117]. Semi-supervised learning comes in particularly

handy when getting labeled data requires a lot of money or effort.

Reinforcement learning : In this sort of learning, an agent picks up skills to interact with its surroundings by acting and then getting feedback in the form of rewards or penalties. The agent's goal is to eventually figure out the best course of action that maximizes cumulative rewards [118]. It is frequently utilized in situations like controlling autonomous vehicles, robotics, and gaming.

Machine learning approaches are diverse due to the specific characteristics, applications, and obstacles of each form of learning. In our case, a supervised technique will be employed.

III.4.3.1 Supervised techniques

Classification : Sorting incoming data into predetermined classes or categories is the aim of this supervised learning activity. The system predicts the class labels of cases that have not yet been encountered by learning from labeled training data. It is frequently used for applications like image recognition, sentiment analysis, and spam detection It works with discrete output values [119].

Regression : Regression is also a supervised learning task but focuses on predicting continuous output values rather than discrete classes. The algorithm learns the relationship between the input features and the continuous target variable. It's used for tasks like predicting house prices, stock prices, and temperature forecasting. Regression aims to find the best-fit line or curve that represents the relationship between input and output variables [120].

Both classification and regression are fundamental techniques in machine learning, each suited to different types of problems and data. They play crucial roles in various domains, including finance, healthcare, marketing, and more.

In our case, we are going to implement classification, utilizing the following model :

III.4.3.2 Random Forest

Random Forest is an ensemble learning algorithm that leverages the power of decision trees to make predictions [121].

Ensemble learning : To increase prediction accuracy and robustness, Random Forest combines several decision trees in an ensemble learning technique [121].

Decision tree integration : To lower the danger of overfitting, it combines several decision trees into a "forest" structure. Each tree is trained using a different subset of the training data and characteristics [121].

Voting mechanism : During prediction, each tree in the forest makes an independent forecast about the event. The predictions are then combined, usually using a majority voting system, to decide the ultimate conclusion [121].

Simpleness and adaptability : Random Forest is renowned for its simplicity and adaptability. It works well with a variety of data types and jobs and maintains performance even in the absence of considerable hyperparameter adjustment [121].

Versatility : It is an adaptable option for a variety of fields due to its broad applicability for both regression and classification problems [121].

Figure III.13 provides a visual representation of a random forest model.

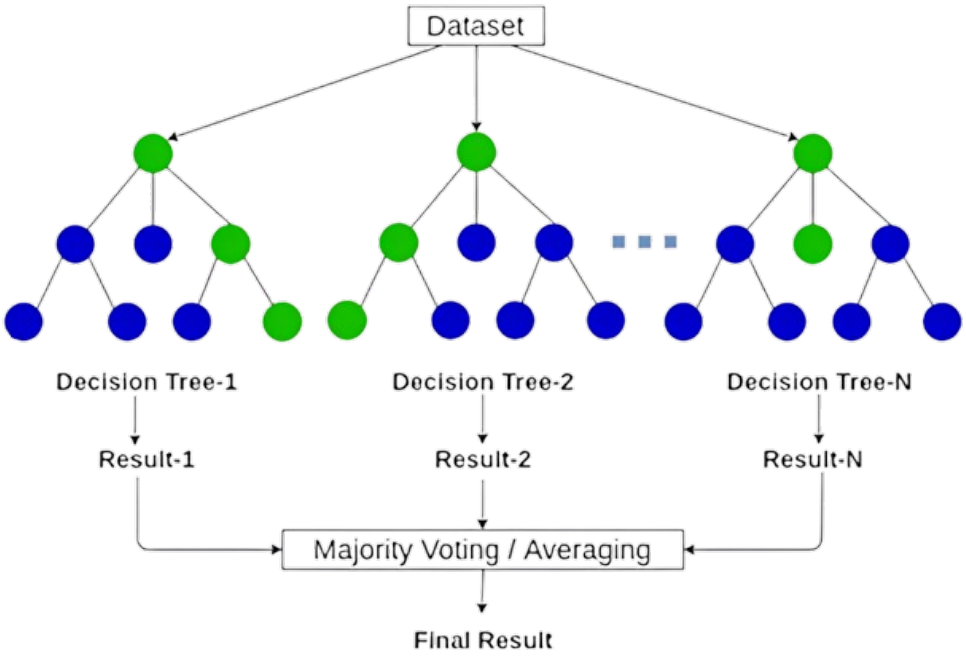

Figure III.13 — Visual representation of a Random Forest model [122]

As shown in Figure III.13, a random forest is an ensemble of decision trees, which is used to improve the performance and accuracy of predictions [122].

III.4.3.3 Model evaluation metrics

III.4.3.4 Accuracy metric

Accuracy is a classification metric that measures the proportion of correctly classified instances out of the total instances evaluated [123, 124]. It provides an overall assessment of a model's predictive capability [125, 124]. The formula for accuracy is Equation (III.4) :

$$\text{Accuracy} = \frac{\text{Number of Correct Predictions}}{\text{Total Number of Predictions}} \tag{III.4}$$

Accuracy ranges from 0 to 1, where 1 represents perfect accuracy. It is intuitive and easy to understand, making it a popular metric for evaluating classification models. However, accuracy may not be the best metric for imbalanced datasets, where one class dominates the others. Additionally, accuracy alone may not provide a complete picture of model performance, especially when classes have unequal importance or misclassification costs [124].

III.4.3.5 AUC-ROC Metric

The Area Under the Receiver Operating Characteristic (ROC) Curve (AUC-ROC) is a metric used to evaluate the performance of binary classification models [126, 124].

- **The ROC curve :** is a graphical plot that illustrates the trade-off between the true positive rate (sensitivity) and the false positive rate (1-specificity) for various threshold values of the classification model [127, 124].
- **AUC-ROC :** quantifies the overall performance of the model by calculating the area under the ROC curve, which ranges from 0 to 1 [128, 124].

A higher AUC-ROC score indicates better discrimination capability of the model in distinguishing between the positive and negative classes. An AUC-ROC score of 0.5 suggests random guessing, while a score of 1 indicates perfect classification [126, 124]. AUC-ROC is widely used because it is threshold-independent and provides a single scalar value to assess the model's overall performance [127, 124]. However, AUC-ROC may not be the most suitable metric for imbalanced datasets where the class distribution is skewed, as it may not adequately reflect the model's performance [127, 124].

III.4.3.6 Using AUC-ROC in multi-class classification

In multi-class classification scenarios, the Area Under the Receiver Operating Characteristic (ROC) Curve (AUC-ROC) can still be useful, albeit with some adaptations [129, 124].

- **One-vs-Rest (OvR) approach :** Convert the multi-class problem into multiple binary classification problems using the One-vs-Rest approach. For each class, consider it as the positive class, while the other classes are combined as the negative class. Compute the ROC curve and AUC separately for each class.
- **Macro-average and micro-average AUC-ROC :**
  - **Macro-average AUC-ROC :** Calculate the AUC-ROC for each class separately and then take the average. This treats all classes equally.

- **Micro-average AUC-ROC :** Aggregate the true positive and false positive rates across all classes before computing the AUC. This method weighs each class by its number of instances.

- **Class imbalance handling :** Assign weights to each class based on their importance or sample size to account for the imbalance.

- **Averaging methods :** Apart from macro and micro averaging, it is also possible to explore other averaging methods such as weighted averaging, geometric averaging, or harmonic averaging, depending on the specific requirements of the problem.

in our case we adopted the techniques One-vs-Rest (OvR) approach.

III.5 Variable importance for Random Forest

Variable importance, or feature importance, is a technique used in machine learning to quantify the relevance of each feature (input variable) in predicting the target variable. It helps in understanding which features are contributing the most to the model's predictions and can guide feature selection, model interpretation, and understanding data relationships [130].
Random Forest, an ensemble learning method, assesses feature importance by evaluating how each feature contributes to reducing the impurity in decision trees [131]. The process involves :
Mean decrease in impurity (MDI) : This method calculates the feature importance by measuring the total decrease in node impurity (Gini impurity or entropy) brought by that feature across all trees in the forest. Features causing larger decreases are considered more important.
Mean decrease accuracy (MDA) : Involves shuffling each feature and measuring the decrease in model accuracy. Features causing larger drops in accuracy are deemed more important.
Permutation importance : This method calculates the drop in model performance (e.g., accuracy) when the values of a feature are randomly shuffled, breaking the relationship between the feature and the target.

In our study Mean decrease in impurity (MDI) was used for feature importance.

III.6 Used approach

III.6.1 Calculation of the reconnaissance drought index (RDI)

The Reconnaissance Drought Index (RDI) was calculated using the DrinC software, which requires precipitation and potential evapotranspiration data. Our dataset ranges from January 1962 to December 2005 and includes data from four meteorological stations : Chlef, Maghnia, Oran, and Saida.

To focus on agricultural impacts, we calculated the RDI for two time scales : 1-month and 3-month periods. The RDI calculation process involves the following :

First, providing precipitation data, it was gathered from the aforementioned meteorological stations.

Second, providing potential evapotranspiration data, was calculated using DrinC. This calculation requires maximum, minimum, and average temperature data. DrinC offers several methods for this calculation, including Hargreaves, Thornthwaite, and Blaney-Criddle. We selected the Hargreaves formula because it provides results closest to those from the Agence Nationale des Ressources Hydriques (ANRH).

Finaly, calculation of the reconnaissance drought index, for each station for the two time scales.

III.6.2 Classification of RDI values

After calculating the RDI for 1-month and 3-month time scales (RDI1 and RDI3), classify the values into seven categories based on the Table III.3 :

Table III.3 — Classification of reconnaissance drought index [132]

Name	Range	Number of Class
Extremely Wet	2+	1
Very Wet	1.5 to 1.99	2
Moderately Wet	1 to 1.49	3
Near Normal	-0.99 to 0.99	4
Moderately Dry	-1 to -1.49	5
Severely Dry	-1.5 to -1.99	6
Extremely Dry	-2 and less	7

III.6.3 Calculation of atmospheric circulation indices (ACI)

The ACI1 is the data from [84]. The ACI3 is to be calculated : For a given month, the ACI3 value is the average of the current month and the two preceding months.

III.6.4 Normalization of ACI Data

Normalize the ACI3 and ACI1 data using the Min-Max Scaler to ensure they are on a comparable scale.

III.6.5 Normalization using Min-Max scaler

Normalization is a crucial step in data preprocessing for machine learning algorithms. It transforms the data into a format that improves the performance and training stability of the models. One commonly used normalization technique is the MinMax Scaler [133].

III.6.5.1 Definition of Min-Max scaler

The MinMax Scaler is a normalization technique that scales the data to a fixed range, usually [0, 1] or [-1, 1]. It is particularly useful when the data needs to be bounded within a specific range, ensuring that each feature contributes equally to the analysis [134].

III.6.5.2 Functioning of Min-Max scaler

The MinMax Scaler operates by transforming each feature individually according to the Equation (III.5) :

$$X_{\text{scaled}} = \frac{X - X_{\text{min}}}{X_{\text{max}} - X_{\text{min}}} \tag{III.5}$$

Where : X is the original value. X_{min} is the minimum value of the feature. X_{max} is the maximum value of the feature. X_{scaled} is the normalized value.

The transformed data, X_{scaled}, is rescaled to the range [0, 1]. The process can be extended to any desired range [a, b] using the Equation (III.6) :

$$X_{\text{scaled}} = a + \frac{(X - X_{\text{min}}) \cdot (b - a)}{X_{\text{max}} - X_{\text{min}}} \tag{III.6}$$

Where : a is the lower bound of the desired range. b is the upper bound of the desired range.

III.6.5.3 Modeling with Random Forest

After scaling the ACI1 and ACI3, we proceed with modeling using the Random Forest algorithm. The input variables for the model are ACI1 for the first series, ACI3 for the second series, and RDI1 as the output for the first series, and RDI3 as the output for the second series. The modeling process involves the following steps :

- **Data splitting :** We divide our dataset into training and testing sets. The training data comprises 70% of the series, while the testing data comprises the remaining 30%. This split allows us to evaluate the model's performance on unseen data.
- **Modeling for each station :** For each station, we perform the modeling process using Random Forest. This involves training the model on the training data and evaluating its performance on the testing data.
- **Model evaluation :** We assess the performance of the model using various metrics, including accuracy and Area Under the Receiver Operating Characteristic Curve (AUC-ROC). Accuracy measures the proportion of correctly classified instances, while AUC-ROC evaluates the model's ability to discriminate between positive and negative instances.

By following these steps, we aim to develop robust models that accurately predict meteorological drought conditions which lead to the agricultural drought based on Atmospheric Circulation Indices (ACI) and Reconnaissance Drought Index (RDI) data for two different short term time scales.

Conclusion

In conclusion, the methodology chapter serves as a comprehensive roadmap for our research endeavors in understanding and predicting meteorological drought and its impacts on agricultural sustainability. We have meticulously detailed the foundational datasets we utilize, the reconnaissance drought index (RDI) and its significance in drought assessment, and the complexities of atmospheric circulation indices.

Furthermore, we have delved into the field of artificial intelligence, distinguishing between basic concepts and cutting-edge techniques, with a particular emphasis on deep learning and machine learning. Through our exploration of the Random Forest method and its application in accurate prediction. we have armed ourselves with a powerful tool for modeling drought dynamics.

Crucially, we have not only outlined each component individually but also integrated them into a cohesive modelization framework. This systematic approach, encompassing

data preprocessing, model training, and evaluation, is pivotal in our mission to develop robust prediction models capable of identifying meteorological drought and its ramifications for agricultural sustainability.

As we move forward with our research, the methodologies elucidated in this chapter will serve as the bedrock upon which we build our analyses and interpretations. By adhering to rigorous statistical analysis, leveraging advanced AI techniques, and continuously refining our models, we endeavor to contribute meaningfully to the understanding and mitigation of drought-related challenges in agricultural ecosystems.

Chapter IV

RESULTS AND DISCUSSION

Introduction

In this chapter, we analyze and interpret the Reconnaissance Drought Index (RDI) and its application to drought assessment in northwestern Algeria, focusing on four key meteorological stations : Chlef, Maghnia, Oran, and Saida. The RDI analysis is conducted on both a monthly (RDI1) and seasonal (RDI3) basis, providing a comprehensive view of drought conditions over different temporal scales. This analysis is complemented by an evaluation of the performance of a Random Forest model in classifying drought conditions, and a detailed feature importance analysis to identify key atmospheric and environmental factors influencing drought variability.

IV.1 Reconnaissance drought index results and interpretation

This section presents the results and interpretation of the Reconnaissance Drought Index (RDI) analysis. The analysis is divided into two parts : RDI1 and RDI3.

Table IV.1 represents how the seasons are defined and classified

Table IV.1 — Seasons classification

Season	Months of the season
1	Sep, Oct and Nov
2	Dec, Jan and Feb
3	Mar, Apr and May
4	Jun, Jul and Aug

Table IV.2 shows the classification of reconnaissance drought index (RDI1 and RDI3) conditions based on the defined ranges. Each classification is color-coded and abbreviated.

Table IV.2 — RDI1 and RDI3 classification scheme

Name	Range	Number	Color	Abbreviation
Extremely Wet	2+	1	Dark Blue	EW
Very Wet	1.5 to 1.99	2	Blue	VW
Moderately Wet	1 to 1.49	3	Light Blue	MW
Near Normal	(−0.99 to 0.99)	4	color White	NM
Moderately Dry	(−1 to −1.49)	5	Yellow	MD
Severely Dry	(−1.5 to −1.99)	6	Orange	SD
Extremely Dry	(−2 and less)	7	Red	ED

IV.1.1 RDI1 analysis

RDI1 is evaluated on a monthly basis for each station. Four tables, each corresponding to a different station, present the RDI1 values. These tables include the year and month, along with the corresponding RDI1 values. The values are color-coded and abbreviated according to their classifications, as shown in IV.2. Each station's RDI1 data is also represented by a percentage circle, which illustrates the proportion of each classification within the data. This visual representation aids in understanding the distribution of drought conditions over time.

IV.1.1.1 RDI1 results and interpretation

The tables : Table IV.2, Table IV.5, Table IV.8 and Table IV.11 present the monthly RDI1 values for each station. These tables include the year and month, along with the corresponding RDI1 values. The values are color-coded and abbreviated according to their classifications, as shown in Table IV.2. Additionally, percentage circles are included to visually represent the proportion of each classification within the data, providing a clearer understanding of the distribution of drought conditions over time.

Figure IV.1, represents a graph for the monthly RDI1 values of Chlef station.

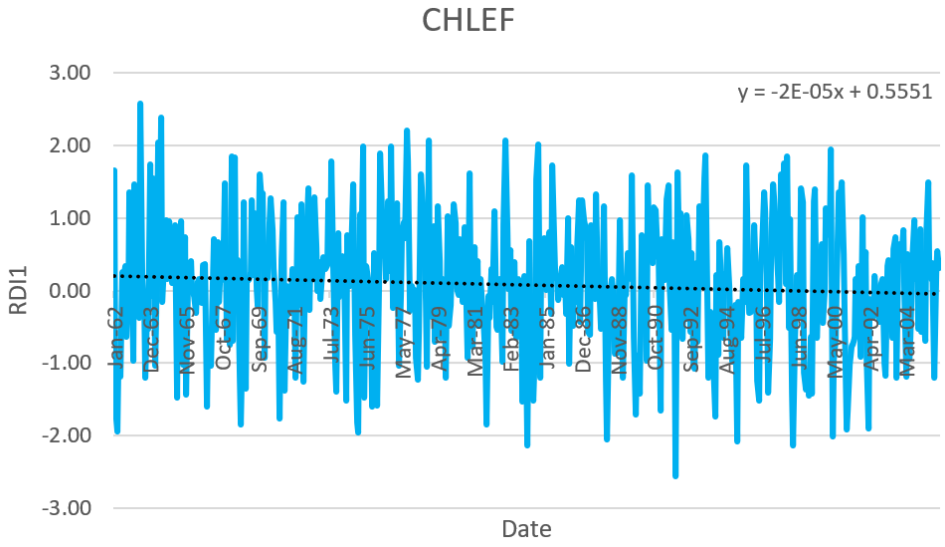

Figure IV.1 — Graph for the monthly RDI1 values for Chlef station

Table IV.2, represent monthly RDI1 values of Chlef station.

Year/Month	Jan	Feb	Mar	Apr	May	Jun	Jul	Aug	Sep	Oct	Nov	Dec
1962	VW	SD	SD	MD	MD	NM	NM	NM	NM	NM	MW	NM
1963	NM	MW	NM	NM	NM	EW	NM	NM	MD	NM	NM	VW
1964	NM	VW	MD	NM	EW	NM	EW	NM	NM	NM	NM	NM
1965	NM	NM	NM	NM	MD	NM	NM	NM	MD	NM	MD	NM
1966	NM	NM	NM	NM	NM	NM	NM	NM	NM	NM	NM	SD
1967	NM	NM	MD	NM	NM	NM	NM	NM	NM	NM	NM	MW
1968	NM	NM	NM	VW	NM	VW	NM	NM	MD	SD	NM	MW
1969	MD	NM	NM	NM	MW	NM	MW	NM	NM	VW	MW	MW
1970	NM	NM	NM	NM	MW	NM	NM	NM	NM	NM	SD	NM
1971	MW	MD	NM	NM	NM	NM	NM	NM	MD	MW	NM	NM
1972	MW	MD	NM	NM	MW	NM	NM	NM	MW	NM	NM	NM
1973	NM	NM	NM	NM	NM	MW	NM	VW	NM	MD	MD	NM
1974	NM	NM	NM	NM	SD	NM	NM	NM	NM	MW	NM	SD
1975	SD	MW	NM	VW	MD	NM	NM	NM	NM	SD	NM	NM
1976	SD	NM	VW	MW	NM	NM	NM	MW	NM	VW	NM	NM
1977	NM	MW	MD	NM	NM	NM	NM	EW	VW	NM	NM	NM
1978	NM	NM	MD	NM	VW	MW	NM	NM	MD	EW	NM	NM
1979	NM	NM	NM	MW	NM	NM	NM	NM	MD	MW	NM	NM
1980	NM	MW	NM	NM	NM	NM	NM	NM	NM	NM	NM	VW
1981	NM	NM	NM	NM	NM	NM	NM	NM	NM	NM	SD	NM
1982	NM	NM	NM	MW	NM	NM	NM	NM	NM	NM	EW	NM
1983	NM	NM	NM	NM	NM	NM	NM	NM	NM	SD	NM	NM
1984	ED	NM	NM	MD	SD	NM	VW	EW	MD	NM	NM	NM
1985	NM	NM	NM	NM	VW	NM	NM	NM	NM	NM	NM	NM
1986	NM	NM	NM	MD	NM	NM	NM	NM	NM	MW	NM	MW
1987	NM	NM	NM	NM	NM	NM	NM	NM	MW	NM	NM	NM
1988	NM	MW	MD	ED	NM	NM	NM	NM	NM	NM	NM	NM
1989	NM	MD	NM	NM	NM	NM	NM	VW	NM	SD	NM	NM
1990	MD	NM	NM	NM	NM	MW	NM	NM	NM	MW	MW	NM
1991	NM	SD	NM	NM	NM	MW	MW	NM	NM	NM	NM	ED
1992	VW	NM	MW	NM	NM	NM	MW	NM	NM	NM	MD	MD
1993	NM	NM	MW	NM	NM	VW	VW	NM	MD	NM	MD	MD
1994	SD	NM	NM	NM	NM	NM	NM	NM	NM	NM	NM	NM
1995	NM	NM	ED	NM	NM	NM	NM	NM	VW	NM	NM	NM
1996	NM	NM	NM	MD	SD	NM	NM	MW	MW	NM	MD	NM
1997	NM	MW	MW	NM	NM	NM	VW	NM	VW	NM	VW	NM
1998	NM	MD	ED	NM	NM	NM	NM	MW	MW	MD	MD	MD
1999	MD	NM	MD	MW	MW	NM	NM	NM	NM	NM	NM	MW
2000	NM	NM	VW	ED	NM	NM	NM	MW	MW	MW	NM	NM
2001	SD	SD	MD	NM	NM	NM	NM	NM	NM	NM	MW	NM
2002	NM	NM	SD	NM	NM	NM	NM	NM	NM	NM	NM	NM
2003	MD	MD	NM	NM	NM	NM	NM	NM	MD	NM	NM	NM
2004	NM	NM	MD	NM	NM	NM	NM	NM	NM	NM	NM	NM
2005	NM	NM	NM	NM	MW	NM	NM	NM	MD	NM	NM	NM

Figure IV.2 — Monthly RDI1 values for Chlef station

IV.1.1.2 The Chlef station

The calculation of the 'RDI' index on a monthly scale (1 month) for the Chlef meteorological station during the period (January 1962 to December 2005) indicates that the high values detected, representing extremely wet months, range between : 2.04 and 2.58, with June 1963 being the wettest month. The low values detected, representing extremely dry months, range between : -2.56 and -2.06, with December 1991 being the driest month detected.

The Figure IV.3 gives a visual representation to the frequency of monthly RDI1 classes for the Chlef meteorological station

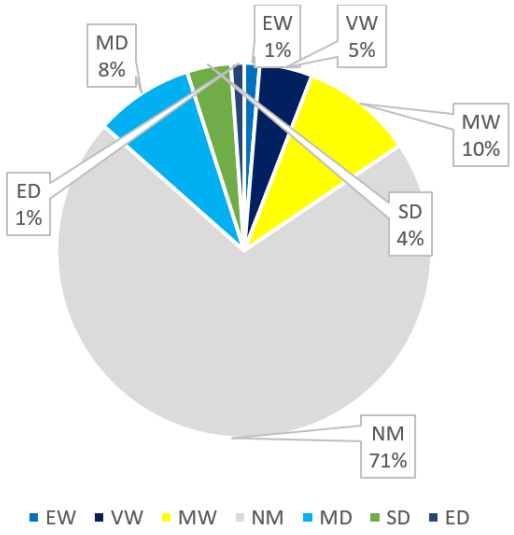

Figure IV.3 — Frequency of monthly RDI1 classes for the Chlef meteorological station

Figure IV.4, represents a graph for the monthly RDI1 values of Maghnia station.

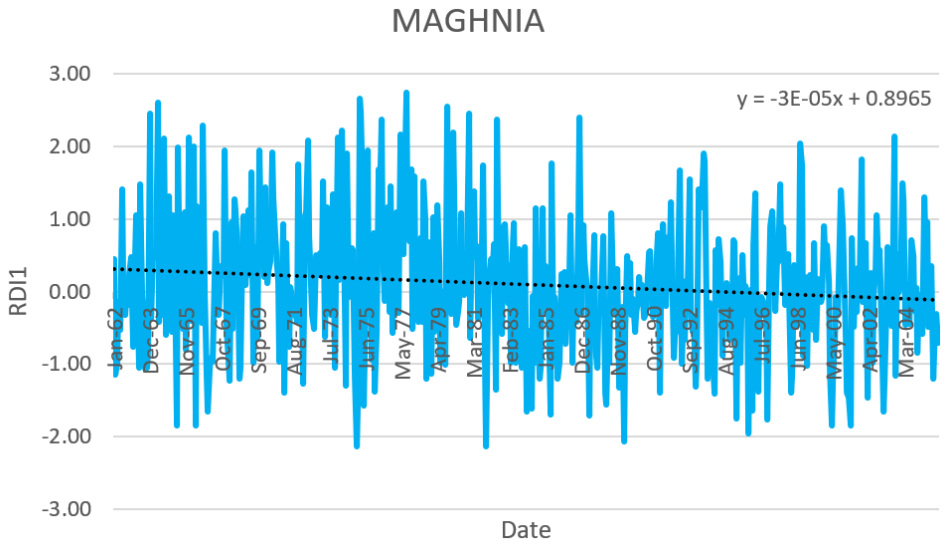

Figure IV.4 — Graph for the monthly RDI1 values for Maghnia station

Table IV.5, represent monthly RDI1 values of Maghnia station.

Year/Month	Jan	Feb	Mar	Apr	May	Jun	Jul	Aug	Sep	Oct	Nov	Dec
1962	NM	MD	NM	NM	NM	MW	NM	NM	NM	NM	NM	NM
1963	NM	NM	MW	NM	MD	MW	NM	NM	MD	MD	NM	EW
1964	NM	NM	NM	NM	EW	NM	VW	NM	EW	NM	NM	MW
1965	NM	NM	MW	NM	SD	VW	NM	NM	NM	MW	NM	NM
1966	EW	NM	NM	VW	SD	MW	NM	NM	NM	EW	NM	MD
1967	SD	MD	NM	NM	NM	NM	NM	NM	NM	NM	NM	VW
1968	NM	NM	MD	NM	NM	MW	MW	NM	MD	MD	NM	MW
1969	NM	NM	MW	NM	VW	NM	NM	NM	NM	VW	NM	NM
1970	NM	MW	NM	NM	NM	VW	MW	NM	NM	NM	NM	NM
1971	NM	MD	NM	NM	NM	NM	NM	NM	NM	NM	VW	NM
1972	NM	MD	MW	MW	EW	NM	NM	NM	NM	NM	NM	NM
1973	NM	NM	VW	NM	MW	NM	NM	NM	MW	MD	NM	EW
1974	NM	MW	EW	NM	MD	VW	NM	NM	NM	NM	MD	ED
1975	SD	EW	EW	MW	SD	NM	VW	NM	NM	NM	NM	MD
1976	NM	VW	MW	EW	NM	NM	NM	MW	NM	MW	NM	NM
1977	NM	MW	NM	EW	MW	NM	MW	EW	MW	NM	VW	NM
1978	VW	NM	NM	NM	NM	NM	VW	NM	MD	NM	NM	MD
1979	MW	NM	NM	MW	NM	NM	NM	NM	MD	EW	NM	NM
1980	NM	EW	NM	NM	NM	NM	MW	NM	NM	NM	NM	EW
1981	NM	MW	MW	NM	NM	NM	NM	NM	VW	MD	ED	NM
1982	NM	NM	NM	NM	MD	EW	NM	NM	NM	NM	NM	NM
1983	NM	NM	NM	NM	NM	NM	NM	NM	NM	MD	NM	NM
1984	SD	NM	NM	SD	NM	NM	MW	NM	MD	MD	MW	NM
1985	NM	NM	NM	SD	VW	NM	NM	NM	MD	NM	NM	NM
1986	NM	NM	NM	NM	MW	NM	NM	NM	NM	MW	EW	NM
1987	NM	NM	NM	NM	SD	NM	NM	NM	NM	MD	NM	NM
1988	NM	NM	MD	SD	NM	NM	MW	NM	NM	NM	NM	MD
1989	MD	NM	ED	NM	NM	NM	NM	NM	NM	NM	NM	NM
1990	NM	NM	NM	NM	NM	NM	NM	NM	NM	NM	NM	NM
1991	NM	MD	NM	NM	NM	NM	NM	NM	MW	NM	NM	NM
1992	NM	NM	VW	NM	NM	NM	NM	NM	VW	NM	NM	NM
1993	MD	NM	MW	MW	MW	VW	VW	NM	MD	NM	NM	NM
1994	MD	NM	NM	NM	NM	NM	NM	NM	NM	NM	NM	NM
1995	NM	NM	SD	NM	NM	NM	NM	NM	NM	NM	SD	NM
1996	SD	NM	MW	NM	MD	NM	NM	NM	NM	NM	SD	NM
1997	NM	MW	NM	NM	NM	NM	MW	NM	NM	NM	NM	NM
1998	NM	MD	MD	NM	NM	NM	NM	EW	VW	NM	NM	MD
1999	NM	NM	NM	NM	NM	NM	NM	NM	NM	NM	NM	NM
2000	NM	NM	MD	SD	MD	NM	NM	NM	NM	MW	NM	NM
2001	NM	MD	MD	SD	NM	NM	NM	NM	NM	NM	VW	NM
2002	NM	NM	MD	NM	NM	NM	NM	NM	MW	NM	NM	NM
2003	SD	MD	NM	NM	NM	NM	NM	EW	MD	NM	NM	NM
2004	MW	MW	NM	NM	NM	NM	NM	NM	NM	NM	NM	NM
2005	NM	NM	MW	NM	NM	NM	NM	NM	MD	NM	NM	NM

Figure IV.5 — Monthly RDI1 values for Maghnia station

IV.1.1.3 The Maghnia station

The calculation of the 'RDI' index on a monthly scale (1 month) for the Maghnia meteorological station during the period (January 1962 to December 2005) indicates that the high values detected, representing extremely wet months, range between : 2.11 and 2.74, with August 1977 being the wettest month. The low values detected, representing extremely dry months, range between : -2.14 and -2.07, with November 1981 and December 1974 being the two driests months detected.

The Figure IV.6 gives a visual representation to the frequency of monthly RDI1 classes for the Maghnia meteorological station

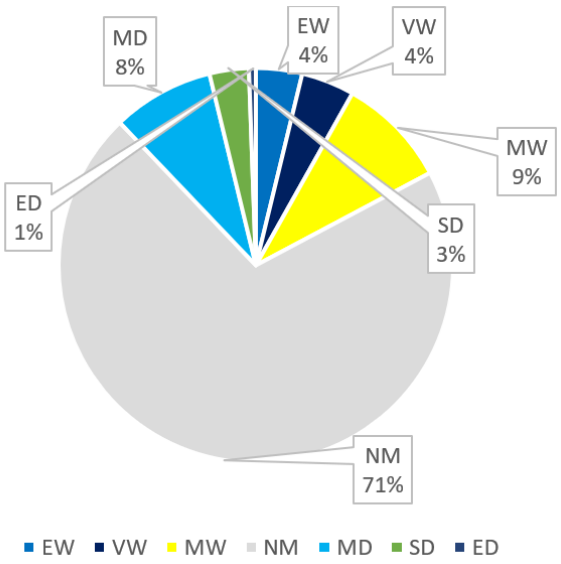

Figure IV.6 — Frequency of monthly RDI1 classes for the Maghnia meteorological station

Figure IV.7, represents a graph for the monthly RDI1 values of Oran station.

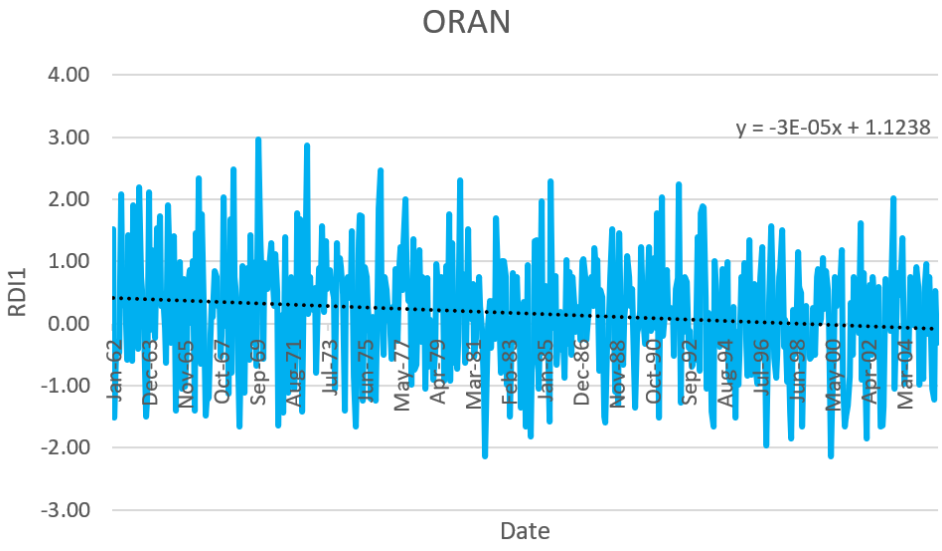

Figure IV.7 — Graph for the monthly RDI1 values for Oran station

Table IV.8, represent monthly RDI1 values of Oran station.

Year/Month	Jan	Feb	Mar	Apr	May	Jun	Jul	Aug	Sep	Oct	Nov	Dec
1962	VW	SD	NM	NM	NM	EW	NM	NM	NM	NM	MW	NM
1963	NM	VW	NM	NM	NM	EW	NM	NM	NM	MD	MD	EW
1964	NM	MW	NM	NM	VW	NM	VW	NM	NM	NM	NM	VW
1965	MW	NM	MW	MW	MD	NM	NM	NM	MD	NM	MD	NM
1966	NM	NM	NM	MW	MD	MW	NM	EW	NM	VW	NM	MD
1967	MD	MD	NM	NM	NM	NM	NM	NM	NM	NM	NM	EW
1968	NM	MW	MD	VW	NM	EW	NM	NM	NM	SD	NM	NM
1969	MD	NM	NM	NM	MW	NM	NM	NM	NM	EW	MW	NM
1970	NM	NM	NM	NM	NM	MW	NM	NM	MW	NM	SD	NM
1971	NM	MD	MW	NM	MD	NM	NM	NM	MD	NM	VW	NM
1972	VW	MD	MW	NM	EW	NM	NM	NM	NM	NM	NM	NM
1973	NM	NM	VW	NM	MW	NM	NM	NM	NM	NM	MD	MW
1974	NM	MW	NM	NM	MD	NM	NM	NM	NM	MW	NM	SD
1975	NM	MW	VW	VW	MD	NM	NM	NM	NM	MD	NM	NM
1976	MD	NM	VW	EW	NM	NM	NM	NM	NM	NM	NM	NM
1977	NM	NM	NM	NM	MW	NM	MW	VW	NM	NM	NM	NM
1978	MW	NM	NM	NM	MW	NM	NM	NM	MD	NM	NM	NM
1979	NM	NM	NM	NM	NM	NM	NM	NM	NM	NM	NM	VW
1980	NM	MW	NM	NM	NM	NM	EW	NM	NM	NM	NM	VW
1981	NM	NM	NM	NM	NM	NM	NM	NM	NM	MD	ED	NM
1982	NM	NM	NM	NM	NM	VW	NM	NM	NM	MW	MW	NM
1983	NM	NM	MD	NM	NM	NM	NM	NM	NM	MD	NM	NM
1984	SD	NM	NM	SD	NM	NM	MW	MW	MD	NM	VW	NM
1985	NM	NM	NM	SD	EW	NM	NM	NM	NM	NM	NM	NM
1986	NM	NM	MW	NM	NM	NM	NM	NM	NM	NM	NM	NM
1987	MW	MW	NM	NM	NM	NM	NM	NM	MW	NM	MW	NM
1988	NM	NM	MD	SD	NM	NM	NM	VW	NM	MD	NM	MD
1989	MW	NM	NM	NM	NM	MW	NM	NM	NM	NM	MD	NM
1990	NM	NM	MW	NM	NM	NM	NM	MW	NM	NM	MW	NM
1991	VW	SD	NM	EW	NM	NM	NM	NM	NM	NM	NM	NM
1992	NM	NM	EW	MD	NM	NM	NM	NM	NM	NM	NM	NM
1993	NM	NM	MW	NM	VW	VW	VW	NM	MD	NM	NM	MD
1994	SD	NM	NM	NM	NM	NM	NM	NM	NM	NM	NM	NM
1995	NM	NM	SD	NM	NM	NM	NM	NM	NM	NM	NM	MW
1996	NM	NM	NM	NM	NM	NM	NM	MW	NM	NM	SD	NM
1997	NM	VW	NM	NM	NM	NM	NM	NM	MW	NM	NM	NM
1998	NM	MD	SD	NM	NM	NM	MW	NM	NM	SD	NM	NM
1999	NM	NM	NM	NM	NM	NM	NM	NM	NM	NM	MW	NM
2000	NM	NM	NM	ED	MD	NM	NM	NM	NM	NM	MW	NM
2001	SD	SD	MD	NM	NM	NM	NM	NM	NM	NM	VW	NM
2002	NM	NM	SD	NM	NM	NM	NM	NM	NM	NM	NM	SD
2003	SD	MD	NM	NM	NM	NM	NM	EW	MD	NM	NM	NM
2004	NM	MW	NM	NM	NM	NM	NM	NM	NM	NM	NM	NM
2005	NM	NM	NM	NM	NM	NM	NM	NM	MD	MD	NM	NM

Figure IV.8 — Monthly RDI1 values for Oran station

IV.1.1.4 The Oran station

The calculation of the 'RDI' index on a monthly scale (1 month) for the Oran meteorological station during the period (January 1962 to December 2005) indicates that the high values detected, representing extremely wet months, range between : 2.24 and 2.95, with October 1969 being the wettest month. The low values detected, representing extremely dry months, are two months with same value : -2.14, November 1981 and April 2000 being the two driests months detected.

The Figure IV.9 gives a visual representation to the frequency of monthly RDI1 classes for the Oran meteorological station

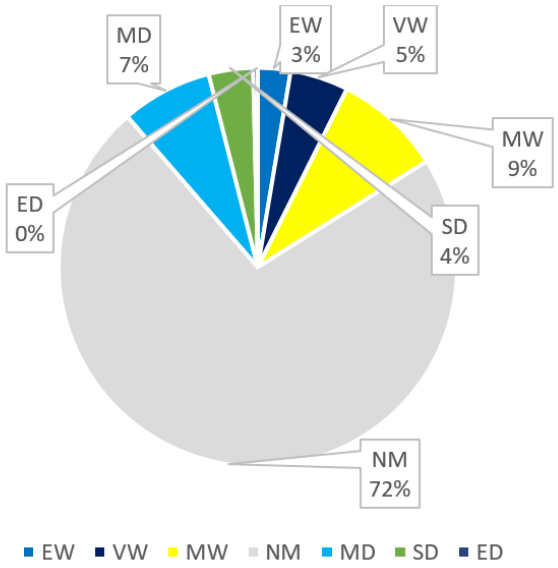

Figure IV.9 — Frequency of monthly RDI1 classes for the Oran meteorological station

Figure IV.10, represents a graph for the monthly RDI1 values of Saida station.

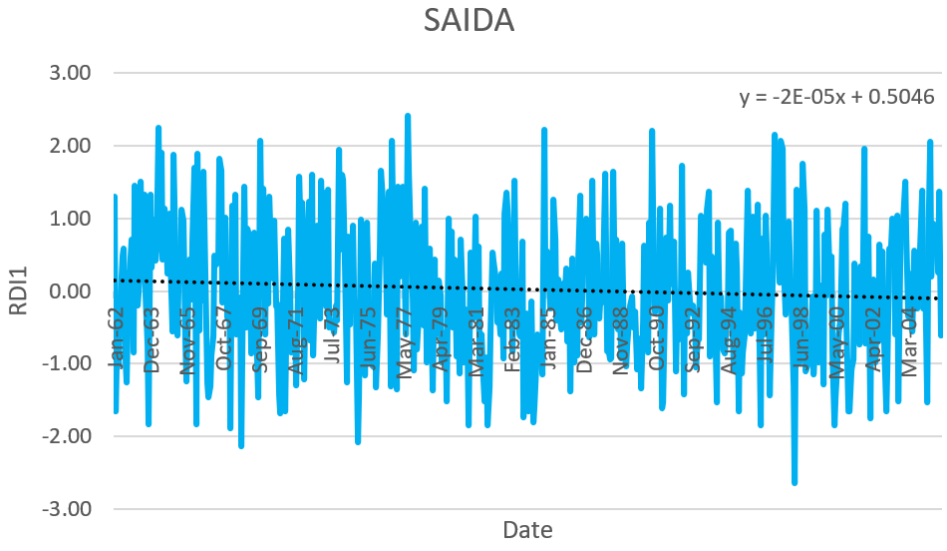

Figure IV.10 — Graph for the monthly RDI1 values for Saida station

Table IV.11, represent monthly RDI1 values of Saida station.

Year/Month	Jan	Feb	Mar	Apr	May	Jun	Jul	Aug	Sep	Oct	Nov	Dec
1962	MW	SD	NM	MD	NM	NM	NM	NM	MD	NM	NM	NM
1963	NM	MW	NM	NM	NM	VW	NM	MW	NM	NM	SD	MW
1964	NM	NM	NM	NM	EW	NM	VW	NM	MW	NM	NM	MW
1965	NM	NM	VW	NM	NM	NM	NM	MW	NM	NM	MD	NM
1966	NM	NM	NM	VW	SD	VW	NM	MW	NM	VW	NM	MD
1967	MD	MD	NM	NM	NM	NM	NM	VW	VW	NM	NM	MW
1968	NM	NM	SD	MW	NM	MW	NM	NM	NM	ED	NM	MW
1969	NM	NM	NM	NM	NM	NM	NM	NM	MD	EW	NM	MW
1970	NM	NM	NM	MW	NM	NM	NM	NM	NM	MD	SD	NM
1971	NM	SD	NM	NM	NM	NM	NM	NM	MD	NM	VW	NM
1972	MW	MD	NM	NM	MW	NM	VW	NM	NM	NM	NM	NM
1973	VW	NM	MW	NM	MW	NM	NM	NM	NM	NM	NM	VW
1974	NM	VW	VW	NM	MD	NM	NM	NM	NM	NM	NM	ED
1975	MD	NM	NM	NM	MD	NM	NM	NM	NM	MD	NM	MD
1976	NM	NM	VW	MW	NM	NM	NM	MW	MD	EW	NM	NM
1977	MD	MW	NM	MW	MW	NM	NM	EW	VW	NM	NM	MD
1978	NM	NM	NM	NM	NM	NM	MW	NM	NM	NM	NM	MD
1979	NM	NM	NM	NM	NM	NM	NM	NM	SD	NM	NM	NM
1980	NM	NM	NM	NM	MD	NM	NM	NM	NM	NM	SD	NM
1981	NM	NM	MW	NM	NM	NM	NM	NM	SD	NM	SD	MD
1982	NM	NM	NM	NM	NM	NM	NM	NM	NM	MW	MW	NM
1983	NM	NM	NM	VW	NM	NM	NM	NM	NM	SD	MD	NM
1984	SD	NM	NM	SD	SD	NM	NM	NM	NM	MD	EW	NM
1985	NM	NM	NM	NM	MW	NM	NM	NM	NM	NM	NM	NM
1986	NM	NM	NM	MD	NM	NM	NM	NM	NM	MW	NM	NM
1987	NM	MW	NM	NM	NM	VW	NM	NM	NM	NM	NM	NM
1988	NM	VW	NM	NM	NM	NM	VW	NM	NM	NM	NM	NM
1989	NM	NM	MD	NM	NM	NM	NM	NM	NM	MD	NM	NM
1990	MD	NM	NM	NM	NM	NM	NM	EW	NM	NM	NM	NM
1991	MW	SD	SD	NM	NM	NM	MW	NM	NM	NM	MD	NM
1992	NM	NM	VW	MD	NM	NM	NM	NM	NM	NM	NM	MD
1993	NM	NM	MW	NM	NM	NM	MW	MW	NM	NM	NM	NM
1994	SD	NM	NM	NM	NM	NM	NM	NM	NM	NM	NM	MD
1995	NM	NM	SD	NM	MD	NM	NM	NM	MW	NM	NM	MW
1996	NM	NM	MW	NM	SD	NM	NM	MW	NM	NM	MD	NM
1997	NM	EW	MW	NM	NM	EW	VW	NM	NM	NM	NM	NM
1998	NM	MD	ED	MW	NM	NM	NM	VW	MW	MD	MD	NM
1999	NM	NM	MD	NM	MW	NM	NM	NM	MD	NM	NM	MW
2000	NM	NM	NM	SD	MD	NM	NM	NM	NM	NM	MW	NM
2001	SD	SD	MD	NM	NM	NM	NM	NM	NM	NM	VW	NM
2002	NM	NM	SD	NM	NM	NM	NM	NM	NM	NM	NM	NM
2003	SD	MD	NM	NM	NM	NM	NM	MW	SD	NM	NM	MW
2004	VW	NM	NM	NM	NM	NM	NM	NM	NM	NM	NM	MW
2005	NM	NM	SD	NM	EW	NM	NM	NM	NM	NM	MW	NM

Figure IV.11 — Monthly RDI1 values for Saida station

IV.1.1.5 The Saida station

The calculation of the 'RDI' index on a monthly scale (1 month) for the Saida meteorological station during the period (January 1962 to December 2005) indicates that the high values detected, representing extremely wet months, range between : 2.07 and 2.41, with August 1977 being the wettest month. The low values detected, representing extremely dry months, range between : -2.64 and -2.08, with March 1998 being the driest month detected.

The Figure IV.12 gives a visual representation to the frequency of monthly RDI1 classes for the Saida meteorological station

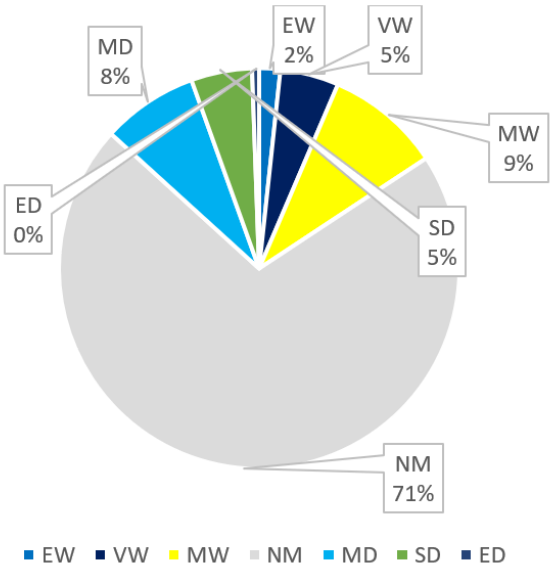

Figure IV.12 — Frequency of monthly RDI1 classes for the Saida meteorological station

IV.1.2 RDI3 analysis

RDI3 is assessed on a seasonal basis. A single table presents the RDI3 values for each year and season. The seasons are defined and classified in Table IV.1, with color codes and abbreviations indicating the RDI3 values for each season, as shown in Table A. Each station's RDI3 data is also represented by a percentage circle, which illustrates the proportion of each classification within the data. This visual representation aids in understanding the distribution of drought conditions over time. The seasonal RDI3 table provides a comprehensive view of drought conditions over the longer term, complementing the monthly analysis provided by RDI1.

IV.1.2.1 RDI3 results and interpretation

The Table IV.13 presents the seasonal RDI3 values for each year and season. The values are color-coded and abbreviated according to their classifications, as shown in Table IV.2. Percentage circles are also included to provide a visual representation of the proportion of each classification within the data, enhancing the understanding of drought conditions over time.

Additionally, graphs representing the RDI3 values for each month are included. These graphs display the RDI3 value for each month over time and include a trend line to

illustrate any tendencies towards dry or wet weather. Similar to RDI1, the slope of the trend line indicates whether there is a tendency towards drier or wetter conditions over time.

Table IV.13, represent seasonal RDI3 values of Chlef, Maghnia, Oran and Saida stations.

\Station	CHLEF				MAGHNIA				ORAN				SAIDA			
Year\Season	1	2	3	4	1	2	3	4	1	2	3	4	1	2	3	4
1962	NM	NM	ED	NM	NM	MD	NM	MW	NM	NM	NM	VW	NM	NM	NM	NM
1963	NM	MW	NM	VW	SD	NM	NM	MW	SD	NM	NM	VW	SD	NM	NM	VW
1964	NM	EW	NM	NM	NM	VW	VW	NM	NM	VW	NM	NM	NM	MW	VW	MW
1965	NM	NM	NM	NM	NM	NM	NM	VW	NM	VW	NM	NM	NM	NM	MW	NM
1966	NM	NM	NM	NM	VW	MW	NM	NM	MW	NM	NM	EW	MW	NM	NM	VW
1967	NM	ED	NM	NM	NM	ED	MD	NM	NM	ED	NM	NM	NM	ED	NM	MW
1968	SD	NM	NM	MW	NM	NM	NM	MW	MD	VW	NM	EW	NM	NM	NM	NM
1969	VW	NM	NM	NM	MW	NM	MW	NM	EW	NM	NM	NM	MW	NM	NM	NM
1970	SD	NM	NM	NM	NM	MW	NM	EW	NM	NM	NM	MW	ED	NM	NM	NM
1971	NM	NM	NM	NM	NM	NM	NM	NM	NM	NM	NM	NM	NM	NM	NM	MD
1972	NM	NM	MW	NM	NM	NM	VW	NM	NM	NM	EW	NM	NM	NM	MW	NM
1973	SD	NM	NM	VW	NM	NM	NM	NM	NM	NM	MW	NM	NM	NM	MW	MD
1974	NM	NM	NM	NM	NM	EW	MW	VW	NM	MW	NM	NM	NM	EW	NM	NM
1975	NM	NM	MW	NM	NM	MW	VW	NM	NM	NM	VW	NM	NM	NM	NM	NM
1976	MW	NM	VW	NM	NM	NM	EW	NM	NM	NM	EW	NM	VW	NM	VW	NM
1977	NM	NM	NM	VW	VW	MW	VW	VW	NM	NM	NM	VW	NM	NM	MW	VW
1978	MW	NM	NM	NM	NM	NM	NM	NM	NM	NM	NM	NM	NM	NM	NM	NM
1979	NM	NM	NM	MD	VW	NM	NM	MD	NM	NM	NM	NM	NM	NM	NM	SD
1980	NM	NM	NM	NM	NM	MW	NM	NM	NM	MW	MD	NM	ED	NM	MD	NM
1981	ED	NM	NM	NM	NM	EW	MW	MD	ED	MW	NM	NM	ED	NM	NM	SD
1982	VW	NM	NM	NM	NM	NM	NM	EW	NM	NM	NM	MW	MW	NM	NM	NM
1983	NM	NM	NM	NM	MD	NM	NM	NM	MD	NM	NM	NM	MD	NM	NM	NM
1984	NM	NM	MD	MW	NM	NM	MD	NM	MW	NM	ED	NM	NM	SD	SD	SD
1985	NM	NM	MW	NM	NM	NM	NM	SD	NM	NM	NM	NM	NM	NM	NM	NM
1986	NM	NM	NM	NM	EW	NM	NM	SD	NM	MD	NM	MD	NM	NM	NM	MD
1987	NM	VW	NM	NM	MD	NM	NM	NM	MW	NM	NM	NM	NM	MW	NM	MW
1988	MD	NM	ED	NM	NM	NM	SD	NM	NM	NM	SD	NM	NM	NM	SD	NM
1989	SD	NM	NM	NM	NM	MD	NM	NM	MD	NM	NM	NM	SD	NM	MD	NM
1990	MW	NM	NM	MW	NM	NM	NM	NM	NM	NM	NM	NM	NM	MD	NM	VW
1991	NM	NM	NM	MW	NM	NM	NM	NM	NM	NM	MW	NM	NM	NM	NM	NM
1992	NM	NM	NM	NM	NM	NM	NM	NM	NM	NM	MW	NM	NM	NM	NM	NM
1993	MD	MD	NM	MW	MD	SD	VW	VW	NM	MD	MW	EW	NM	MD	MW	MW
1994	NM	SD	NM	NM	NM	NM	NM	MD	NM	NM	NM	NM	NM	NM	NM	MD
1995	NM	MD	SD	MD	MD	NM	MD	MD	NM	NM	MD	NM	NM	NM	SD	NM
1996	NM	NM	MD	NM	SD	NM	NM	NM	ED	NM	NM	NM	NM	NM	NM	NM
1997	VW	NM	NM	NM	NM	NM	NM	NM	NM	NM	NM	NM	NM	MW	NM	VW
1998	NM	NM	MD	NM	NM	NM	NM	NM	NM	MD	MD	NM	NM	NM	NM	NM
1999	NM	ED	MW	MD	NM	NM	NM	NM	NM	NM	NM	NM	NM	MD	NM	NM
2000	MW	MW	NM	NM	MW	NM	ED	MD	MW	NM	MD	MD	MW	NM	ED	SD
2001	NM	ED	SD	MD	MW	NM	NM	MD	MW	ED	MD	MD	NM	ED	NM	NM
2002	NM	NM	MD	NM	NM	NM	NM	NM	NM	NM	NM	MD	NM	NM	NM	SD
2003	NM	SD	NM	NM	NM	ED	NM	NM	NM	ED	NM	NM	NM	ED	NM	NM
2004	NM	NM	NM	NM	NM	MW	NM	NM	NM	MW	MD	MD	NM	VW	NM	NM
2005	NM	NM	NM	NM	MD	NM	MW	NM	NM	NM	NM	NM	NM	NM	NM	NM

Figure IV.13 — Seasoned RDI3 values for stations : Chlef, Maghnia, Oran and Saida

Figure IV.14, represents a graph for the monthly RDI3 values of Chlef station.

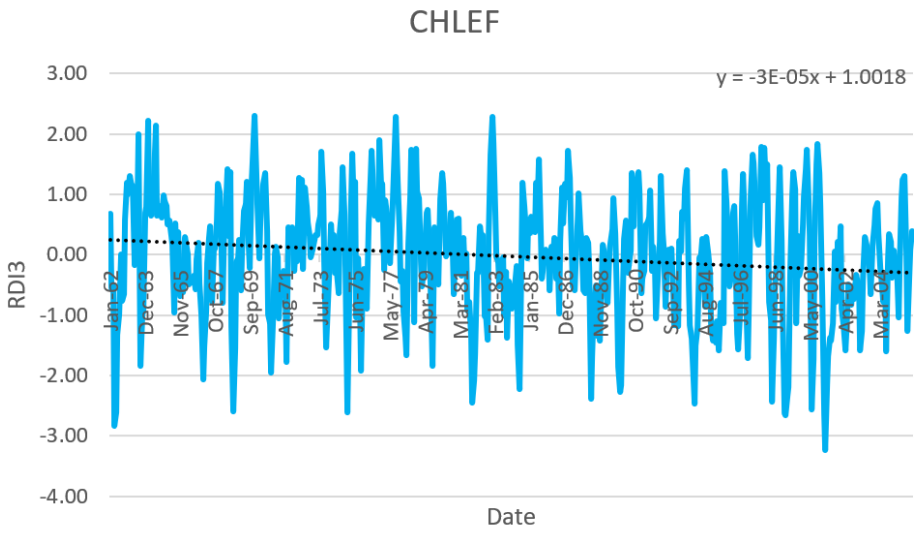

Figure IV.14 — Monthly RDI3 values for Chlef station

Figure IV.15, represents a graph for the monthly RDI3 values of Maghnia station.

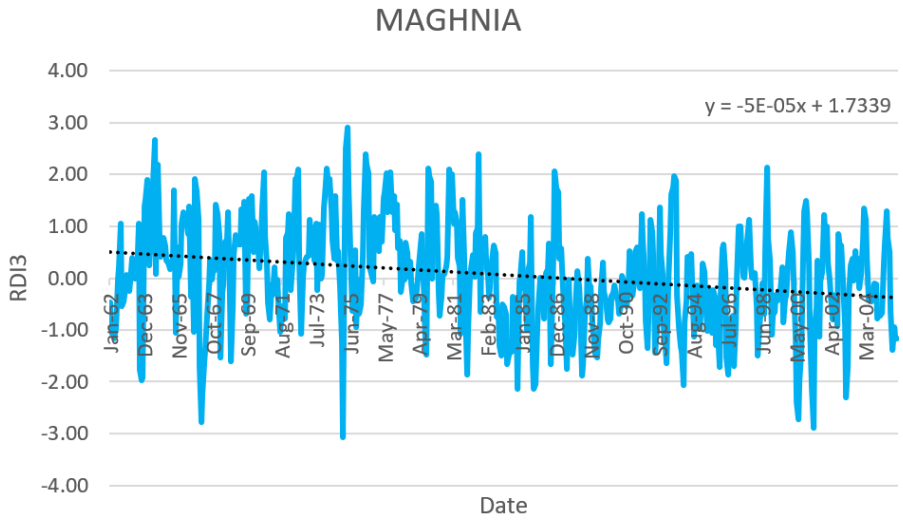

Figure IV.15 — Monthly RDI3 values for Maghnia station

Figure IV.16, represents a graph for the monthly RDI3 values of Oran station.

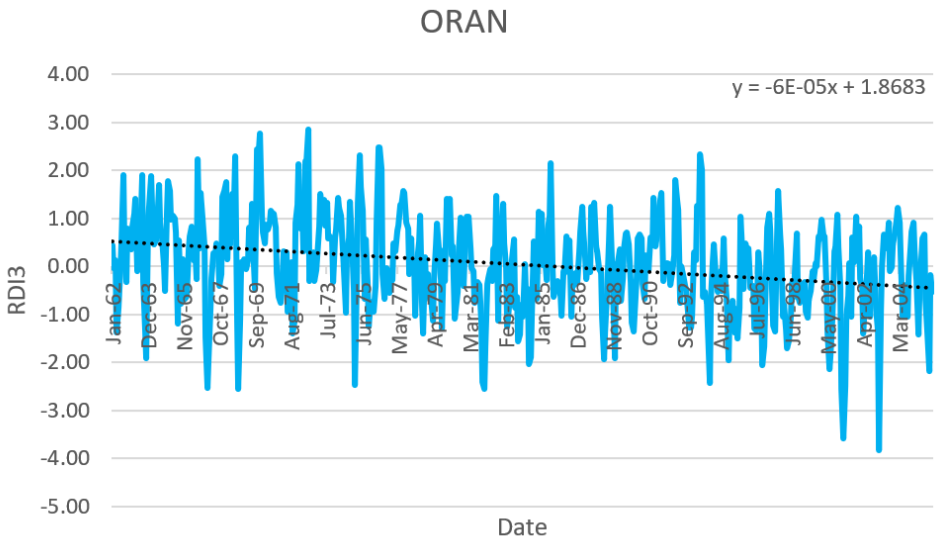

Figure IV.16 — Monthly RDI3 values for Oran station

Figure IV.17, represents a graph for the monthly RDI3 values of Saida station.

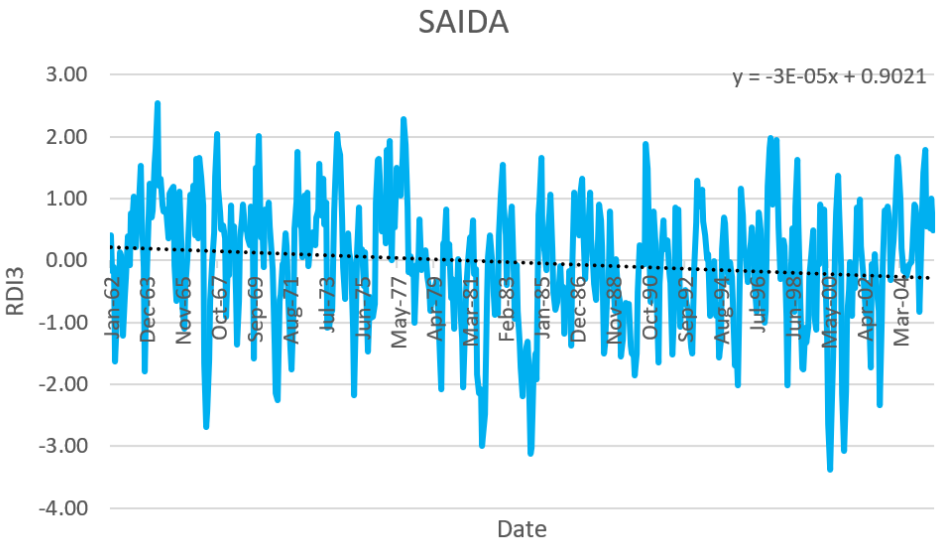

Figure IV.17 — Monthly RDI3 values for Saida station

IV.1.2.2 RDI3 of Chlef, Maghnia, Oran and Saida stations

The computation of the 'RDI' index on a seasonal scale (3 months) spanning from January 1962 to December 2005 for each meteorological station reveals distinct patterns.

For the Chlef station, the analysis indicates that the range of high values, representing extremely wet seasons, falls between 2 and 2.22. The wettest season was observed in second season, 1964. Conversely, the range of low values, indicative of extremely dry seasons, varies from -2.06 to -2.64, with second season, 2001 being identified as the driest

season.

Similarly, for the Maghnia station, the analysis indicates that the range of high values, representing extremely wet seasons, falls between 2.07 and 2.4. The wettest season was observed in fourth season, 1982. Conversely, the range of low values, indicative of extremely dry seasons, varies from -2.4 to -2.77, with second season, 1967 being identified as the driest season.

Likewise, for the Oran station, the analysis indicates that the range of high values, representing extremely wet seasons, falls between 2 and 2.48. The wettest season was observed in third season, 1976. Conversely, the range of low values, indicative of extremely dry seasons, varies from -2.04 to -3.84, with second season, 2003 being identified as the driest season.

Lastly, for the Saida station, the analysis indicates that the high value, representing extremely wet season, is 2.04. This wettest season was observed in second season, 1974. Conversely, the range of low values, indicative of extremely dry seasons, varies from -2.04 to -3, with first season, 1981 being identified as the driest season.

These findings provide valuable insights into the variability of wet and dry seasons across the different meteorological stations.

The Figure IV.18 gives a visual representation to the frequency of seasonal RDI3 classes for the Chlef meteorological station

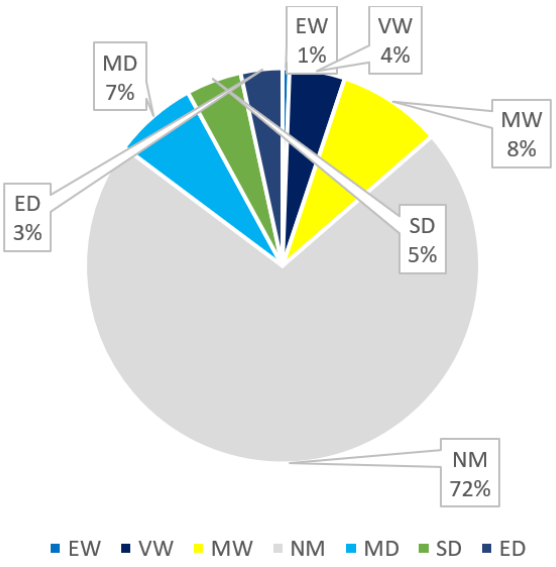

Figure IV.18 — Frequency of seasonal RDI3 classes for the Chlef meteorological station

The Figure IV.19 gives a visual representation to the frequency of seasonal RDI3 classes for the Maghnia meteorological station

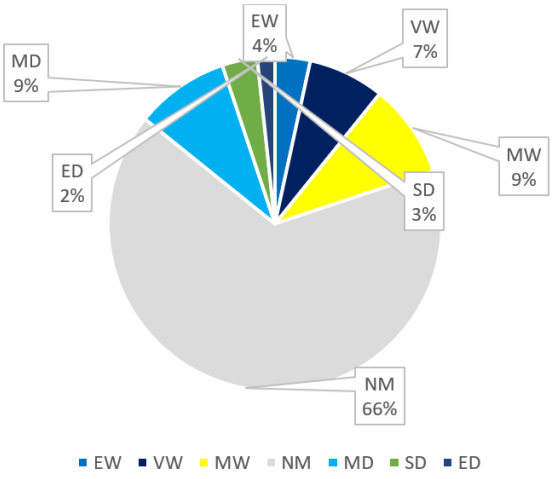

Figure IV.19 — Frequency of seasonal RDI3 classes for the Maghnia meteorological station

The Figure IV.20 gives a visual representation to the frequency of seasonal RDI3 classes for the Saida meteorological station

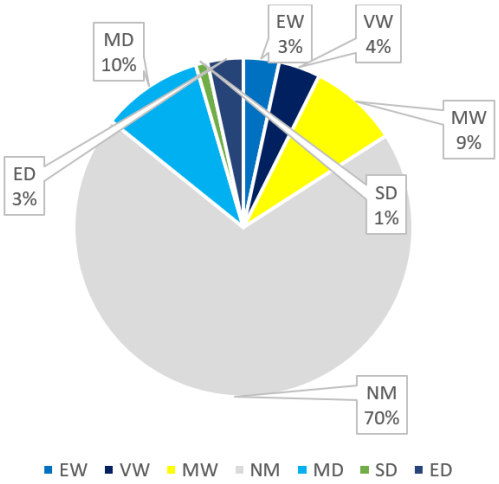

Figure IV.20 — Frequency of seasonal RDI3 classes for the Oran meteorological station

The Figure IV.21 gives a visual representation to the frequency of seasonal RDI3 classes for the Oran meteorological station

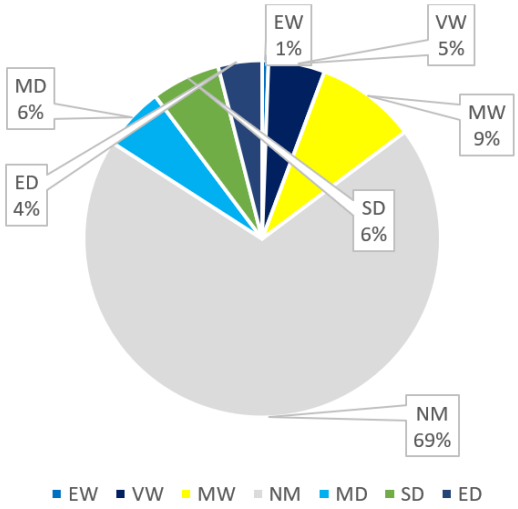

Figure IV.21 — Frequency of seasonal RDI3 classes for the Saida meteorological station

IV.2 Atmospheric Circulation Indices analysis

In this section, we delve into the analysis of atmospheric circulation indices (ACIs) and their relationship with drought indices, aiming to gain deeper insights into the dynamics of drought occurrence and its potential atmospheric drivers. The analysis focuses on two series : ACI1 and ACI3, examining their correlations with the corresponding drought indices, RDI1 and RDI3.

IV.2.1 Correlation analysis between atmospheric and drought indices

The correlation analysis serves as a pivotal component in understanding the interplay between atmospheric circulation patterns and drought occurrence. By quantifying the relationship between atmospheric circulation indices and drought indices, we gain valuable insights into the potential influence of large-scale atmospheric processes on regional drought conditions.

Figure IV.22, represent the correlation between ACI1 and RDI1

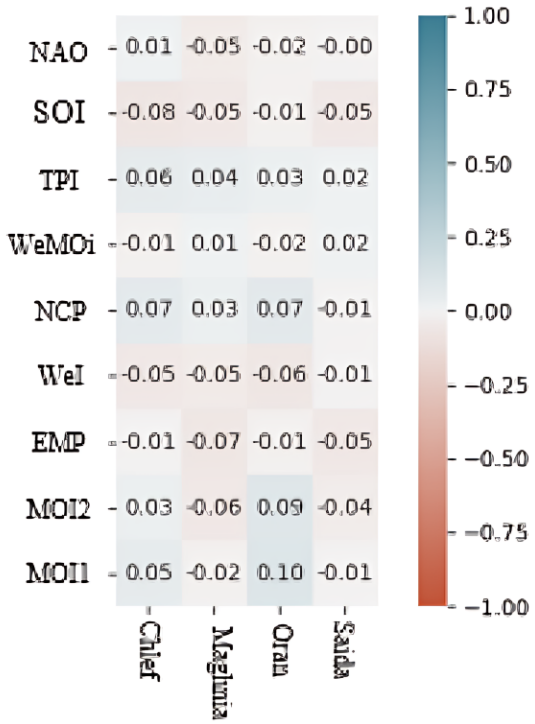

Figure IV.22 — Correlation between ACI1 and RDI1

Figure IV.23, represent the correlation between ACI3 and RDI3

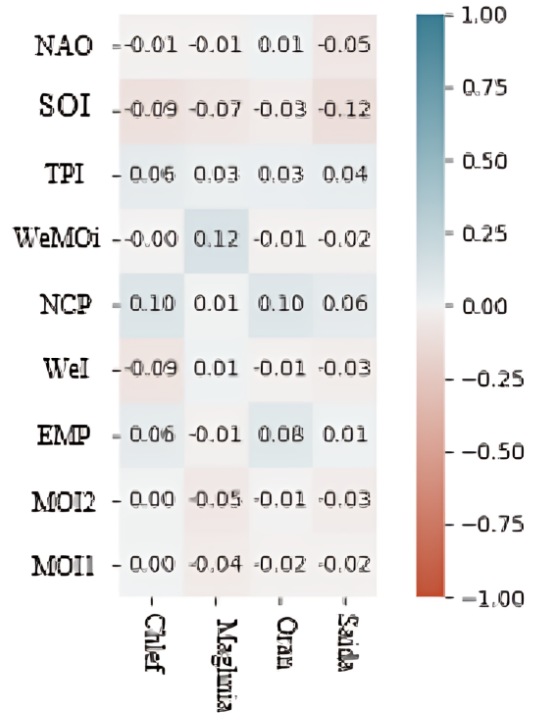

Figure IV.23 — Correlation between ACI3 and RDI3

The absence of a significant correlation between ACI1 and RDI1 suggests that the atmospheric circulation patterns represented by ACI1 may not directly influence the monthly variations in drought severity captured by RDI1. This finding indicates that other factors or local-scale dynamics may play a more dominant role in driving monthly drought conditions at the study area.

Similarly, the lack of a significant correlation between ACI3 and RDI3 implies that the seasonal atmospheric circulation patterns characterized by ACI3 may not be strongly associated with the longer-term drought conditions captured by RDI3. This suggests that broader climatic factors or regional-scale processes might be more influential in shaping the multi-seasonal variability of drought occurrences.

In both cases, it's essential to acknowledge the complexity of drought dynamics and recognize that the absence of correlation does not necessarily negate the potential influence of atmospheric circulation patterns on drought. Other factors, such as local geography, land surface characteristics, and anthropogenic influences, could also contribute to the observed drought variability. Further investigation into these factors may provide a more comprehensive understanding of drought dynamics in the study area.

IV.3 Model performance : Random Forest performance

In this section, we present the performance evaluation of the Random Forest model for each meteorological station. The evaluation is based on key performance metrics, including accuracy and ROC-AUC values, providing insights into the model's ability to accurately classify drought conditions.

IV.3.1 Model performance by station

For each meteorological station (Saida, Chlef, Maghnia, and Oran), the Random Forest model's performance is evaluated based on accuracy and ROC-AUC values. The results are summarized in Table IV.3 and Table IV.4.

Table IV.3 — Accuracy scores for Random Forest model for the stations : Chlef, Maghnia, Oran and Saida

Model/Station	**CHLEF**	**MAGHNIA**	**ORAN**	**SAIDA**
RDI1 accuracy				
Random forest	0.7	0.77	0.67	0.7
RDI3 accuracy				
Random forest	0.69	0.67	0.69	0.74

Table IV.4 — AUC-ROC scores for Random Forest model for the stations : Chlef, Maghnia, Oran and Saida

Model/Station	CHLEF	MAGHNIA	ORAN	SAIDA
RDI1 AUC-ROC				
Random forest	0.65	0.56	0.51	0.55
RDI3 AUC-ROC				
Random forest	0.55	0.55	0.5	0.53

These metrics provide insights into the model's performance across different stations, aiding in the assessment of its effectiveness in classifying drought conditions in north west of Algeria.

IV.4 Variable importance

In this section, we present the variable importance analysis for each station based on the models developed using the two series : ACI1, RDI1 and ACI3, RDI3. Understanding the importance of each variable helps in identifying which factors contribute the most to the model's predictions, providing insights into the underlying mechanisms driving the observed phenomena.

IV.4.1 ACI1 and RDI1 series

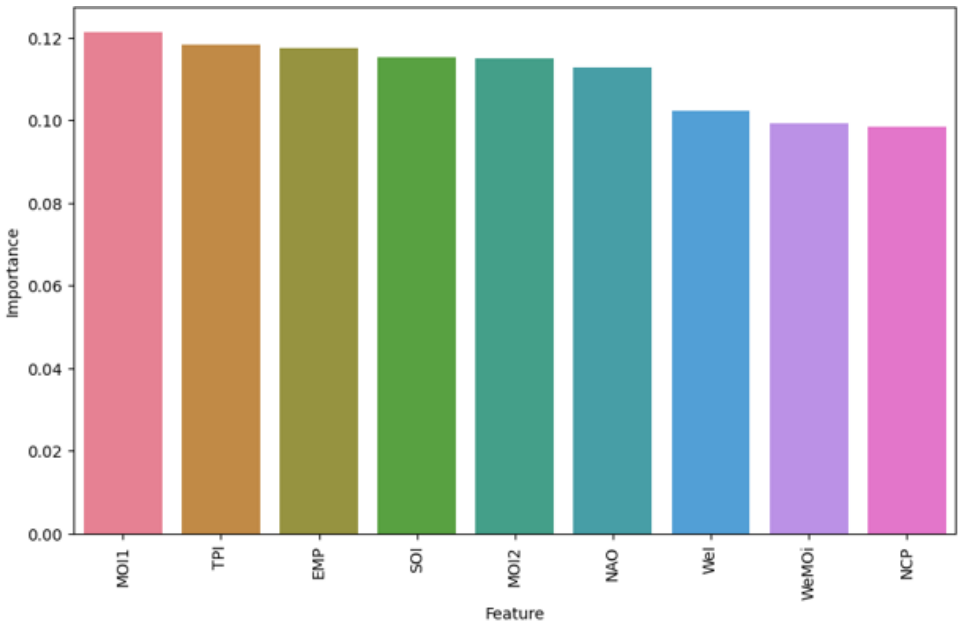

Figure IV.24 — Feature importance for series 1 at Chlef station

The first set of models was developed using the ACI1 and RDI1 series. Feature importance scores were computed to evaluate the contribution of each variable to the model's performance. Figures IV.24, IV.25, IV.26, and IV.27 illustrate the feature importance for Chlef, Maghnia, Oran, and Saida, respectively.

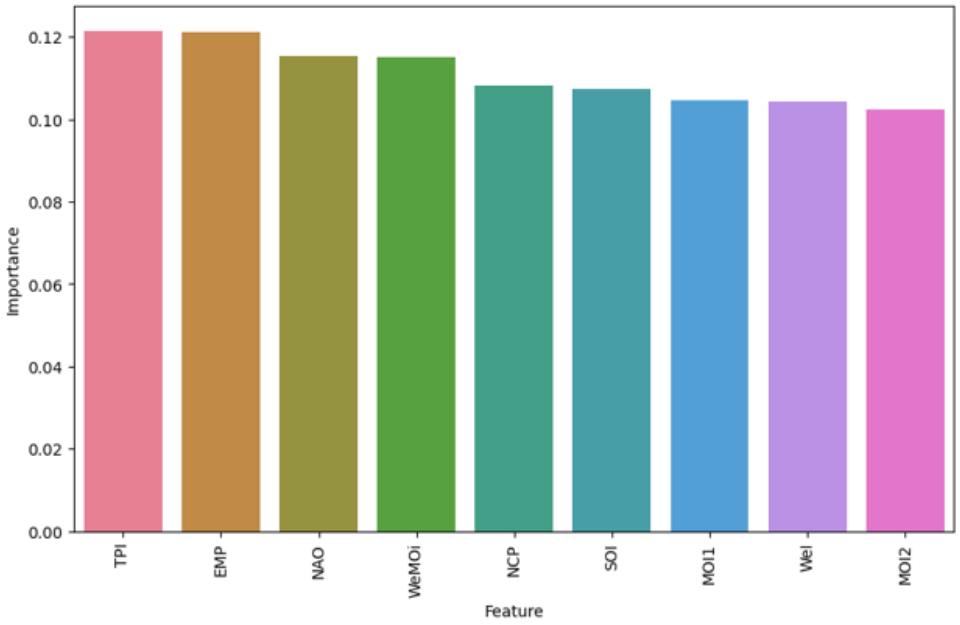

Figure IV.25 — Feature importance for series 1 at Maghnia station

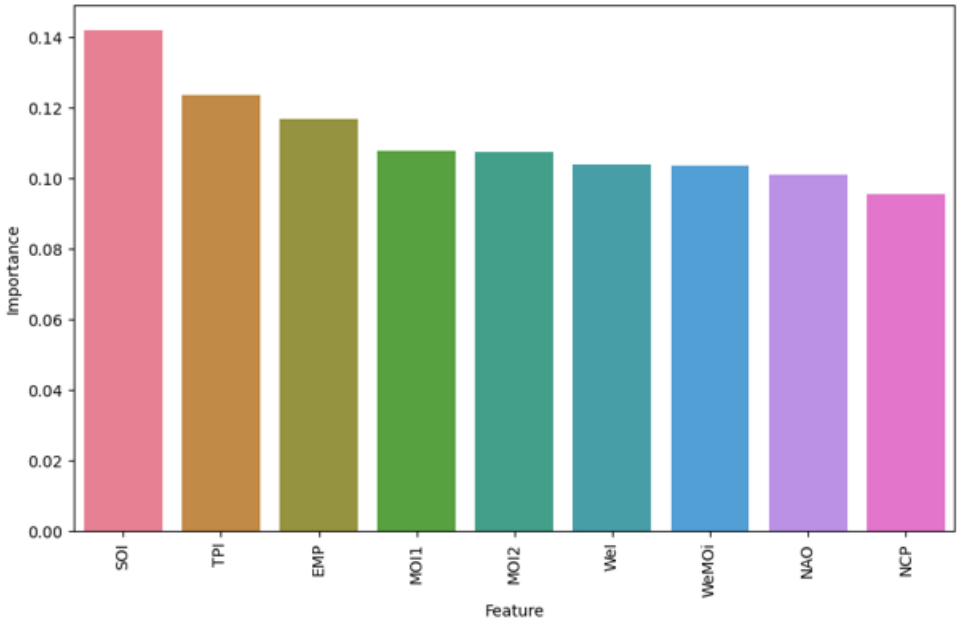

Figure IV.26 — Feature importance for series 1 at Oran station

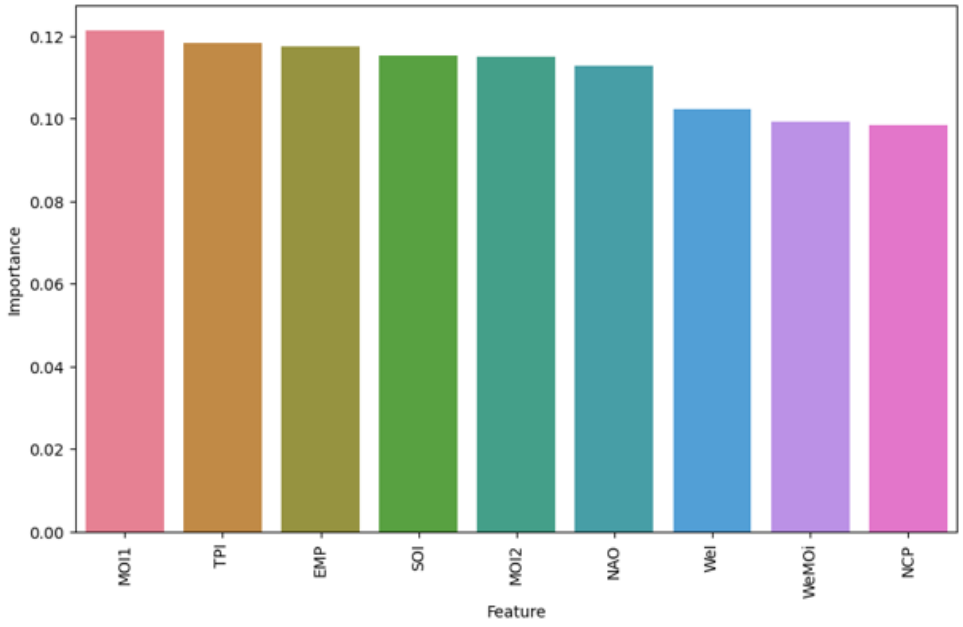

Figure IV.27 — Feature importance for series 1 at Saida station

IV.4.2 ACI3 and RDI3 series

Similarly, the second set of models was developed using the ACI3 and RDI3 series. Feature importance scores for this series were also computed to identify the key variables influencing the model's predictions. Figures IV.28, IV.29, IV.30, and IV.31 display the feature importance for Chlef, Maghnia, Oran, and Saida, respectively.

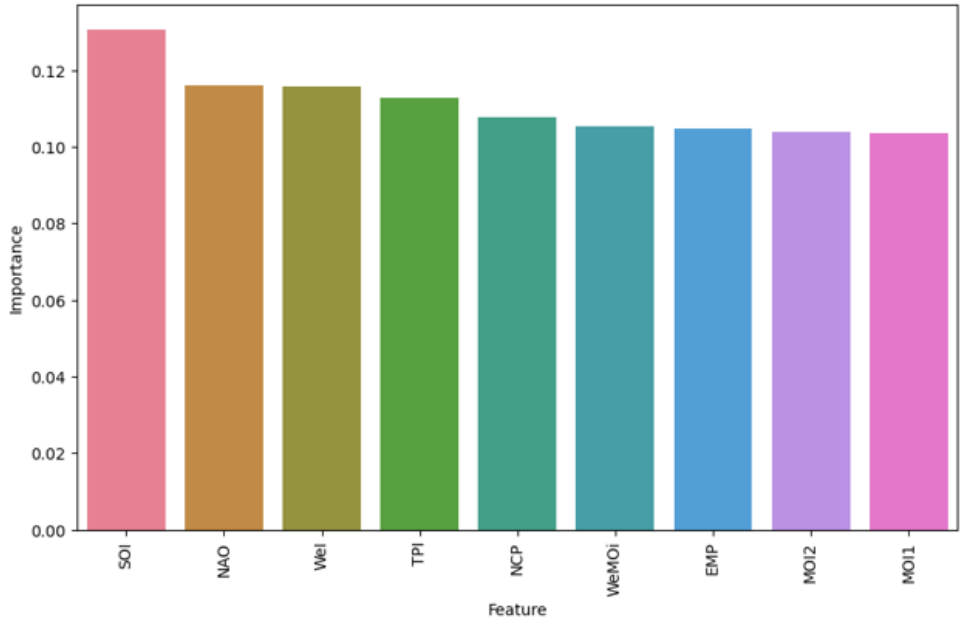

Figure IV.28 — Feature importance for series 2 at Chlef station

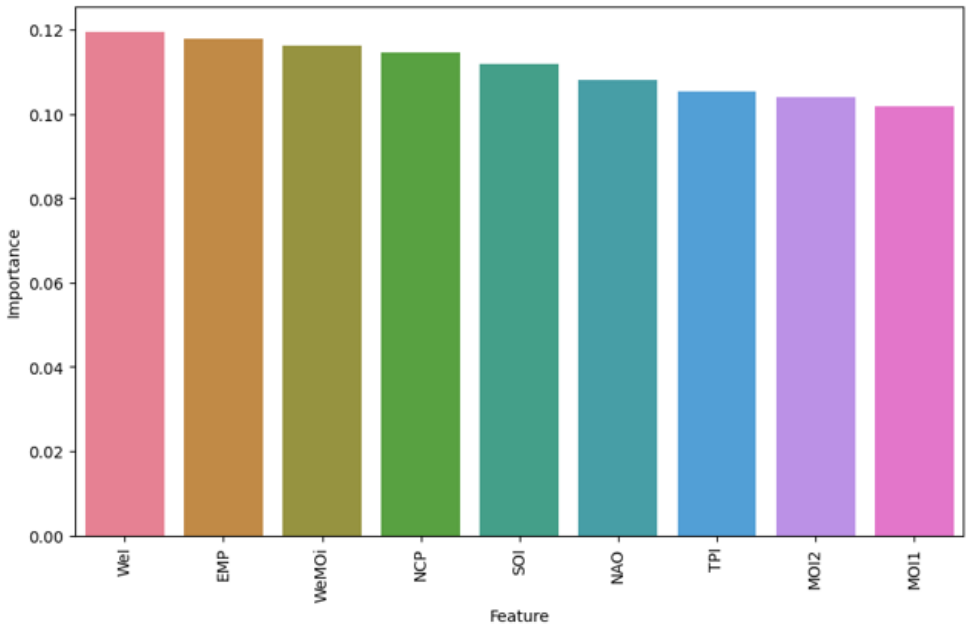

Figure IV.29 — Feature importance for series 2 at Maghnia station

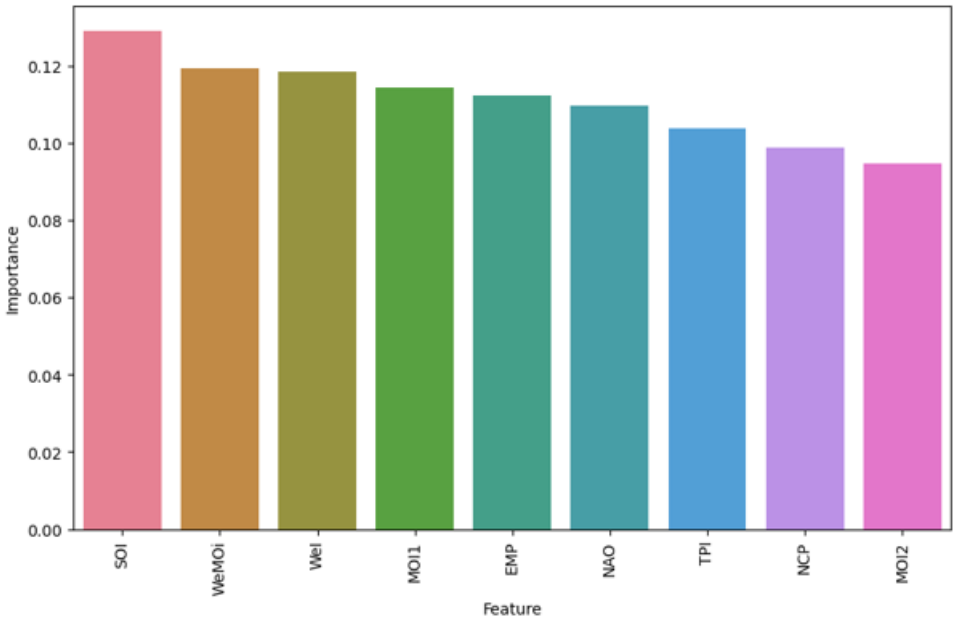

Figure IV.30 — Feature importance for series 2 at Oran station

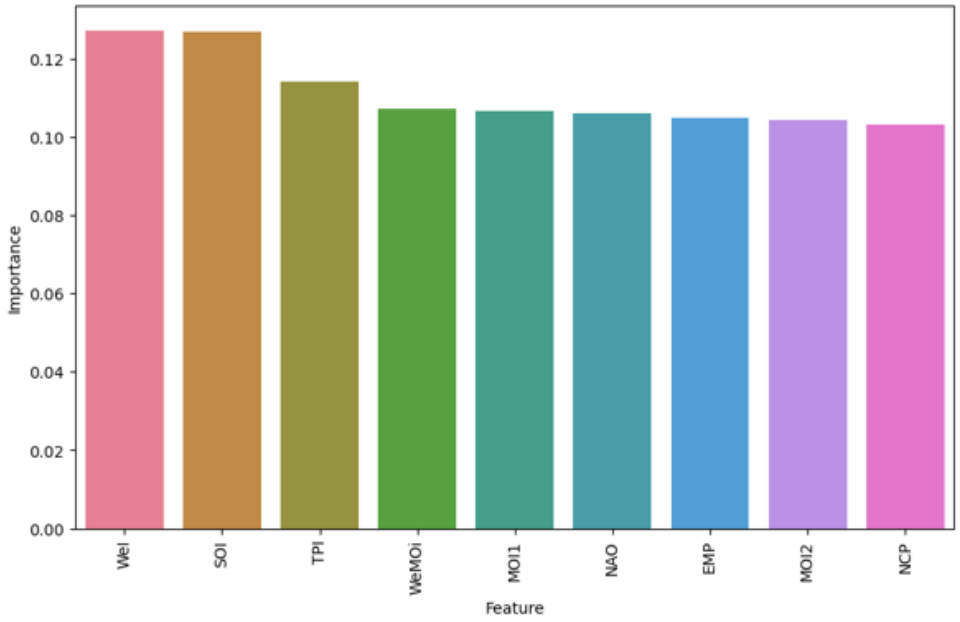

Figure IV.31 — Feature importance for series 2 at Saida station

IV.4.3 Interpretation

The feature importance results reveal which variables are most influential in predicting drought conditions at each station. High importance scores indicate that a variable significantly contributes to the model's predictive power. By examining these scores, we can gain a deeper understanding of the factors driving drought variability and improve our predictive models.

- For Chlef, the most important features in the ACI1 and RDI1 model are MOI1, TPI, and EMP (refer to Figure IV.24). In the ACI3 and RDI3 model, the key features are SOI, NAO, and WeI (refer to Figure IV.28).
- For Maghnia, the top contributing variables in the ACI1 and RDI1 model are TPI, EMP, and NAO (refer to Figure IV.25). In the ACI3 and RDI3 model, significant features include WeI, EMP, and WeMOi (refer to Figure IV.29).
- For Oran, important features in the ACI1 and RDI1 model are SOI, TPI, and EMP (refer to Figure IV.26). In the ACI3 and RDI3 model, the influential variables are SOI, WeMOi, and WeI (refer to Figure IV.30).
- For Saida, the most impactful variables in the ACI1 and RDI1 model are MOI1, TPI, and EMP (refer to Figure IV.27). In the ACI3 and RDI3 model, the top features are WeI, SOI, and TPI (refer to Figure IV.31).

Overall, the feature importance analysis provides valuable insights into the relative contribution of each variable in predicting drought conditions across different stations.

These findings can guide future research and model development, helping to enhance our understanding and management of drought risks.

Conclusion

The results of our analysis reveal significant patterns and insights into drought conditions across the four meteorological stations in northwestern Algeria. The monthly and seasonal RDI assessments highlight distinct wet and dry periods, with notable variability across different seasons and years. The Random Forest model demonstrates varying levels of accuracy and discrimination performance across the stations, with generally moderate accuracy but lower ROC-AUC scores, indicating room for improvement in model performance.

The feature importance analysis further elucidates the key variables influencing drought conditions, with notable differences observed between the stations. Variables such as TPI, EMP, SOI, NAO, and WeI consistently emerge as significant contributors, underscoring the complex interplay of atmospheric and environmental factors driving drought variability.

Overall, this comprehensive analysis enhances our understanding of drought dynamics in the region, providing valuable insights for improving drought prediction models and informing effective drought management strategies. Further research integrating additional variables and refining model algorithms could yield even more robust predictive capabilities, ultimately aiding in the mitigation of drought impacts in northwestern Algeria.

CONCLUSION AND PERSPECTIVES

Conclusion and perspectives

In conclusion, our project addresses the critical challenge of drought mitigation through the innovative application of Artificial Intelligence techniques, the Reconnaissance Drought Index, and atmospheric circulation patterns to find relationship between atmospheric and drought indices. Droughts, exacerbated by climate change, pose severe threats to communities worldwide, underscoring the urgency of effective forecasting and management strategies. By integrating advanced technological solutions with comprehensive meteorological indices, we aim to enhance early warning systems and bolster decision-making processes in drought-prone regions like northwestern Algeria.

Reflecting on the state-of-the-art, our review highlighted the evolving landscape of drought indices and their complex interplay with atmospheric variables. Understanding these relationships is pivotal for improving the accuracy and reliability of drought predictions, thereby minimizing their socio-economic impacts.

Moreover, characterizing the study area provided essential insights into the geographical, geological, and climatic factors influencing drought vulnerability in northwestern Algeria. This contextual understanding informed the development of tailored methodologies for our research, emphasizing the integration of diverse data sources and cutting-edge AI algorithms.

Our methodology centered on leveraging the Reconnaissance Drought Index and exploring atmospheric circulation indices, demonstrating their efficacy in predicting and assessing drought conditions over various temporal scales. The application of the Random Forest model underscored significant advancements in drought classification accuracy, facilitated by robust feature importance analysis that elucidated key environmental drivers of drought variability.

The results and discussions presented herein not only validate our approach but also contribute valuable insights into enhancing drought resilience strategies. By bridging the gap between theoretical research and practical application, our findings lay a foundation for future advancements in drought monitoring and response frameworks. This project exemplifies a proactive step towards sustainable water resource management, offering tangible benefits for local communities and ecosystems alike.

In essence, our endeavor exemplifies the transformative potential of interdisciplinary research and technological innovation in safeguarding against the adverse impacts of climate change. Moving forward, continued collaboration and refinement of methodologies will be essential to further fortify our defenses against the escalating challenges posed by droughts globally.

We hope that this project will serve as a solid foundation for future research and contribute to advancing drought resilience. There is still much to explore and improve upon, but we are confident in our ability to meet these challenges and continue making progress in this field.

Perspectives

Based on our work, we propose the following points for further development :

- Utilize longer time scales to enhance resource management.
- Implement advanced artificial intelligence models and techniques to further improve prediction accuracy.
- Expand the network of monitoring stations and extend the data collection timeframe to enhance accuracy.
- Explore additional drought indices, particularly those integrating atmospheric circulation indices, to better understand and predict drought dynamics.

Bibliographie

[1] S. K. Sigaroodi, Q. Chen, S. Ebrahimi, A. Nazari, and B. Choobin, "Long-term precipitation forecast for drought relief using atmospheric circulation factors : a study on the maharloo basin in iran," *Hydrology and Earth System Sciences*, vol. 18, no. 5, pp. 1995–2006, 2014.

[2] D. A. Wilhite, *Drought and water crises : science, technology, and management issues*. Crc Press, 2005.

[3] J. A. Dracup, K. S. Lee, and E. G. Paulson Jr, "On the definition of droughts," *Water resources research*, vol. 16, no. 2, pp. 297–302, 1980.

[4] R. L. Jones, D. Guha-Sapir, and S. Tubeuf, "Human and economic impacts of natural disasters : can we trust the global data ?," *Scientific data*, vol. 9, no. 1, p. 572, 2022.

[5] R. Hao, H. Yan, and Y.-M. Chiang, "Forecasting the propagation from meteorological to hydrological and agricultural drought in the huaihe river basin with machine learning methods," *Remote Sensing*, vol. 15, no. 23, p. 5524, 2023.

[6] F. Ma, X. Yuan, and A. Ye, "Seasonal drought predictability and forecast skill over china," *Journal of Geophysical Research : Atmospheres*, vol. 120, no. 16, pp. 8264–8275, 2015.

[7] H. Escobar, "Drought triggers alarms in brazil's biggest metropolis," 2015.

[8] Y. Song and M. Park, "Assessment of quantitative standards for mega-drought using data on drought damages," *Sustainability*, vol. 12, no. 9, p. 3598, 2020.

[9] D. A. Wilhite and M. H. Glantz, "Understanding : the drought phenomenon : the role of definitions," *Water international*, vol. 10, no. 3, pp. 111–120, 1985.

[10] R. R. Heim Jr, "A review of twentieth-century drought indices used in the united states," *Bulletin of the American Meteorological Society*, vol. 83, no. 8, pp. 1149–1166, 2002.

[11] Z. Hao and V. P. Singh, "Drought characterization from a multivariate perspective : A review," *Journal of Hydrology*, vol. 527, pp. 668–678, 2015.

[12] S. Park, J. Im, E. Jang, and J. Rhee, "Drought assessment and monitoring through blending of multi-sensor indices using machine learning approaches for different climate regions," *Agricultural and forest meteorology*, vol. 216, pp. 157–169, 2016.

[13] D. Rajsekhar, V. P. Singh, and A. K. Mishra, "Multivariate drought index : An information theory based approach for integrated drought assessment," *Journal of Hydrology*, vol. 526, pp. 164–182, 2015.

[14] A. A. M. Society), "Statement on meteorological drought," *Bull Am Meteorol Soc*, vol. 85, pp. 771–773, 2004.

[15] Indeed, "Statistical methods."

[16] DataScientest, "Machine learning : Tout savoir," 2024. Accessed : 2024-06-23.

[17] JavaTpoint, "Machine learning techniques."

[18] S. E. Haupt, T. C. McCandless, S. Dettling, S. Alessandrini, J. A. Lee, S. Linden, W. Petzke, T. Brummet, N. Nguyen, B. Kosović, *et al.*, "Combining artificial intelligence with physics-based methods for probabilistic renewable energy forecasting," *Energies*, vol. 13, no. 8, p. 1979, 2020.

[19] A. Giannikopoulou, E. Kampragkou, F. Gad, A. Kartalidis, D. Assimacopoulos, *et al.*, "Drought characterisation in cyclades complex, greece," *Eur Water*, vol. 47, pp. 31–43, 2014.

[20] R. Mohammed and M. Scholz, "Impact of evapotranspiration formulations at various elevations on the reconnaissance drought index," *Water Resources Management*, vol. 31, pp. 531–548, 2017.

[21] A. M. Society, "Meteorological drought-policy statement," *Bulletin of the American Meteorological Society*, vol. 78, pp. 847–849, 1997.

[22] D. G. Friedman, *The prediction of long-continuing drought in south and southwest Texas*. No. 1, Travelers Insurance Company, 1957.

[23] M. D. Svoboda, B. A. Fuchs, *et al.*, *Handbook of drought indicators and indices*, vol. 2. World Meteorological Organization Geneva, Switzerland, 2016.

[24] W. J. Gibbs and J. V. Maher, "Rainfall deciles drought inddicators," 1967.

[25] J. J. Keetch and G. M. Byram, *A drought index for forest fire control*, vol. 38. US Department of Agriculture, Forest Service, Southeastern Forest Experiment ..., 1968.

[26] M. J. Hayes, C. Alvord, and J. Lowrey, *Drought indices*. National drought mitigation center, University of Nebraska, 2002.

[27] W. S. P. I. U. Guide, M. Svoboda, M. Hayes, and D. Wood, "Wmo-no. 1090," *WMO : Geneva, Switzerland*, 2012.

[28] H. Wu, M. J. Hayes, D. A. Wilhite, and M. D. Svoboda, "The effect of the length of record on the standardized precipitation index calculation," *International Journal of Climatology : A Journal of the Royal Meteorological Society*, vol. 25, no. 4, pp. 505–520, 2005.

[29] N. B. Guttman, "Comparing the palmer drought index and the standardized precipitation index 1," *JAWRA Journal of the American Water Resources Association*, vol. 34, no. 1, pp. 113–121, 1998.

[30] N. B. Guttman, "Accepting the standardized precipitation index : a calculation algorithm 1," *JAWRA Journal of the American Water Resources Association*, vol. 35, no. 2, pp. 311–322, 1999.

[31] M. Hayes, M. Svoboda, N. Wall, and M. Widhalm, "The lincoln declaration on drought indices : universal meteorological drought index recommended," *Bulletin of the American Meteorological Society*, vol. 92, no. 4, pp. 485–488, 2011.

[32] T. B. McKee, N. J. Doesken, J. Kleist, *et al.*, "The relationship of drought frequency and duration to time scales," in *Proceedings of the 8th Conference on Applied Climatology*, vol. 17, pp. 179–183, California, 1993.

[33] B. Lyon, "The strength of el niño and the spatial extent of tropical drought," *Geophysical Research Letters*, vol. 31, no. 21, 2004.

[34] E. De Martonne, *Traité de géographie physique*, vol. 3. A Colin, 1927.

[35] E. Baltas, "Spatial distribution of climatic indices in northern greece," *Meteorological Applications : A journal of forecasting, practical applications, training techniques and modelling*, vol. 14, no. 1, pp. 69–78, 2007.

[36] H. Wu, M. J. Hayes, A. Weiss, and Q. Hu, "An evaluation of the standardized precipitation index, the china-z index and the statistical z-score," *International Journal of Climatology : A Journal of the Royal Meteorological Society*, vol. 21, no. 6, pp. 745–758, 2001.

[37] D. C. Edwards, T. B. McKee, *et al.*, *Characteristics of 20 th century drought in the United States at multiple time scales*, vol. 97. Colorado State University Fort Collins, 1997.

[38] W. C. Palmer, "Keeping track of crop moisture conditions, nationwide : the new crop moisture index," 1968.

[39] H. N. Bhalme and D. A. Mooley, "Large-scale droughts/floods and monsoon circulation.," 1980.

[40] G. Tsakiris and H. Vangelis, "Establishing a drought index incorporating evapotranspiration," *European water*, vol. 9, no. 10, pp. 3–11, 2005.

[41] H.-R. Byun and D. A. Wilhite, "Objective quantification of drought severity and duration," *Journal of climate*, vol. 12, no. 9, pp. 2747–2756, 1999.

[42] G. Selyaninov, "About climate agricultural estimation," *Proc. Agric. Meteorol*, vol. 20, no. 165-651, p. 177, 1928.

[43] N. D. Strommen and R. P. Motha, "An operational early warning agricultural weather system," in *Planning For Drought*, pp. 153–162, Routledge, 2019.

[44] W. M. Alley, "The palmer drought severity index : limitations and assumptions," *Journal of Applied Meteorology and Climatology*, vol. 23, no. 7, pp. 1100–1109, 1984.

[45] W. C. Palmer, "Meteorological drought. us," *Weather Bureau Res. Paper*, vol. 45, pp. 1–58, 1965.

[46] M. Van Rooy, "A rainfall anomally index independent of time and space, notos," 1965.

[47] E. Kraus, "Subtropical droughts and cross-equatorial energy transports," *Monthly weather review*, vol. 105, no. 8, pp. 1009–1018, 1977.

[48] N. Wells, S. Goddard, and M. J. Hayes, "A self-calibrating palmer drought severity index," *Journal of climate*, vol. 17, no. 12, pp. 2335–2351, 2004.

[49] R. W. Katz and M. H. Glantz, "Anatomy of a rainfall index," *Monthly Weather Review*, vol. 114, no. 4, pp. 764–771, 1986.

[50] S. M. Vicente-Serrano, S. Beguería, and J. I. López-Moreno, "A multiscalar drought index sensitive to global warming : the standardized precipitation evapotranspiration index," *Journal of climate*, vol. 23, no. 7, pp. 1696–1718, 2010.

[51] P. Woli, J. W. Jones, K. T. Ingram, and C. W. Fraisse, "Agricultural reference index for drought (arid)," *Agronomy Journal*, vol. 104, no. 2, pp. 287–300, 2012.

[52] S. J. Meyer, K. G. Hubbard, and D. A. Wilhite, "A crop-specific drought index for corn : I. model development and validation," *Agronomy Journal*, vol. 85, no. 2, pp. 388–395, 1993.

[53] S. J. Meyer, K. G. Hubbard, and D. A. Wilhite, "A crop-specific drought index for corn : Ii. application in drought monitoring and assessment," *Agronomy Journal*, vol. 85, no. 2, pp. 396–399, 1993.

[54] K. Weghorst, "The reclamation drought index : guidelines and practical applications," in *North American water and environment congress & destructive water*, pp. 637–642, ASCE, 1996.

[55] G. Tsakiris, "Meteorological drought assessment, paper prepared for the needs of the european research program medroplan," *Mediterranean Drought Preparedness and Mitigation Planning), Zaragoza*, 2004.

[56] R. G. Allen, L. S. Pereira, D. Raes, M. Smith, *et al.*, "Crop evapotranspiration-guidelines for computing crop water requirements-fao irrigation and drainage paper 56," *Fao, Rome*, vol. 300, no. 9, p. D05109, 1998.

[57] D. Tigkas, H. Vangelis, and G. Tsakiris, "Introducing a modified reconnaissance drought index (rdie) incorporating effective precipitation," *Procedia engineering*, vol. 162, pp. 332–339, 2016.

[58] M. A. A. Zarch, B. Sivakumar, and A. Sharma, "Droughts in a warming climate : A global assessment of standardized precipitation index (spi) and reconnaissance drought index (rdi)," *Journal of hydrology*, vol. 526, pp. 183–195, 2015.

[59] N. Arain, A. Akber, S. Shah, and L. Ahmad, "Analysis of historical drought using standardized precipitation index and reconnaissance drought index (rdi) in tharparkar, sindh," *Environ. Ecol*, vol. 39, no. 1, pp. 65–70, 2021.

[60] Y. Mohammed and A. Yimam, "Analysis of meteorological droughts in the lake's region of ethiopian rift valley using reconnaissance drought index (rdi)," *Geoenvironmental Disasters*, vol. 8, no. 1, p. 13, 2021.

[61] H. Vangelis, D. Tigkas, and G. Tsakiris, "The effect of pet method on reconnaissance drought index (rdi) calculation," *Journal of Arid Environments*, vol. 88, pp. 130–140, 2013.

[62] A. Memon and N. Shah, "Assessment and comparison of spi and rdi meteorological drought indices in panchmahals district of gujarat, india," *International Journal of Current Microbiology and Applied Sciences*, vol. 8, no. 08, pp. 1995–2004, 2019.

[63] R. Mohammed and M. Scholz, "Adaptation strategy to mitigate the impact of climate change on water resources in arid and semi-arid regions : a case study," *Water Resources Management*, vol. 31, pp. 3557–3573, 2017.

[64] R. Mohammed and M. Scholz, "Climate variability impact on the spatiotemporal characteristics of drought and aridityin arid and semi-arid regions," *Water Resources Management*, vol. 33, no. 15, pp. 5015–5033, 2019.

[65] Y. Yin, H. Ke, Y. Tu, X. Wang, Y. Chen, and S. Jiao, "Changes of summer meteorological drought and their relationship with the dry and wet circulation patterns in the huai river basin, china," *Journal of Hydrology : Regional Studies*, vol. 52, p. 101710, 2024.

[66] K. Migała, E. upikasza, M. Osuch, M. Opała-Owczarek, and P. Owczarek, "Linking drought indices to atmospheric circulation in svalbard, in the atlantic sector of the high arctic," *Scientific Reports*, vol. 14, no. 1, p. 2160, 2024.

[67] E. Cherenkova, "The role of atmospheric circulation changes in the increasing frequency of summer droughts in european russia," *Russian Meteorology and Hydrology*, vol. 48, no. 9, pp. 765–777, 2023.

[68] H. Bouguerra, O. Derdous, S. E. Tachi, M. Hatzaki, and H. Abida, "Spatiotemporal investigation of meteorological drought variability over northern algeria and its relationship with different atmospheric circulation patterns," *Theoretical and Applied Climatology*, vol. 155, no. 2, pp. 1507–1518, 2024.

[69] R. Beranová and J. Kyselỳ, "Large-scale heavy precipitation over the czech republic and its link to atmospheric circulation in cordex regional climate models," *Theoretical and Applied Climatology*, pp. 1–12, 2024.

[70] Z. Qian, Y. Sun, Q. Ma, Y. Gu, T. Feng, and G. Feng, "Understanding changes in heat waves, droughts, and compound events in yangtze river valley and the corresponding atmospheric circulation patterns," *Climate Dynamics*, vol. 62, no. 1, pp. 539–553, 2024.

[71] T. Xue, Y. Ding, and C. Lu, "Interdecadal variability of summer precipitation in northwest china and associated atmospheric circulation changes," *Journal of Meteorological Research*, vol. 36, no. 6, pp. 824–840, 2022.

[72] A. Araźny, A. Bartczak, R. Maszewski, and M. Krzemiński, "The influence of atmospheric circulation on the occurrence of dry and wet periods in central poland in 1954–2018," *Theoretical and Applied Climatology*, vol. 146, no. 3, pp. 1079–1095, 2021.

[73] S. H. Mahmoud, T. Y. Gan, R. P. Allan, J. Li, and C. Funk, "Worsening drought of nile basin under shift in atmospheric circulation, stronger enso and indian ocean dipole," *Scientific Reports*, vol. 12, no. 1, p. 8049, 2022.

[74] Y. Zhang, P. Wang, Y. Chen, J. Yang, D. Wu, Y. Ma, Z. Huo, and S. Liu, "The optimal time-scale of standardized precipitation index for early identifying summer

maize drought in the huang-huai-hai region, china," *Journal of Hydrology : Regional Studies*, vol. 46, p. 101350, 2023.

[75] H. Meddi and M. Meddi, "Annual variability of precipitation in the northwest of algeria," *Science et changements planétaires/Sécheresse*, vol. 20, no. 1, pp. 57–65, 2009.

[76] F. HALLOUZ, S. ALIRAHMANI, H. KARAHACANE, M. MEDDI, and G. MAHE, "Variabilité climatique et événements extrêmes et l'impact sur les ressources en eau dans le nord-ouest d'algérie. climate variability and extreme events and the impact on water resources in the northwest of algeria,"

[77] Esri, 2024. Accessed : 2024-05-05.

[78] A. M. L. Henia, "Regionalisation of annual rainfall in the north-western parts of algeria," *Revue Géographique de L'Est*, vol. 45, no. 2, p. 113, 2005.

[79] M. Meddi and B. Morsli, "Etude d'érosion et du ruissellement sur bassins versants expérimentaux dans les monts de beni-chougrane (ouest d'algérie) ; etude d'érosion et du ruissellement sur bassins versants expérimentaux dans les monts de beni-chougrane (ouest d'algérie) ; erosion and runoff in beni-chougrane's mountains (western algeria)," *Zeitschrift fur Geomorphologie*, vol. 45, no. 4, pp. 443–452, 2001.

[80] M. MEDDI and H. MEDDI, "Sécheresse météorologique et agricole dans le nord-ouest de l'algérie," in *Deuxieme colloque méditerranéen sur l'eau et l'environnement, Alger*, 2002.

[81] Tiempo, "Climat - informations et statistiques météorologiques." `https://fr.tutiempo.net/climat`. Accessed : 2024-02-15.

[82] National Centers for Environmental Information (NCEI), "Climate data online (cdo)." `https://www.ncei.noaa.gov/cdo-web/`. Accessed : 2024-02-15.

[83] Climatic Research Unit (CRU), University of East Anglia, "Cru high-resolution gridded datasets." `https://crudata.uea.ac.uk/cru/data/hrg/`. Accessed : 2024-02-15.

[84] University of East Anglia Climatic Research Unit, "CRU Time-Series Datasets of Precipitation and Temperature : Per Capita Indicators." `https://crudata.uea.ac.uk/cru/data/pci.htm`, 11/03/2024.

[85] G. Tsakiris, D. Pangalou, and H. Vangelis, "Regional drought assessment based on the reconnaissance drought index (rdi)," *Water resources management*, vol. 21, pp. 821–833, 2007.

[86] G. Tsakiris, A. Loukas, D. Pangalou, H. Vangelis, D. Tigkas, G. Rossi, A. Cancelliere, *et al.*, "Drought characterization," *Drought management guidelines technical annex*, vol. 58, pp. 85–102, 2007.

[87] M. A. Asadi Zarch, H. Malekinezhad, M. H. Mobin, M. T. Dastorani, and M. R. Kousari, "Drought monitoring by reconnaissance drought index (rdi) in iran," *Water resources management*, vol. 25, pp. 3485–3504, 2011.

[88] S. A. Shamsnia *et al.*, "Comparison of reconnaissance drought index (rdi) and standardized precipitation index (spi) for drought monitoring in arid and semi-arid regions," *Ind J Fundam Appl Life Sci*, vol. 4, no. 3, pp. 39–44, 2014.

[89] Encyclopædia Britannica, "Weather."

[90] National Oceanic and Atmospheric Administration (NOAA), "Global atmospheric circulations."

[91] Copernicus Climate Change Service, "Atmospheric circulation."

[92] C. F. Ropelewski and P. D. Jones, "An extension of the tahiti–darwin southern oscillation index," *Monthly weather review*, vol. 115, no. 9, pp. 2161–2165, 1987.

[93] R. J. Allan, N. Nicholls, P. D. Jones, and I. J. Butterworth, "A further extension of the tahiti-darwin soi, early enso events and darwin pressure," *Journal of Climate*, vol. 4, no. 7, pp. 743–749, 1991.

[94] G. P. Können, P. D. Jones, M. Kaltofen, and R. J. Allan, "Pre-1866 extensions of the southern oscillation index using early indonesian and tahitian meteorological readings," *Journal of Climate*, vol. 11, no. 9, pp. 2325–2339, 1998.

[95] J. W. Hurrell, "Decadal trends in the north atlantic oscillation : Regional temperatures and precipitation," *Science*, vol. 269, no. 5224, pp. 676–679, 1995.

[96] T. J. Osborn, "Winter 2009/2010 temperatures and a record-breaking north atlantic oscillation index," *Weather*, vol. 66, no. 1, pp. 19–21, 2011.

[97] T. Osborn, "Simulating the winter north atlantic oscillation : the roles of internal variability and greenhouse gas forcing," *Climate Dynamics*, vol. 22, no. 6, pp. 605–623, 2004.

[98] P. D. Jones, T. Jónsson, and D. Wheeler, "Extension to the north atlantic oscillation using early instrumental pressure observations from gibraltar and south-west iceland," *International Journal of Climatology : A Journal of the Royal Meteorological Society*, vol. 17, no. 13, pp. 1433–1450, 1997.

[99] B. Vinther, K. K. Andersen, A. Hansen, T. Schmith, and P. Jones, "Improving the gibraltar/reykjavik nao index," *Geophysical Research Letters*, vol. 30, no. 23, 2003.

[100] C. D. Jones and P. M. Cox, "Constraints on the temperature sensitivity of global soil respiration from the observed interannual variability in atmospheric co2," *Atmospheric Science Letters*, vol. 2, no. 1-4, pp. 166–172, 2001.

[101] R. C. Cornes, P. D. Jones, K. R. Briffa, and T. J. Osborn, "A daily series of mean sea-level pressure for london, 1692–2007," *International Journal of Climatology*, vol. 32, no. 5, pp. 641–656, 2012.

[102] R. C. Cornes, P. D. Jones, K. R. Briffa, and T. J. Osborn, "A daily series of mean sea-level pressure for paris, 1670–2007," *International Journal of Climatology*, vol. 32, no. 8, pp. 1135–1150, 2012.

[103] R. C. Cornes, P. D. Jones, K. R. Briffa, and T. J. Osborn, "Estimates of the north atlantic oscillation back to 1692 using a paris–london westerly index," *International Journal of Climatology*, vol. 33, no. 1, pp. 228–248, 2013.

[104] J. Palutikof, M. Conte, J. Casimiro Mendes, C. Goodess, and F. Espirito Santo, "Climate and climatic change," *Mediterranean desertification and land use*, vol. 43, p. 86, 1996.

[105] M. Conte, A. Giuffrida, and S. Tedesco, "The mediterranean oscillation : impact on precipitation and hydrology in italy," 1989.

[106] J. Palutikof, "Analysis of mediterranean climate data : measured and modelled," *Mediterranean climate : variability and trends*, pp. 125–132, 2003.

[107] H. Kutiel and Y. Benaroch, "North sea-caspian pattern (ncp)–an upper level atmospheric teleconnection affecting the eastern mediterranean : Identification and definition," *Theoretical and Applied Climatology*, vol. 71, pp. 17–28, 2002.

[108] A. Pittock, "Patterns of climatic variation in argentina and chile—i precipitation, 1931–60," *Monthly weather review*, vol. 108, no. 9, pp. 1347–1361, 1980.

[109] A. B. Pittock, "On the reality, stability, and usefulness of southern hemisphere teleconnections," *Australian meteorological Magazine Canberra*, vol. 32, no. 2, pp. 75–82, 1984.

[110] P. Jones, M. Salinger, and A. Mullan, "Extratropical circulation indices in the southern hemisphere based on station data," *International Journal of Climatology : A Journal of the Royal Meteorological Society*, vol. 19, no. 12, pp. 1301–1317, 1999.

[111] M. Hatzaki, H. Flocas, D. Asimakopoulos, and P. Maheras, "The eastern mediterranean teleconnection pattern : identification and definition," *International Journal of Climatology : A Journal of the Royal Meteorological Society*, vol. 27, no. 6, pp. 727–737, 2007.

[112] TechTarget, "Ai (artificial intelligence)."

[113] H. Hirsch-Kreinsen, "Artificial intelligence : a "promising technology"," *AI & SOCIETY*, pp. 1–12, 2023.

[114] TechTarget, "Machine learning (ml)." https://www.techtarget.com/searchenterpriseai/definition/machine-learning-ML#:~:text=Classical%20machine%20learning%20is%20often,semisupervised%20learning%20and%20reinforcement%20learning., 2024. Accessed : 2024-05-14.

[115] Baeldung, "An introduction to machine learning." https://www.baeldung.com/cs/machine-learning-intro, 2024. Accessed : 2024-05-14.

[116] NVIDIA, "Supervised vs. unsupervised learning : What's the difference ?." https://blogs.nvidia.com/blog/supervised-unsupervised-learning/, 2024. Accessed : 2024-05-14.

[117] AltexSoft, "Semi-supervised learning." https://www.altexsoft.com/blog/semi-supervised-learning/, 2024. Accessed : 2024-05-14.

[118] TechTarget, "Types of learning in machine learning explained." https://www.techtarget.com/searchenterpriseai/tip/Types-of-learning-in-machine-learning-explained, 2024. Accessed : 2024-05-14.

[119] A. Vidhya, "Regression vs classification." https://www.analyticsvidhya.com/blog/2023/05/regression-vs-classification/, 2023. Accessed : 2024-05-14.

[120] GeeksforGeeks, "Ml | classification vs regression." https://www.geeksforgeeks.org/ml-classification-vs-regression/, 2024. Accessed : 2024-05-14.

[121] B. In, "Random forest algorithm."

[122] A. Brital, "Random forest," 2021.

[123] N. Satsawat, "Evaluation metrics reference guides." https://medium.com/@net_satsawat/evaluation-metrics-reference-guides-7c3a2a055351, May 2019. Accessed : June 9, 2024.

[124] Y. Hasnaoui, S. E. Tachi, H. Bouguerra, S. Benmamar, G. Gilja, R. Szczepanek, J. Navarro-Pedreño, and Z. M. Yaseen, "Enhanced machine learning models development for flash flood mapping using geospatial data," *Euro-Mediterranean Journal for Environmental Integration*, pp. 1–21, 2024.

[125] EvidentlyAI, "Classification metrics : Accuracy, precision, recall." https://www.evidentlyai.com/classification-metrics/accuracy-precision-recall#:

~:text=Accuracy%20is%20a%20metric%20that,often%20the%20model%20is%20right%3F. Accessed : June 9, 2024.

[126] Unknown, "Metrics to evaluate your machine learning algorithm," *Towards Data Science*. Accessed : June 9, 2024.

[127] H. Face, "Hugging face evaluation metric : Accuracy." https://huggingface.co/spaces/evaluate-metric/accuracy. Accessed : June 9, 2024.

[128] Cohere, "A guide to classification evaluation metrics." https://cohere.com/blog/classification-eval-metrics. Accessed : June 9, 2024.

[129] K. Boyd, "Roc graphs : Notes and practical considerations for researchers," 2013.

[130] Unknown, "Feature importance : How to choose the right metrics for machine learning models." https://builtin.com/data-science/feature-importance. Accessed : June 9, 2024.

[131] scikit learn, "Feature importances with forests of trees." https://scikit-learn.org/stable/auto_examples/ensemble/plot_forest_importances.html. Accessed : June 9, 2024.

[132] D. Jang, "Assessment of meteorological drought indices in korea using rcp 8.5 scenario," *Water*, vol. 10, no. 3, 2018.

[133] F. Pedregosa, G. Varoquaux, A. Gramfort, V. Michel, B. Thirion, O. Grisel, M. Blondel, P. Prettenhofer, R. Weiss, V. Dubourg, *et al.*, "Scikit-learn : Machine learning in python," *the Journal of machine Learning research*, vol. 12, pp. 2825–2830, 2011.

[134] scikit-learn, "MinMaxScaler."